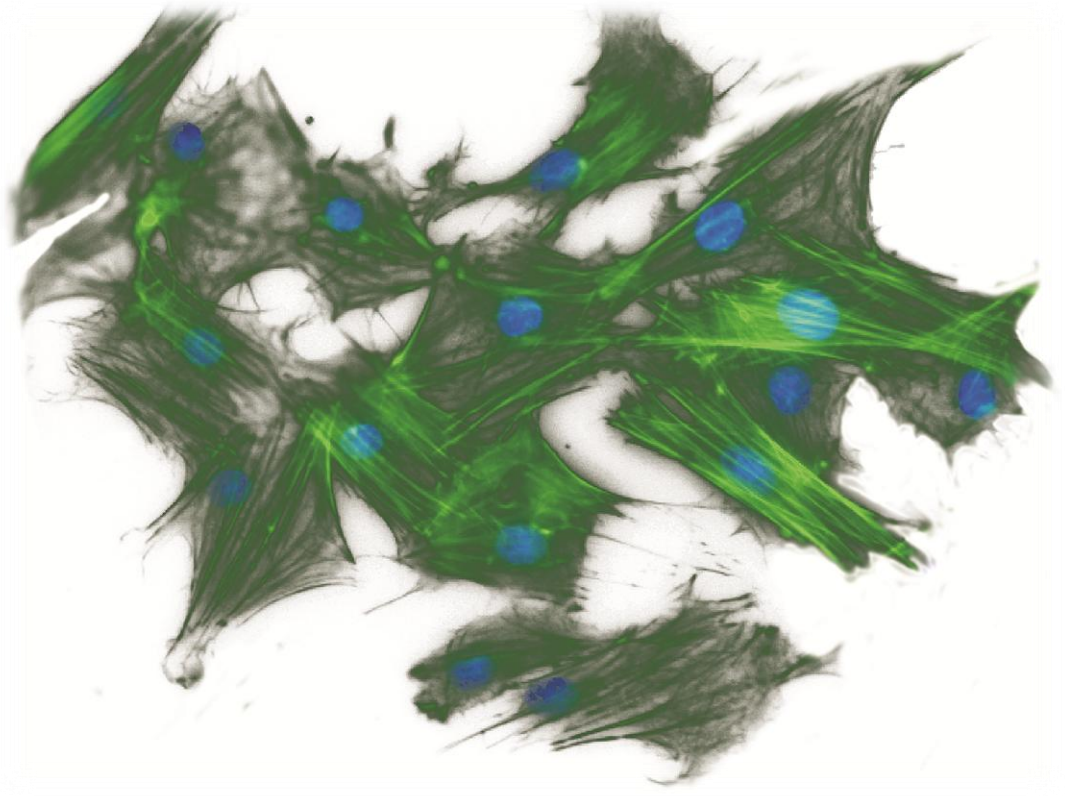


Chondrocyte response to matrix elasticity



Elena Schuh

2010

Chondrocyte response to matrix elasticity

Inauguraldissertation

Zur Erlangung der Doktorwürde

der Universität zu Lübeck

- Aus der Technisch-Naturwissenschaftlichen Fakultät -

Angefertigt am

Institut für Virologie und Zellbiologie,

Universität zu Lübeck

und am

Institut für Biomechanik,

ETH Zürich

vorgelegt von

Elena Schuh

aus Bad Pyrmont

Lübeck 2010

Die vorliegende Arbeit wurde in der Zeit von November 2006 bis Juli 2008 am Institut für Virologie und Zellbiologie der Universität zu Lübeck und von August 2008 bis Mai 2010 am Institut für Biomechanik der ETH Zürich angefertigt. Sie wurde im Rahmen des “integrierten PhD Programms” des europäischen Exzellenznetzwerks EXPERTISSUES erstellt.

1. Berichterstatter: Prof. Dr. Holger Notbohm, Universität zu Lübeck, Deutschland
2. Berichterstatterin: Prof. Dr. Nicole Rotter, Universitätsklinikum Ulm, Deutschland

Tag der mündlichen Prüfung: 06.09.2010

Table of contents

Table of contents	III
Acknowledgements	IV
Abbreviations	VI
Summary.....	VIII
Zusammenfassung.....	XIII
1 Introduction.....	3
1.1 Specific aims.....	5
1.2 Outline of the thesis.....	6
2 Background	9
2.1 Rationale for cartilage tissue engineering (TE).....	11
2.2 Matrix elasticity in skeletal TE	16
3 Chondrocyte response to matrix elasticity in 2D	37
3.1 Adaptation of a validated 2D PA system	39
3.2 Chondrocyte response to matrix elasticity in 2D	42
4 Chondrocyte response to matrix elasticity in 3D: evaluation of a porous system	59
4.1 Characterization of a porous silk-based system.....	61
4.2 Chondrocyte response to pore size	71
5 Chondrocyte response to matrix elasticity in a 3D hydrogel system	81
5.1 Development of a tunable 3D hydrogel system.....	83
5.2 Chondrocyte response to matrix elasticity in 3D	94
5.3 Chondrocyte redifferentiation in 3D.....	107
6 Synthesis	125
6.1 Innovations	127
6.2 Limitations and future work	130
6.3 Conclusions	131
References.....	132
Scientific manuscripts.....	144
Curriculum Vitae.....	145

Acknowledgements

The present work would not have been possible without the help of several people.

I want to thank Prof. Dr. Holger Notbohm and Prof. Dr. Nicole Rotter for giving me the opportunity to perform this integrated PhD programme and for both, helpful scientific advice when necessary, but also the high degree of freedom I was given during this work.

My sincerest thanks go to Prof. Dr. Ralph Müller for welcoming me in his institute and enabling research continuation in Zürich, for always having an open office door when advice was needed, and for providing critical, yet always very constructive scientific input.

Furthermore, I would like to thank people from the Institute of Virology and Cell Biologie at the University of Lübeck. ‘Thank you’ to Prof. Dr. Jürgen Rohwedel and Dr. Jan Kramer for allowing me to join their research group and for many fruitful, scientific discussions during that time. Further thanks go to Barbara Andresen and Alexandra Tiedke for always offering technical advice and a helpful hand, to Dr. Silke Erdmann for her very valuable introduction into the work with chondrocytes and to Dr. Thomas Gutschmann for the AFM work.

I would also like to thank all members of the Institute for Biomechanics at the ETH Zürich for contributing to the nice working atmosphere by being, not only colleagues but also friends. Special thanks go to Dr. Sandra Hofmann for always taking her time for in depth discussions and valuable advice for my scientific work. Further thanks go to her and the rest of the Tissue Engineering group, Silke Wuest, Benjamin Thimm and Dr. Ming Chang for creating such a great atmosphere in the group by being uncomplicated, jolly and always ready to help me and each other. Many thanks also to Dr. Kathryn Stok for her introduction into mechanical testing and Marius Elkuch for his contributions to the silk scaffold project.

A big ‘thank you’ goes to all my friends in Germany, Switzerland and the rest of Europe, especially Anna, Kerstin and Ingrid, to my Volleyball teams and to my flatmates, for so

many good times besides work and for dragging me out of the lab when I needed a break.

Particular thanks go to Thomas for his love and support and for making Switzerland something like a home for me.

My sincerest thanks go to my parents and siblings, for always supporting and believing in me, for planting the confidence in me that all things turn out well eventually, and for contributing significantly to keeping this true. Thank you so much!

Finally, the financial support from the European Network of Excellence, EXPERTISSUES, is gratefully acknowledged.

Abbreviations

AA	–	Acrylamide
AAD	–	Adipic acid hydrazide
ACI	–	Autologous chondrocyte implantation
AFM	–	Atomic force microscopy
ALP	–	Alcaline phosphatase
ANOVA	–	Analysis of variance
BrdU	–	5-bromo-2-deoxyuridine
BSA	–	Bovine serum albumine
DAPI	–	2-(4-amidinophenyl)-1H -indole-6-carboxamide
DNA	–	Deoxyribonucleic acid
2D	–	Two-dimensional
3D	–	Three-dimensional
ECM	–	Extracellular matrix
EGTA	–	glycol-bis(2-aminoethylether)- <i>N,N,N',N'</i> -tetraacetic acid
EDTA	–	2,2',2'',2'''-(ethane-1,2-diyl)dinitrilo)tetraacetic acid
FA	–	Focal adhesion
FBS	–	Fetal bovine serum
FITC	–	Fluoresceinisothiocyanat
GAG	–	Glycosaminoglycan
HEPES	–	4-(2-hydroxyethyl)-1-piperazineethanesulfonic acid
H&E	–	Haematoxylin and Eosin
HFIP	–	1,1,1,3,3,3-Hexafluoro-2-propanol
IHC	–	Immunohistochemistry

LOWESS	–	Locally weighted scatterplot smoothing
LSD	–	Least significant difference
MAPK	–	Mitogen activated protein kinase
Micro-CT	–	Micro-computed tomography
MMP	–	Matrix metalloproteinase
MSCs	–	Mesenchymal stem cells
PA	–	Polyacrylamide
PBS	–	Phosphate buffered saline
PCM	–	Pericellular matrix
PEG	–	Poly(ethylene)-glycol
PEGDA	–	Poly(ethylene)-glycol diacrylate
RGD	–	Arg-Gly-Asp
RGE	–	Arg-Gly-Glu
RNA	–	Ribonucleic acid
RT	–	Room temperature
RT-PCR	–	Reverse transcriptase polymerase chain reaction
SD	–	Standard deviation
SE	–	Standard error of mean
SEM	–	Scanning electron microscopy
SMC	–	Smooth muscle cell
Sulfo-SANPAH	–	<i>N</i> -Sulfosuccinimidyl-6-(4'-azido-2'-nitrophenylamino) hexanoate
TE	–	Tissue engineering
UPW	–	Ultrapure water

Summary

Due to the limited capability of cartilage for self repair, tissue engineering (TE) solutions provide an attractive alternative to conventional clinical treatments of cartilage defects [1]. In order to produce functional cartilage substitutes, stem cells or primary chondrocytes can be immobilized and cultured in supporting materials. The physical properties of such scaffolds have been shown to vastly impact cellular behavior [2-5] and may be tuned in novel materials to induce a desired cellular response. The importance of matrix elasticity, as one of these properties, gained increasing interest over the last few years. It has been shown that cells actively probe the elasticity of the matrix and react to it in a cell type specific way [4, 6, 7]. However, knowledge about the influence of this material property on chondrocyte behavior is still largely lacking. Based on this gap, the objective of the thesis is a comprehensive investigation of chondrocyte response to matrix elasticity.

The different possible culture scenarios in cartilage TE should, hereby, be covered. These are: (i) chondrocyte expansion in monolayer after isolation (ii) chondrocyte incorporation and expansion in a three-dimensional (3D) setting after isolation and (iii) 3D redifferentiation of chondrocytes after expansion in monolayer. I hypothesized that matrix elasticity influences the proliferation and differentiation state of chondrocytes in both, the two-dimensional (2D) and 3D culture systems. To investigate this hypothesis, suitable culture systems needed to be adapted or, if necessary, developed. A polyacrylamide (PA) system was adapted for the study in 2D culture as it has been well characterized and was widely used in other studies in this field. A suitable 3D culture system still needed to be identified, since studies about cellular response to matrix elasticity in 3D are largely lacking. In a first step, the suitability of a porous system was investigated, as porous systems have been used for other studies in this field. Since the porous system did not provide satisfactory conditions for my purpose, a tunable hydrogel system was then developed to provide an improved, well-controlled environment to study chondrocyte response to matrix elasticity in 3D.

Chapter 2 provides the background for this work. It explains the main constituents of

cartilage and strategies for cartilage repair and cartilage TE. Furthermore, the current knowledge about the importance of stiffness sensing in the broader field of skeletal TE is summarized.

Chapter 3 investigates chondrocyte response to matrix elasticity in a 2D-environment. When chondrocytes are cultured in monolayer, on cell culture plastic, they lose their chondrogenic phenotype in a process called dedifferentiation [8]. Dedifferentiated cells produce tissue substitutes with inferior mechanical properties compared to fully differentiated chondrocytes [9]. I hypothesized that the elasticity of the substrate, the cells are cultured on, influences the maintenance of the chondrogenic phenotype. To examine this hypothesis, a 2D culture system was used in which PA gels with different concentrations of bis-acrylamide were coated with collagen type I. Matrices with Young's moduli of 4 kPa, 10 kPa, 40 kPa, and 100 kPa were produced, as determined by atomic force microscopy (AFM). Porcine chondrocytes were cultivated on these matrices at low density for seven days. The proliferation of cells was analyzed by 5-Bromo-2'-deoxy-uridine (BrdU) incorporation. Maintenance of the chondrogenic phenotype was analyzed by measuring collagen type I, type II and aggrecan gene expression, immunofluorescence staining for collagen type II, and phalloidin staining for actin filaments. Compared to cells cultured on stiffer substrates, cellular proliferation and actin organization was decreased on matrices of 4 kPa. The differentiated phenotype of the chondrocytes grown on matrices of 4 kPa was stabilized, indicated by higher collagen type II and aggrecan, and lower collagen type I expression in comparison to chondrocytes on stiffer substrates. These findings indicate that chondrocytes sense the elasticity of the matrix and that soft substrates support the chondrogenic phenotype in 2D.

Since cells often find themselves in a more complex, 3D environment in TE applications and *in vivo*, this research was extended into the third dimension, in a next step. The elasticity of a 3D system can be altered by different means. I tested two potential approaches: 1) a porous system, in which pore size has been shown to change the mechanical properties and 2) a hydrogel system where the mechanical properties can be tuned by using different concentrations of a starting material.

Chapter 4 investigates the suitability of a porous system to study stiffness sensing in 3D.

Different pore sizes have been shown to result in different mechanical properties of the bulk material, with smaller pores resulting in stiffer, and larger pores in softer materials [10, 11]. Pore size might, however, also directly impact cellular behavior [12, 13]. I hypothesized larger pores would result in softer scaffolds which, in turn, -based on the experience in the 2D culture system- would be favorable for the chondrogenic phenotype. Porous silk scaffolds with different average pores sizes ($98.5 \pm 1.5 \mu\text{m}$ = small; $142 \pm 11.5 \mu\text{m}$ = medium and $196.9 \pm 20.2 \mu\text{m}$ = large pores) could be produced as confirmed by micro-computed tomography (micro-CT) measurements. However, mechanical testing of the scaffolds showed that even groups of scaffolds with the same average pore size had high deviations in mechanical properties, and that scaffolds with different pore sizes consequently did not differ significantly in their mechanical properties. Analysis of the TE constructs after 4 weeks of culture showed that cells were more evenly distributed in scaffolds with small pores, but that the amount of DNA and glycosaminoglycans (GAGs) was not significantly different between the different scaffold types. Cells maintained their chondrogenic phenotype independent of the pore size as indicated by a round morphology and a high collagen type II production. However, they had only little contact to the substrate and were not evenly distributed, but formed a dense layer at the outside of the scaffold with only sparse cell numbers in the center. In conclusion, pore size had a small influence on cell distribution but not on proliferation, extracellular matrix (ECM) production or the maintenance of the chondrogenic phenotype. The investigated porous system was furthermore shown to be an unsuitable system to study stiffness sensing, due to the heterogeneous mechanical properties, the limited contact between cells and substrates, and the inhomogeneous cell distribution.

Based on the knowledge obtained in **Chapter 4**, the first section of **Chapter 5** covers the development of a hydrogel system. I hypothesized that a hydrogel system would provide an improved, controlled environment for studying stiffness sensing in 3D. To furthermore assure a separation of mechanical properties and adhesion site density, an approach was chosen in which an inert material with tunable mechanical properties can be modified with a controlled number of adhesion sites. Agarose was chosen as inert bulk material, while RGD (Arg-Gly-Asp) was chosen as an adhesion sequence, to enable active stiffness sensing of the cells. Agarose type VII displayed stable mechanical properties

under cell culture conditions and could be modified with RGD. Hydrogels with different mechanical properties were produced by varying the concentration of agarose in the gel. Cells interacted with the RGD and cellular viability was not diminished in modified, when compared to plain agarose. The developed agarose model system, thus, seemed to be suitable to study chondrocyte stiffness sensing in 3D culture.

The second section of **Chapter 5** applies the developed model system to investigate the effect of matrix elasticity on the maintenance of the chondrogenic phenotype in 3D-culture. Based on the findings in 2D, I hypothesized that soft materials would also promote the chondrogenic phenotype in 3D culture. To investigate this hypothesis, agarose was modified with RGD, or RGE (Arg-Gly-Glu) as a chemically similar control that does not provide adhesion sites. Hydrogels with different mechanical properties were produced. Primary chondrocytes were incorporated into the gel, cultured for up to two weeks and constructs were analyzed. Cells were surrounded by their own ECM from an early stage and maintained their chondrogenic phenotype, independent of substrate composition, as indicated by a high collagen type II and a lack of collagen type I production. However, softer gels showed a higher DNA and GAG content and larger cell clusters than stiff gels, in both, RGD- and RGE-modified agarose. I concluded that matrix elasticity does not influence the maintenance of the chondrogenic phenotype in 3D-agarose-culture, but influences the size of the formed cell-ECM clusters. The deviation of these findings from the previous results in 2D culture stresses the importance of transferring results from mechanosensing from 2D into 3D culture systems, as these are more closely mimicking the natural environment of cells

The third section of **Chapter 5** applies the developed hydrogel system to investigate the influence of adhesion site density and stiffness on the redifferentiation of expanded chondrocytes. To obtain sufficient cell numbers for cartilage TE with autologous chondrocytes, cells are typically expanded in monolayer culture. The resulting loss of the chondrogenic phenotype can be reversed upon transfer into a 3D-environment. I hypothesized that the properties of this 3D-environment, namely adhesion site density and substrate elasticity, would influence this redifferentiation process. To test this hypothesis, chondrocytes were expanded in monolayer and their phenotypical transition was analyzed. Agarose hydrogels with different RGD densities and mechanical properties

were produced, cells were incorporated into the gels to induce redifferentiation and constructs were analyzed after two weeks of 3D-culture. The availability of adhesion sites inhibited cellular redifferentiation: GAG production per cell was diminished by RGD in a dose dependant manner and cells incorporated into gels with the highest RGD density, continued to synthesize collagen type I and produced the least amount of collagen type II. Substrate stiffness, in contrast, did not significantly influence cellular redifferentiation, but softer gels contained higher cell numbers and amounts of ECM after two weeks of culture. These findings might prove useful to choose appropriate biomaterials for the 3D-redifferentiation of expanded chondrocytes.

In conclusion, different model systems were developed in this thesis and applied to investigate the response of chondrocytes in 2D culture, 3D culture and during redifferentiation in 3D culture. I showed that chondrocytes sense matrix elasticity and that their response is very different in 2D compared to 3D culture. Substrate stiffness influences the chondrogenic phenotype in 2D but not in 3D culture. However, cell proliferation and cluster formation is influenced by matrix elasticity in 3D and the availability of adhesion sites influences chondrogenic redifferentiation. This fundamental knowledge can be used in future TE applications to optimize cell-material interactions through the controlled manipulation of biomaterials.

Zusammenfassung

Geschädigtes Knorpelgewebe besitzt nur sehr begrenzte Möglichkeiten, sich ohne Eingriff von außen zu regenerieren. Das Züchten von Knorpelgewebe (Knorpel Tissue Engineering, TE) bietet die Möglichkeit einen entstandenen Knorpeldefekt dauerhaft zu beheben [1]. Um beschädigtes Gewebe zu ersetzen, können hierbei adulte Stammzellen oder Chondrozyten auf einem geeigneten Trägermaterial (Matrix) immobilisiert werden. Sowohl die chemischen als auch physikalischen Eigenschaften dieses Trägermaterials haben einen direkten Einfluss auf das Verhalten der Zellen, und damit auf die erfolgreiche Entstehung des Gewebeersatzes [2-4]. Es konnte beispielsweise gezeigt werden, dass Zellen die Elastizität des Materials detektieren und darauf reagieren. Die Forschung der letzten Jahre bestätigte, dass gerade diese Eigenschaft einen bisher unterschätzten Einfluss auf das Zellverhalten hat. Ob und wie sich dieser Einfluss auswirkt, scheint jedoch sehr stark vom Zelltyp abzuhängen [2, 6, 7]. Da bislang kaum Kenntnisse über die Auswirkung dieser Materialeigenschaft auf Chondrozyten vorhanden sind, war das Ziel dieser Arbeit eine umfassende Untersuchung des Einflusses von Matrixelastizität auf das Verhalten von Chondrozyten. Hierbei sollte der Einfluss der Matrixelastizität auf die verschiedenen Aspekte im Knorpel TE untersucht werden: (i) Die Expansion von Chondrozyten im Monolayer, also in einem 2D-Kultursystem, (ii) die Inkorporation und Vermehrung von Chondrozyten in verschiedenen 3D-Kultursystemen und (iii) die 3D-Kultur zur Redifferenzierung von Chondrozyten die im Monolayer vermehrt wurden. Die Ausgangshypothese dieser Studie war, dass die Elastizität der Matrix sowohl den chondrogenen Phenotyp, als auch die Proliferation von Chondrozyten in den verschiedenen Kultursystemen beeinflusst. Um diese Hypothese zu untersuchen wurden verschiedene Kultursysteme adaptiert, auf ihre Tauglichkeit geprüft und wenn nötig neu implementiert. Zur Untersuchung des Einflusses der Matrixelastizität in 2D-Kultur wurde ein bereits etabliertes und gut charakterisiertes 2D-Kultursystem auf Basis von Polyacrylamid (PA)-Gelen ausgewählt. Da bisher kaum Studien über den Einfluss von Matrixelastizität in 3D-Kultur durchgeführt wurden, musste zunächst ein angemessenes

3D-Kultursystem identifiziert werden. In einem ersten Schritt wurde hierzu die Tauglichkeit eines porösen Systems untersucht, da poröse Systeme bereits für andere Studien in diesem Bereich verwendet wurden. Da dieses Kultursystem jedoch nur unzureichende Eigenschaften für meine Zwecke vorweisen konnte, wurde in einem nächsten Schritt ein Hydrogel basiertes Kultursystem entwickelt um Untersuchungen des Einflusses der Matrixelastizität auf Chondrozyten in einer verbesserten, kontrollierte 3D-Umgebung zu ermöglichen.

Kapitel 2 legt die Hintergründe der vorliegenden Forschungsarbeit dar. Sowohl die Grundkomponenten von Knorpelgewebe, als auch die heutigen Möglichkeiten zur Behandlung von Knorpeldefekten, wie zum Beispiel Knorpel TE, werden beschrieben. Zusätzlich werden die aktuellen Erkenntnisse zur Auswirkung der Matrixelastizität auf Zellen für den Gewebeersatz im weiteren Feld des Bewegungsapparates zusammengefasst.

Kapitel 3 behandelt die Auswirkung von Matrixelastizität auf Chondrozyten in einem 2D-Kultursystem. Wenn Chondrozyten im Monolayer in Zellkulturflaschen kultiviert werden, verlieren sie mit der Zeit ihren differenzierten Phänotyp [8]. Knorpelgewebe, das mit Hilfe dieser dedifferenzierten Zellen gezüchtet wird, besitzt unzureichende mechanische Eigenschaften um einen Knorpeldefekt dauerhaft und vollständig reparieren zu können [9].

Die Ausgangshypothese dieser Studie war, dass der Erhalt des differenzierten Phänotyps in Monolayerkultur von der Elastizität der Matrix beeinflusst wird. Um diese Hypothese zu untersuchen wurde ein bereits etabliertes Modellsystem adaptiert, in dem PA-Gele mit unterschiedlichen Konzentrationen von bis-Acrylamid vernetzt werden, um Substrate mit verschiedenen Elastizitäten zu erhalten. Ein Adhäsionsprotein, in diesem Fall Kollagen I, kann anschließend kovalent an die Substrate gekoppelt werden, um die aktive Detektion der Elastizität durch die Zellen zu ermöglichen.

Porcine Chondrozyten wurden in geringer Dichte für bis zu 7 Tagen auf Gelen mit Young's Moduli von 4 kPa, 10 kPa, 40 kPa und 100 kPa kultiviert. Anschließend wurde der Phänotyp der Zellen auf den unterschiedlichen Substraten analysiert. Im Vergleich zu härteren Gelen wurden bei Zellen auf weichen Gelen eine geringere Proliferation und eine weniger stark ausgeprägte Organisation des Aktin-Zytoskelets nachgewiesen. Eine

höhere Expression von Kollagen Typ II und Aggrekan und eine geringere Expression von Kollagen Typ I zeigten weiterhin, dass der differenzierte Phänotyp durch die Kultur auf weichen Substraten stabilisiert werden konnte. Diese Ergebnisse legen den Schluss nahe, dass Chondrozyten die Elastizität des Materials detektieren können und dass weiche Materialien den Verlust des differenzierten Phänotyps von Chondrozyten in Monolayerkultur verzögern können.

Da Zellen sich sowohl *in vivo*, als auch bei der Erstellung von Gewebeersatz oft in einer komplexeren, 3D-Umgebung befinden sollte in einem nächsten Schritt untersucht werden, wie weit Ergebnisse aus einem 2D-Kultursystem auf das Verhalten von Chondrozyten in einem 3D-Kultursystem übertragbar sind. Ich stellte die Hypothese auf, dass die, im 2D-Kultursystem beobachtete Reaktion der Chondrozyten auf die Elastizität des Materials auch in einem 3D-Kultursystem beobachtet werden kann. Um diese Hypothese zu untersuchen musste zunächst ein geeignetes 3D-Kultursystem entwickelt werden. Die mechanischen Eigenschaften eines 3D-Kultursystems können auf verschiedene Arten verändert werden. Die Studien zur Entwicklung eines geeigneten 3D-Kultursystems basieren auf zwei Kernhypothesen 1) Ein geeignetes Kultursystem kann auf Basis eines porösen Materials, dessen Elastizität über die Porengröße reguliert wird, entwickelt werden und 2) Ein geeignetes Kultursystem kann auf Basis eines Hydrogels, dessen Elastizität durch die Konzentration des Ausgangsmaterials reguliert wird, entwickelt werden.

Kapitel 4 untersucht die Eignung eines porösen Systems zur Erforschung des Einflusses von Matrixelastizität auf das Verhalten von Chondrozyten in 3D-Kultur. Bisherige Untersuchungen haben gezeigt, dass unterschiedliche Porengrößen zu unterschiedlichen Elastizitäten führen, wobei kleine Poren zu steiferen und große Poren zu weicherem Scaffolds führt [10, 11]. Die Porengröße selbst kann sich jedoch auch direkt auf das Zellverhalten auswirken [12, 13]. Ausgangshypothese in diesem Kapitel war, dass Scaffolds mit unterschiedlichen mechanischen Eigenschaften durch ein Einbringen verschieden großer Poren produziert werden können und dass weiche Scaffolds -wie in der Kultur in 2D- den chondrogenen Phänotyp unterstützen. Porogene unterschiedlicher Größe konnten dazu verwendet werden, poröse Seidenscaffolds mit unterschiedlichen Porengrößen ($98.5 \pm 1.5 \mu\text{m}$ = kleine; $142 \pm 11.5 \mu\text{m}$ = mittlere und $196.9 \pm 20.2 \mu\text{m}$ =

große Poren) zu produzieren, wie anhand von micro-CT Analysen bestätigt werden konnte. Die mechanischen Tests der Scaffolds zeigten jedoch, dass selbst Scaffolds mit derselben Porengröße sehr unterschiedliche elastische Moduli hatten. Unterschiedliche Porengrößen führten deshalb nicht zu signifikant unterschiedlichen elastischen Moduli der Scaffolds. Die Analyse der für 4 Wochen mit Zellen kultivierten Konstrukte ergab, dass die Zellen eine etwas gleichmäßigere Verteilung in Scaffolds mit kleinen Poren zeigten, die Menge von DNA und ECM-Komponenten auf den verschiedenen Scaffoldtypen jedoch nicht signifikant unterschiedlich war. Der differenzierte Phänotyp der Chondrozyten wurde außerdem unabhängig von der Porengröße der Scaffolds erhalten.

Durch die Bildung von Zell-ECM Aggregaten, vor allem an der Oberfläche der Scaffolds, hatte der Großteil der Zellen jedoch nur sehr begrenzten Kontakt zum Trägermaterial. Die Zellen zeigten bildeten dichte Schichten am Rand und verteilten sich nur spärlich bis in die Mitte der Scaffolds.

Zusammenfassend lässt sich sagen, dass die Porengröße keinen Einfluss auf den Erhalt des differenzierten Phänotyps, die Proliferation und die Produktion von ECM-Komponenten der Zellen zu haben scheint. Eine eindeutige Trennung der Porengröße von anderen physikalischen Scaffold-Eigenschaften ist jedoch nicht möglich. Das untersuchte, poröse System ist zudem durch die inhomogenen mechanischen Eigenschaften, den eingeschränkten Kontakt der Zellen zum Trägermaterial und die ungleichmäßige Zellverteilung nicht als Modellsystem für Untersuchungen zum Einfluss der Matrixelastizität geeignet.

Basierend auf den Erfahrungen mit dem porösen System, beschäftigt sich der erste Teil des **Kapitels 5** mit der Entwicklung eines Hydrogel-Modellsystems. Dies soll eine verbesserte, kontrollierte Umgebung für die Untersuchung des Einflusses der Matrixelastizität auf Chondrozyten in 3D-Kultur bieten. Um zudem zu gewährleisten, dass die Veränderung der Elastizität unabhängig von einer Veränderung in der Dichte der Adhäsionsstellen in dem Material erfolgt, wurde ein Ansatz gewählt, in dem ein inertes Ausgangsmaterial mit einer kontrollierten Anzahl von Adhäsionsmolekülen modifiziert wurde. Als Adhäsionsmolekül, das eine aktive Detektion der Matrixelastizität durch die Zellen ermöglichen soll, wurde RGD verwendet. Als inertes Ausgangsmaterial wurde

Agarose Typ VII gewählt, da es stabile mechanische Eigenschaften unter Zellkulturkonditionen aufweist. Die Agarose konnte erfolgreich mit RGD modifiziert werden. Hydrogele mit reproduzierbaren mechanischen Eigenschaften und Young's Moduli von etwa 4 kPa bis 53 kPa konnten durch den Einsatz verschiedener Konzentrationen von Agarose produziert werden. Zellen adhärten zudem an der modifizierten Agarose und zeigten eine gute Vitalität nach Inkorporation in das Material. Das entwickelte Modellsystem war somit geeignet den Einfluss der Matrixelastizität auf Chondrozyten in einem 3D-Kultursystem zu untersuchen.

Im zweiten Teil des Kapitels wurde das entwickelte Modellsystem angewandt, um den Einfluss der Matrixelastizität auf Chondrozyten in 3D zu untersuchen. Agarose wurde mit RGD modifiziert und RGE-modifizierte Hydrogele wurden, als chemisch ähnliches Kontrollsystem ohne Adhäsionsmöglichkeiten, hergestellt. Harte (53 kPa) und weiche (4 kPa) Hydrogele wurden erzeugt. Chondrozyten wurden in die Gele inkorporiert, für bis zu zwei Wochen kultiviert, und die entstandenen Konstrukte analysiert. Die Chondrozyten waren bereits in einem frühen Stadium der Zellkultur von ihrer eigenen ECM umgeben. Das Ausmaß der Kollagen II Produktion und das komplette Fehlen von Kollagen I zeigten zudem, dass der differenzierten Phänotyp unabhängig von den Eigenschaften des Trägermaterials bewahrt wurde. Unabhängig von der Art der Modifizierung, enthielten weiche Gele jedoch signifikant mehr DNA und GAG und größere Zell-ECM Cluster als harte Gelen. Die Ergebnisse deuten darauf hin, dass die Elastizität des Materials keinen Einfluss auf die Erhaltung des differenzierten Phänotyps in einer 3D-Umgebung hat, jedoch die Zellmenge und die Größe der geformten Cluster beeinflusst. Die Abweichung dieser Ergebnisse von den Ergebnissen im 2D-Kultursystem unterstreicht hierbei zudem die Notwendigkeit, Untersuchungen des Einflusses der Matrixelastizität auf 3D-Kultursysteme auszuweiten.

Im letzten Teil des Kapitels wurde das entwickelte Modellsystem angewandt, um den Einfluss von Matrixelastizität und Adhäsionsmoleküldichte auf die Redifferenzierung expandierter Chondrozyten zu untersuchen. Um ausreichend Zellen für die Züchtung von Knorpelgewebe zu erhalten, müssen Chondrozyten typischerweise in Monolayerkultur vermehrt werden. Hierbei verlieren sie ihren differenzierten Phänotyp. Dieser Vorgang kann jedoch durch die Kultur in einem geeigneten 3D-Trägermaterial

wieder rückgängig gemacht werden. Die Ausgangshypothese dieser Studie war, dass die Eigenschaften des Trägermaterials, in diesem Falle die Dichte der Adhäsionsmoleküle und die Elastizität des Materials, den Erfolg dieser Redifferenzierung beeinflussen können. Um diese Hypothese zu untersuchen, wurden Chondrozyten im Monolayer vermehrt und der Verlust des differenzierten Phänotyps wurde analysiert. Hydrogele mit verschiedenen RGD Konzentrationen und verschiedenen mechanischen Eigenschaften (hart = ~53 kPa oder weich = 4 kPa) wurden produziert und die expandierten Zellen wurden für zwei Wochen in den Hydrogelen kultiviert, um die Redifferenzierung zu ermöglichen.

RGD hatte einen inhibierenden Effekt auf die Wiedererlangung des differenzierten Phänotyps: Die GAG Produktion pro Zelle nahm mit zunehmender RGD-Konzentration im Hydrogel ab und Zellen, die in Gele mit der höchsten RGD Dichte inkorporiert wurden, waren auch nach der Redifferenzierungs-Phase positiv für Kollagen Typ I und produzierten nur geringe Mengen Kollagen Typ II. Die Elastizität des Materials hatte hingegen keinen Einfluss auf den Redifferenzierungsprozess. Weiche Gele enthielten am Ende der Kulturzeit jedoch wiederum mehr Zellen und GAG als harte Gele. Diese Erkenntnisse zum Einfluss der Materialeigenschaften auf den Redifferenzierungsprozess können in Zukunft dazu verwendet werden passende Trägermaterialien für die 3D-Redifferenzierung von Chondrocyten auszuwählen.

Im Rahmen der vorliegenden Forschungsarbeit wurden verschiedene Kultursysteme angewandt, und wenn nötig neu implementiert, um den Einfluss von Matrixelastizität auf das Verhalten von Chondrozyten zu untersuchen. Die verschiedenen Studien behandelten dabei unterschiedliche Aspekte, die im Bereich des Knorpel TE von Bedeutung sind.

Es konnte gezeigt werden, dass Chondrozyten in 2D-Kultursystemen anders auf die Elastizität der Matrix reagieren als in 3D-Kultursystemen. Die Elastizität beeinflusste die Erhaltung des differenzierten Phänotyps in 2D-, jedoch nicht in 3D-Kultur. Im 3D-System konnte jedoch ein Einfluss der Elastizität auf die Zellproliferation und die Größe der formierten Zellcluster festgestellt werden. Die Elastizität hatte jedoch keinen messbaren Einfluss auf die Redifferenzierung expandierter Chondrozyten. Es konnte hingegen ein inhibierender Einfluss von Adhäsionsmolekülen auf diesen Vorgang festgestellt werden.

Durch die, im Rahmen dieser Forschungsarbeit durchgeführten, Studien konnte grundlegendes Wissen über vorteilhafte Materialeigenschaften für die verschiedenen Szenarien der Zellkultur im Knorpel TE erlangt werden. Dieses Wissen kann in Zukunft dazu genutzt werden Biomaterialien für TE-Applikationen gezielt zu manipulieren, um Zell-Material Interaktionen zu optimieren.

1 Introduction

1.1 Specific aims

In an aging population, the need for clinical solutions to compensate for the wear of the skeletal system is constantly increasing. Amongst those, chondral injuries affect a large and ever increasing fraction of the population. Cartilage in itself has very limited ability for self repair and therefore even minor lesions can pose a major problem and in a consequence disable joint movement and vastly restrict daily activities. Several surgical treatments have been applied to avoid total or partial replacement of joints. Nevertheless, articial joints are still often the only resort to effectively treat joint degeneration. Tissue engineering (TE) on the other side provides an attractive alternative to artificial implants, which have a limited life span. In this biological approach, the combination of cells and biomaterials could produce tissue substitutes that fully integrate with the host tissue, are remodeled over time, and with that allow adaptation and growth in line with the patient's needs and lifestyle.

The optimal physical properties of biomaterials for cartilage TE are, to date, mainly identified by trial and error methods for each promising material. To reduce this cost and labor intensive procedure and facilitate the intentional design of novel biomaterials, a fundamental knowledge about favorable physical properties needs to be obtained.

The elasticity of a material was, hereby, shown to have a high influence on cellular behavior and may be tuned to optimize cell-material interactions. However, only little is known about the influence of elasticity on the chondrogenic phenotype and chondrocyte behavior. This thesis aims to help filling this gap through a comprehensive study about chondrocyte response to matrix elasticity. The studies, conducted in the scope of this thesis, should, hereby, cover the different possible scenarios in cartilage TE: chondrocyte culture in monolayer, chondrocyte culture in a 3D culture system and 3D redifferentiation of chondrocytes that were expanded in monolayer. To achieve this, four specific aims were formulated.

Specific aim 1: The adaptation of a validated 2D model system to study chondrocyte

response to matrix elasticity in 2D monolayer culture.

Specific aim 2: Test known 3D culture systems for their suitability to study stiffness sensing in 3D, identify possible pitfalls of this more complex setting and develop a suitable, well defined model system, if necessary.

Specific aim 3: Investigate chondrocyte response to matrix elasticity in 3D culture.

Specific aim 4: Investigate the influence of matrix elasticity on chondrocyte redifferentiation in 3D culture after monolayer expansion.

1.2 Outline of the thesis

The following five chapters introduce the area of research, highlight the gap of knowledge that should be filled in the scope of this thesis, address the formulated specific aims, and summarize the findings in a comprehensive synthesis.

Chapter 2 provides the background for this work by introducing the field of cartilage TE and the current knowledge about cellular response to matrix elasticity in the broader field of skeletal TE.

In **Chapter 3**, a 2D hydrogel system is adapted in which PA gels with different elasticities are modified with collagen type I to provide adhesion. This system is then applied to study chondrocyte response to matrix elasticity in 2D monolayer culture.

Chapter 4 investigates the suitability of porous silk scaffolds with different pore sizes as a 3D model system to study chondrocyte response to matrix elasticity. Porous silk scaffolds are produced through the application of differently sized porogens. The scaffolds are characterized with respect to pore size and mechanical properties and cultured with chondrocytes. The resulting TE constructs are then analyzed.

In **Chapter 5**, knowledge from **Chapter 4** is taken into account to develop a hydrogel system that provides an improved, well-defined environment to study chondrocyte stiffness sensing in 3D. Agarose-hydrogels with tunable elasticity

are, hereby, modified with the adhesion sequence RGD to enable active probing of the stiffness by the cells. Chondrocytes are then incorporated into modified hydrogels with different elasticities to study cellular response to matrix elasticity in 3D.

Finally, the 3D hydrogel system is applied to study the differential effects of adhesion site density and matrix elasticity on the redifferentiation process of expanded chondrocytes.

The thesis is concluded by **Chapter 6** presenting a comprehensive synthesis of the thesis, including the established 2D and 3D model system, cellular response to matrix elasticity observed in the different systems, the limitations of the studies and possible future work.

2 Background

2.1 Rationale for cartilage tissue engineering (TE)

2.1.1 Cartilage

Cartilage is a specialized soft tissue that is found in different parts of the body as, for instance, ear, nose or ribcages. Articular cartilage covers the surface of diarthroidal joints and fulfils essential mechanical functions as load bearing and shock absorption and provides a smooth surface for frictionless joint movements [14].

Cartilage is an avascular and alymphatic tissue that is mainly composed of a dense mesh of highly hydrated ECM (extracellular matrix). It contains only a single cell type, the chondrocyte, which is sparsely distributed in the ECM and obtains its nutrient supply through convective diffusion [1]. In joints, the tissue is organized into three zones with distinct ECM composition and organization and chondrocytes in the zones differ in proliferation rate and biosynthesis.

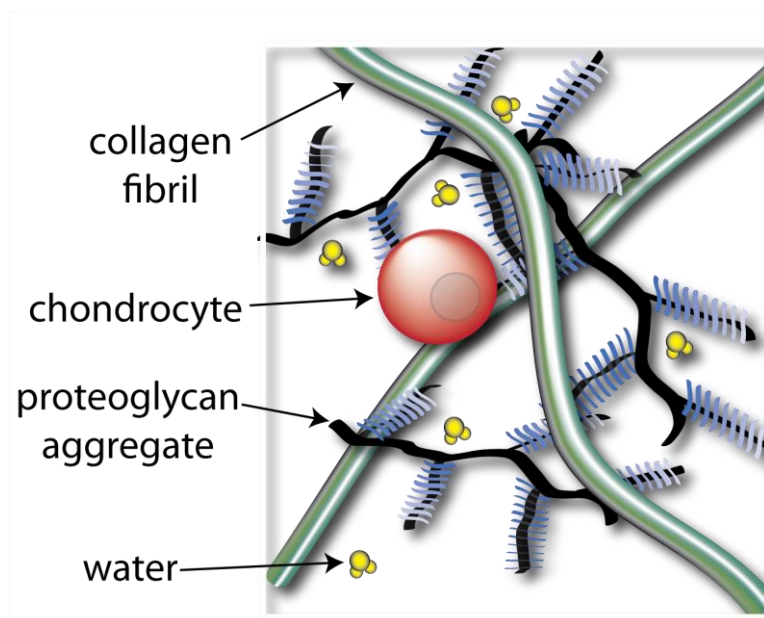


Figure 2.1: Major constituents of cartilage. Chondrocytes are embedded in a matrix composed of hydrated proteoglycans and a constraining network of collagen fibrils.

Chondrocytes surround themselves with a territorial, pericellular matrix (PCM), thought to be mainly responsible for mechanotransduction, and an inter-territorial matrix providing mechanical strength to the bulk material [15]. The main constituents of the matrix are collagens, predominantly type II, and proteoglycans, mainly aggrecan (Figure 2.1). Proteoglycans consist of a core protein and glycosaminoglycan (GAG) chains attached to it and can form large aggregates with the help of linker proteins. They are highly hydrated due to their negative charge and, with that, provide the compressive strength of cartilage [16]. Collagens organize into triple-helical structures and have the ability to form a fibrillar network [17]. The collagenous network constrains the swollen proteoglycan component and provides the tensile and shear properties of cartilage. The interplay of the different ECM components and the fluid, water phase provides cartilage with the ability to withstand very high compressive loads and the associated compressive and shear stresses [14].

2.1.2 Cartilage damage and current clinical solutions

Cartilage has very limited ability for self repair due to the avascular nature of the tissue, the inability of mature chondrocytes to proliferate or change their biosynthesis, and the immobility of the cells. Even minor lesions can, therefore, pose a major problem and in a consequence disable joint movement and vastly restrict daily activities. Chondral injuries affect people of all ages but have different origins: lesions, due to acute trauma or repetitive micro-trauma, are the most frequent cause in younger people while degenerative joint diseases, as osteoarthritis, are the most common cause in older people [18]. 250,000 knee and hip replacements are performed each year, alone in the United States [19]. However, total joint replacements have a limited life span and should only be performed when all other treatments failed.

Several surgical treatments, aiming to relief pain and restore cartilage functionality have, therefore, been applied to avoid total or partial replacement of the knee joint. They can be divided into three categories: (1) symptomatic treatments, (2) procedures that facilitate access to the vascular system to initiate healing, and (3) tissue transplantation [20, 21].

The first category includes the debridement or lavage of cartilage [22] to minimize

mechanical problems as locking, catching, or crepitus, but provides only a temporary relief since repair is not stimulated [23].

The second category usually involves a penetration of the subchondral bone to allow all factors associated with the vascularization dependent healing process, most importantly mesenchymal stem cells (MSCs), to enter the damaged tissue. Different surgical methods are applied to achieve this, including microfracture, abrasion arthroplasty [24], Pridie drilling [25] and spongialization [26]. The outcome of these procedures is, however, highly variable and often leads to the development of fibrocartilage, with inferior mechanical properties and limited life-span, as compared to hyaline tissue [27].

To overcome the limitations of the above mentioned procedures, interest in the third category of cartilage repair, the formation or direct transplantation of tissue from autogenous or autologous sources, is constantly increasing. Transplantations of osteochondral plugs, taken from non-load bearing regions of the joint, are performed to facilitate integration of the cartilage through bone on bone healing. The application of mosaicplasties, where a collection of small osteochondral cylinders is assembled at the site of defect, was hereby shown to further improve the outcome of the transplantation, since the curvature of the articular surface could be reconstructed [28] (Figure 2.2 A).

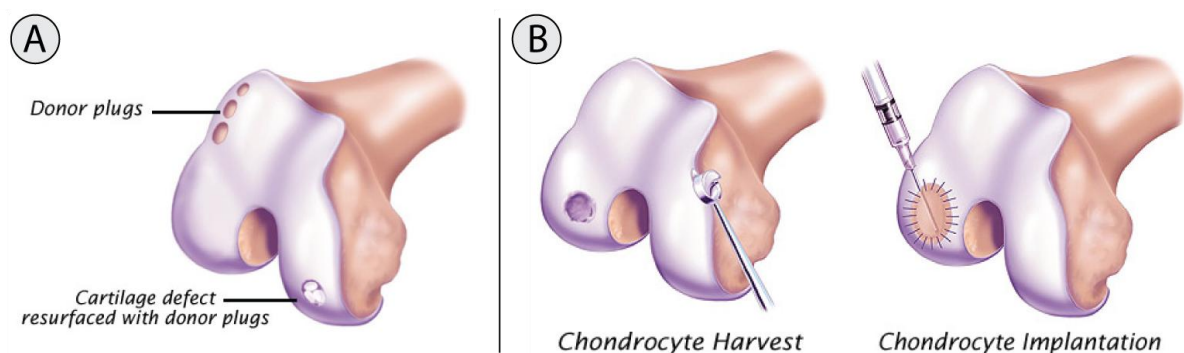


Figure 2.2: Cartilage repair: **A:** Application of osteochondral grafts to fill a defect. **B:** Autologous chondrocyte implantation. Chondrocytes are isolated from the patient, expanded, and introduced into the site of defect under a periosteal flap. Images reprinted with permission from <http://www.sosmed.org>.

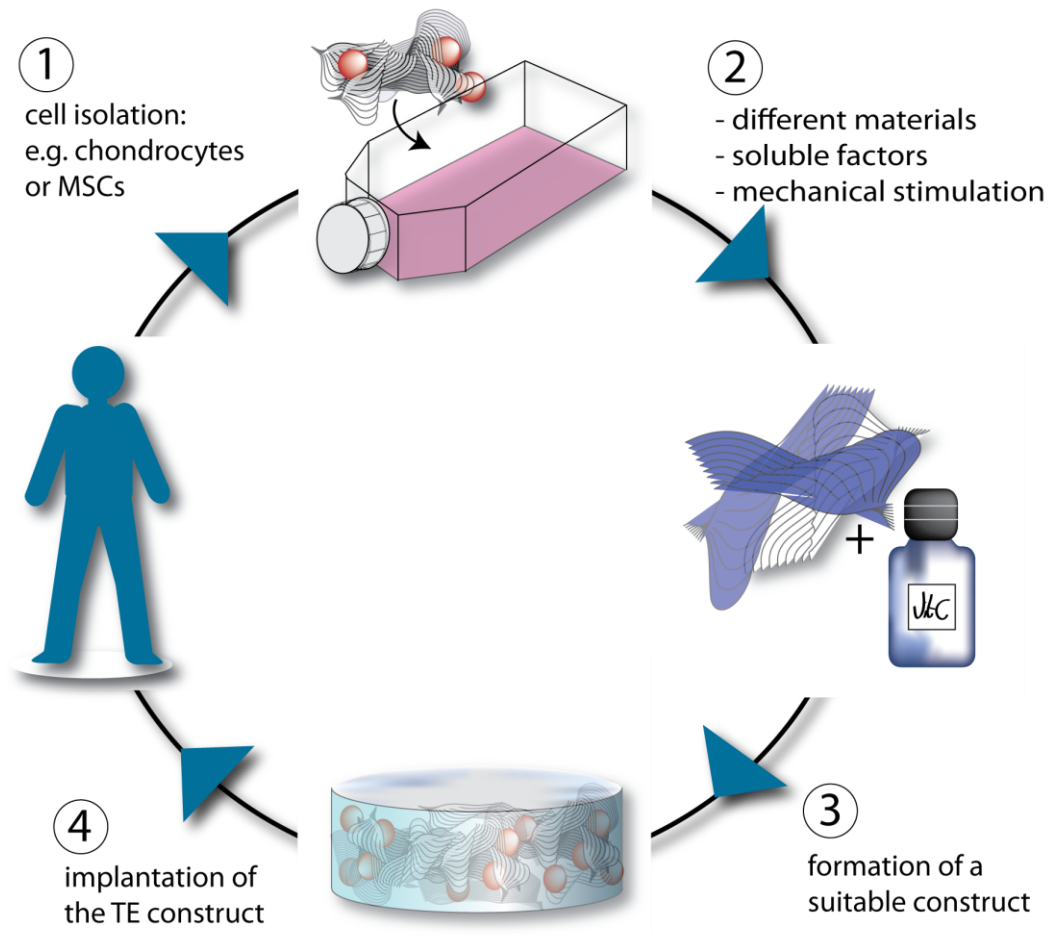


Figure 2.3: Cartilage TE: 1: Cells are isolated from the patient. 2: They are combined with different scaffold materials and can be further stimulated through soluble factors or mechanical stimulation. 3: This leads to the formation of a tissue substitute 4: that is then reimplanted into the patient.

The most commonly applied cell based therapy is autologous chondrocyte transplantation (ACI) where chondrocytes are isolated from the patient, expanded *in vitro*, and injected into the site of defect that is then closed with a periosteal flap [29] (Figure 2.2 B). While this method showed better clinical results than other procedures, especially in younger patients, it is still associated with certain complications, as chondrocyte leakage, detachment or hypertrophy of the periosteal graft [30] and the formation of fibrocartilage. As a consequence, much effort has been spent on tissue engineering based solutions and the development of new generations of cell-based repair techniques [29].

The evolving field of TE is a highly interdisciplinary field that combines knowledge from materials science, biology, medicine and engineering. It aims to find an optimal

combination of cells, materials, soluble factors, and mechanical stimuli to produce a biological substitute that can integrate and grow with the patient (Figure 2.3). Research conducted in the field of cartilage TE involves the combination of different cell sources and a variety of materials.

The optimal cell source for cartilage TE is still to be identified. Although fibroblasts [31, 32] and embryonic stem cells [33-36] show chondrogenic capacity as well, chondrocytes and mesenchymal stem cells (MSCs) seem to have the highest potential for cartilage TE, to date.

Chondrocytes have been widely applied as cell source for cartilage substitutes, as in ACI applications. Differentiated chondrocytes are characterized by a round morphology, produce collagen type II and proteoglycans and show a low proliferation rate. The main problem associated with chondrocytes as cell source is their limited availability. As mentioned above, cartilage is mainly composed of ECM and water. Chondrocytes account for only 5-10 % of the tissue [1] and have to be expanded before implant formation. During expansion in monolayer they change into a fibroblastoid phenotype in a process called dedifferentiation [37]. TE with these cells leads to the formation of fibrocartilage with inferior mechanical properties [9]. However, the dedifferentiation process can be reversed when cells are transferred into a suitable 3D environment [38].

MSCs have recently gained much interest as an alternative to autologous chondrocytes. Higher cell numbers can be obtained with a lower risk of donor site morbidity, since the cells can be isolated from different tissues of the patient, as bone marrow or adipose tissue [39, 40], and expanded in monolayer. Chondrogenesis of stem cells can be induced in 3D culture systems as pellet or micromass culture [41] or on different scaffold materials [42-44], and usually additionally requires media supplementation with soluble factors as TGF β [41]. While these cells are likely to play an increasingly important role in the future, TE cartilage with MSCs, so far, leads to constructs with inferior mechanical properties when compared with constructs formed with chondrocytes [45].

To immobilize and further instruct the cells for cartilage tissue formation, cells are combined with different supporting materials, so called scaffolds. These need to facilitate certain requirements for both *in vitro* tissue formation and implantation. Initially, easy cell

seeding procedures, maintained cell viability, proliferation and differentiation are crucial for tissue formation while in the long term, integration into the site of defect and controlled scaffold degradation are required to successfully substitute cartilage tissue.

A number of different materials have been used for the formation of suitable scaffolds. Natural materials include protein based polymers such as collagen [46, 47] or silk fibroin [44, 48] and carbohydrate based polymers such as agarose [49-51], alginate [52, 53], chitosan [54] or hyaluronic acid [55]. Common synthetic materials are, for instance, poly(vinyl) alcohol [56] and poly(ethylene) glycol (PEG) [57-59]. These materials have been processed in many different ways: they have been mixed for conjugate formation [60, 61], modified with bioactive peptides [57, 62, 63] and manufactured into different forms such as fibers, sponges and hydrogels [1].

Much of the research, aiming to find the optimal material and manufacturing process, has been performed on a trial and error basis. The physical properties of a substrate, such as porosity [64-67], nanotopology [68, 69] and elasticity [70] have been shown to influence attachment, migration, differentiation and nutrient diffusion in a scaffold. To facilitate the intentional design of scaffolds for TE applications, systematic studies are needed that investigate the influence of isolated material properties on cellular behavior.

This thesis investigates the role of matrix elasticity for cartilage TE. I hypothesized that chondrocytes sense the elasticity of the matrix and respond to it. To provide a context for this work, the following section will describe the current state of research about the principles of stiffness sensing and about the importance of matrix elasticity in the broader field of skeletal TE.

2.2 Matrix elasticity in skeletal TE

Interest in cellular response to the elasticity of a material emerged within the last few years as it became evident that this property plays a, so far underestimated, role not only for cell spreading and adhesion [71], but also for cellular proliferation and differentiation [7, 72]. Several 2D model systems have been developed to study the correlation of mechanical

properties and cellular behavior, and recently increasing effort has been made to transfer this knowledge into 3D systems.

One fundamental issue in this field of research seems to be that the mechanical cues sensed by a cell during *in vitro* culture and expansion often do not match *in vivo* conditions. Common cell culture dishes, for instance, are significantly stiffer than most environments a cell would be surrounded by in the human body [73]. These discrepancies seem to have a high impact on cellular behavior *in vitro*. In fact, many cell types show cell type specific behavior when cultured on substrates with stiffness, viscoelastic properties and strength that match the conditions they would sense in their *in vivo* environment [74]. Studies on cytoskeleton formation, proliferation and differentiation [75-77] consequently show that responses towards elasticity are highly cell type specific. To produce functional tissue in *in vitro* culture, matching intrinsic mechanical properties need to be identified and may then be adapted to the respective cell type, and stage of development.

2.2.1 Mechanisms responsible for stiffness sensing

While the exact mechanisms by which cells respond to the stiffness of the ECM are still not completely understood, several components involved, have been identified and new experimental evidence is constantly emerging. Simplified, the elasticity of a substrate is defined by the amount of force necessary to induce a certain substrate deformation. As cells seem to “sense” this property and then adapt their behavior to the degree of stiffness [78] a potential stiffness sensor needs to fulfill at least two requirements. It needs the ability to pull at the matrix to actively probe its stiffness and it needs to facilitate a transformation of the derived mechanical information into a biochemical signal to induce a response [7].

Cells can probe their microenvironment through actin-myosin contractility which can be measured as cellular prestress. Nonmuscle myosins have been implied to be involved in this process of actively probing the matrix as they have the ability to tension cortical actin structures. Evidence for this hypothesis comes from a study from Engler et al. [7] where expression of nonmuscle myosin II A-C was shown to be affected by changes in matrix stiffness. Inhibiting its function by blebbistatin treatment suppressed the cellular response

towards this matrix property. Recent studies further confirmed the essential role of myosin type II for the response to matrix mechanics [79] and experimental evidence from muscle cells also indicates a synergistic action of Rho-A, a small GTPase that enhances actin contractility, and matrix compliance in governing cellular behavior [80].

The force needed for active probing of the microenvironment needs to be transmitted to the ECM via a direct physical link. Integrins are extended across the cell membrane and provide a link between the matrix on the extracellular side and the actin cytoskeleton - associated with potential signaling molecules- on the intracellular side (reviewed in [81]). The application of forces to cytoskeleton-integrin-ECM connections leads to the maturation of focal adhesions (FAs) and organization of the cytoskeleton. Loss of force in return leads to the disassembly of FAs and stress fibers [82]. In the concrete context of stiffness sensing it was repeatedly shown that FAs grow from undetectable confuse

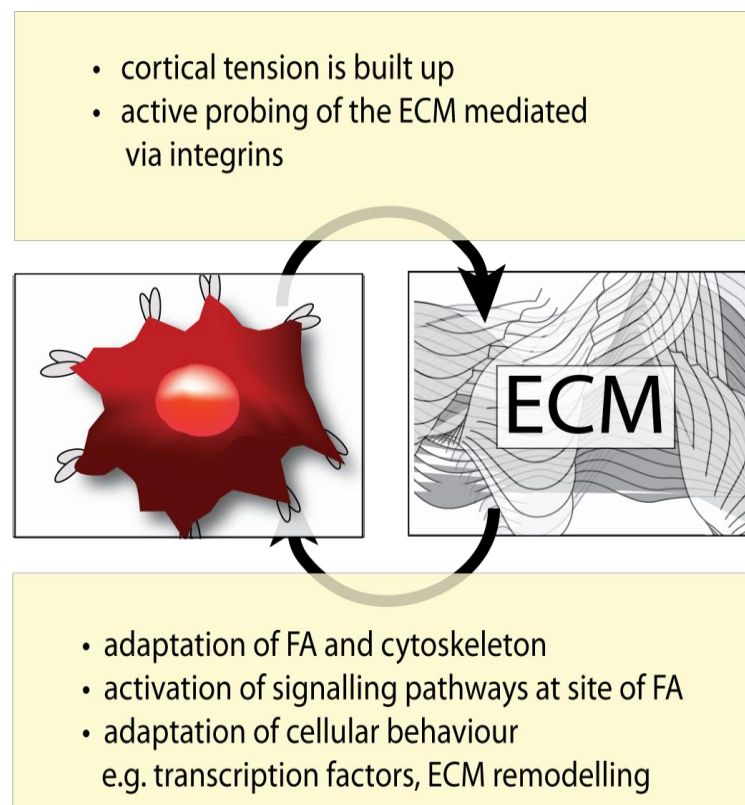


Figure 2.4: Principles of a possible mechanism of stiffness sensing. The cell actively probes its environment and adapts its behavior, via a FA and cytoskeleton mediated pathway.

contacts to well defined adhesions with increasing substrate stiffness [7, 71]. Thus, the mechanism of stiffness sensing seems to involve force transmission over FAs.

It has been hypothesized that components of the force signaling pathway must be located at the site of the cytoskeleton-integrin junction where the force is applied [82]. Friedland et al. very recently showed that the integrin $\alpha_5\beta_1$ switches between two different states in response to myosin II generated intracellular tension [79] and subsequently leads to the activation of FA kinase. This kinase is then involved in the activation of different downstream signaling cascades [83].

Possible mechanisms on how the sensor could work have been post including its direct stimulation through cytoskeletal stretch (that can for instance cause protein folding or unfolding) or indirect stimulation through binding to a deformed force sensor component of the integrin-cytoskeleton complex [82]. Talin, a protein that links integrins to the cytoskeleton was shown to also undergo a conformational change in response to the application of force. This change leads to the exposition of binding sites for vinculin, a protein that is involved in cytoskeletal reorganization.

The force balance paradigm states that integrins mediate a bidirectional force balance between the cell and its surrounding. It is based on mathematical models of tensegrity (for review see [84-86]) and implies that a change in matrix elasticity leads to a cytoskeletal adaption of the cell in order to compensate and re-establish the homeostatic balance. While the tensegrity hypotheses is still under discussion it has been clearly shown that cellular prestress increases with increasing matrix stiffness [87] and that a stiffer matrix also produces stiffer and increasingly tensed cells [7].

Taken together, all experimental evidence obtained so far hints towards a high importance of adhesion sites, actin cytoskeleton and integrin signaling in the cellular response towards matrix elasticity (Figure 2.4). Since all these factors are very different in a two-dimensional (2D) when compared to a three dimensional (3D) setting [88] it becomes evident that findings from 2D culture systems might not be easily transferable into a 3D environment. This stresses the need for validation in 3D settings. Several different 2D model systems for the analysis of stiffness sensing are evolving and recently much effort has been spend on bringing this research into the third dimension.

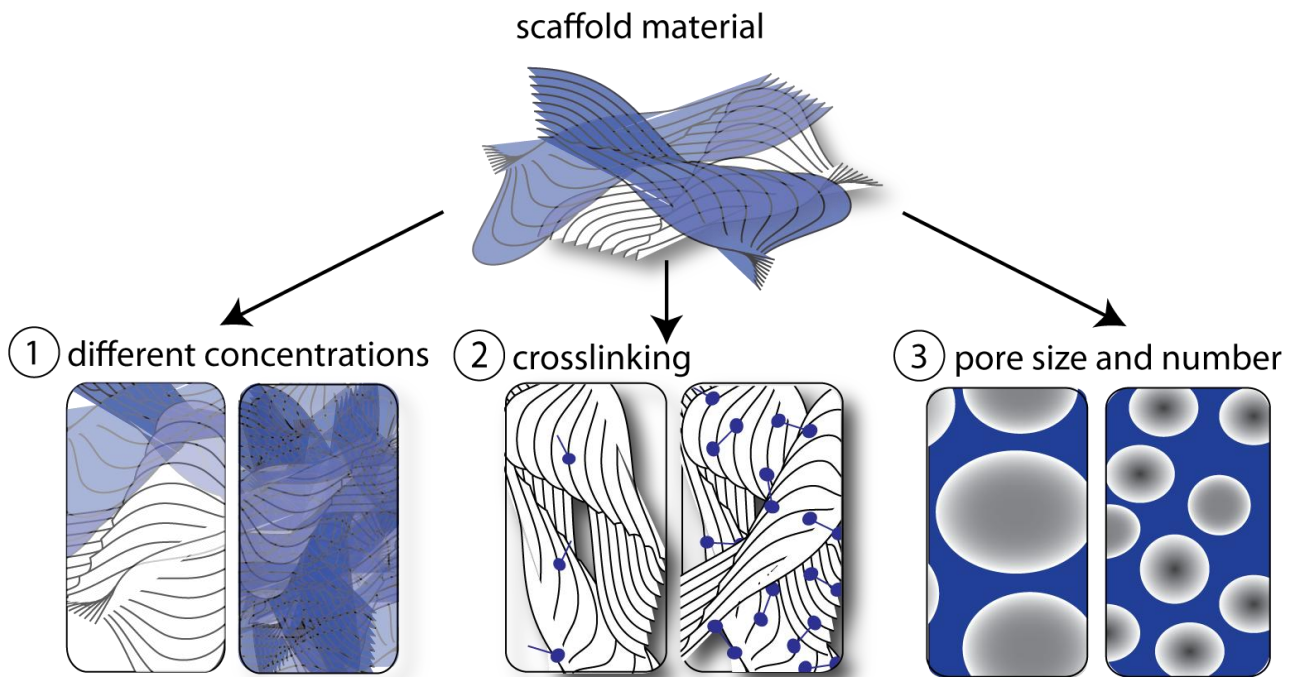


Figure 2.5: Altering the stiffness of a scaffold. Changes in stiffnesses can be achieved through differently processing the original scaffold material: 1) Different concentrations of the original material can be applied. 2) The material can be physically or chemically crosslinked and 3) the bulk elasticity of porous scaffolds can be altered by varying the size and amount of pores.

2.2.2 Model systems for the investigation of matrix elasticity

Requirements and limitations of a tunable substrate

The stiffness of a substrate can be altered in different ways. Matrices with different elasticities can be produced by altering the concentration of a material, differently crosslinking a material, or, in porous substrates altering pore number or size (Figure 2.5).

To study the influence of substrate mechanics, an ideal system should fulfill several criteria: (1) The material should facilitate cellular attachment as cellular stiffness sensing seems to be mediated via FAs. (2) The mechanical properties should be stable and reproducible (3) Matrix elasticity should ideally be altered independently of all other material properties to truly contribute effects to the substrate mechanics.

Obviously, the ideal system able to clearly fulfill all these requirements is hardly achievable. The last requirement, a segregation of substrate mechanics from all other

material properties, is probably the most challenging one.

Procedures that lead to an alteration in the Young's modulus of the substrate are always likely to also change other material properties. These properties, in turn, might account for a good part of the changes that are observed in cellular behavior.

Which properties are affected depends on the material and the method by which the elastic modulus is altered. The availability of adhesion sites as well as the microstructure and nutrient diffusion rate are likely to be affected by many methods applied to change the elastic modulus. To judge the influence of elasticity changes, possible contributions of these factors need to be considered as well.

Adhesion peptide density

Especially in protein based matrices where an increase in stiffness may be achieved by elevating the overall protein concentration, a higher elastic modulus is often accompanied by a higher density of adhesion sites. Assuming that actin contractility is a central part of the stiffness sensing mechanism an alteration in adhesion site density might be an important problem. Besides a change in stiffness, actin contractility can also be directly influenced by changing the number of interactions with the substrate, thus, by changing the number of adhesion sites (Figure 2.6). An increase in adhesion site density was indeed shown to affect cytoskeleton organization [89], migration [90, 91], and differentiation [92] as shown in studies in which ligand density and substrate stiffness were altered independently.

Studies with MSCs cultured in agarose modified with RGD showed that binding to this sequence promotes MSC spreading in a density dependent manner. A higher RGD density increased cytoskeletal organization and decreased the GAG deposition of cells cultured in chondrogenic medium. Expression of osteogenic marker proteins, in contrast, was enhanced [93]. Smooth muscle cells (SMCs) cultured in RGD-modified PEG-hydrogels respond similarly. SMCs spread to a significantly higher degree on hydrogels with high ligand densities and increasing the RGD-density increased the relative area of FAs [93]. Test systems should therefore ideally provide the possibility to separately alter the mechanical properties and the ligand density of the material to clearly contribute

observed effects to either of them. The material could ideally also facilitate the coupling of different ECM ligands since the type of ligand bound is very likely to also influence cellular behavior [94, 95].

Microstructure and pore size

When changing the mechanics of a substrate, not only adhesion sites but also the texture of the materials surface can be subject to change. This can have an impact on cellular behavior as well. PEG chain length for instance was shown to influence differentiation and cytoskeleton organization of chondrocytes [96]. The microstructure might also influence cellular shape and this, in turn, can influence cellular growth, proliferation [97] and differentiation [98]. When MSCs were cultured on micropatterned substrates in mixed media containing adipogenic and osteogenic differentiation factors, fibronectin islands that supported a round shape induced adipogenesis while islands that promoted a spread shape induced osteogenesis [98]. An additional structural factor that is likely to be

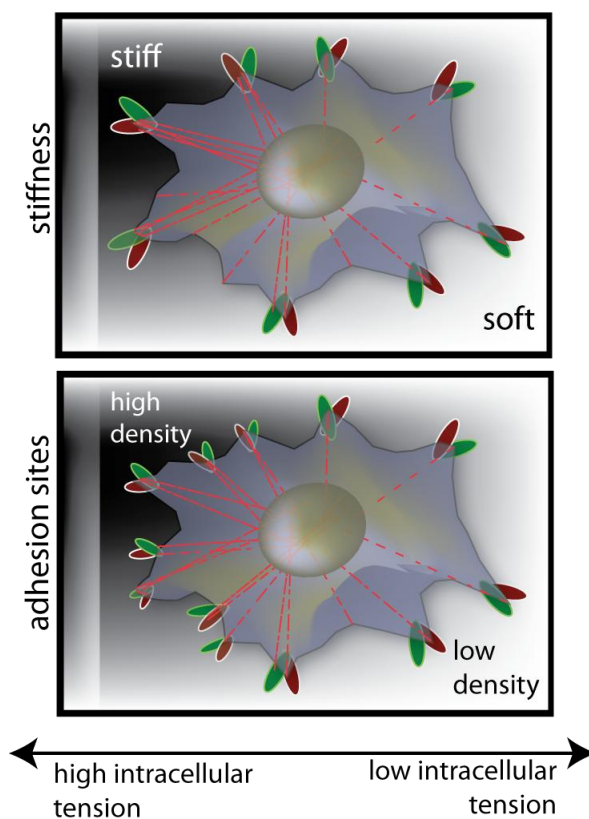


Figure 2.6: Intracellular tension.

Both, an increase in stiffness or in adhesion sites density increases the intracellular tension and cellular spreading.

affected by methods to change the stiffness is the pore size of a material.

The average pore size of hydrogels, as well as its change related to increases in stiffness, is very material specific. PEG hydrogels as one example have been shown to have a very small pore size. Altering their stiffness from 34 to 1370 kPa therefore only increased the pore size from 40 to 140 Å [3]. This small size can be an advantage as the change is still in the range of Å in comparison to hydrogels from other materials such as silk [99] where pore size can vary in the range of nm when stiffness is altered. Recent experiments with PEG fibrinogen hydrogels, on the other hand, showed that cellular viability was only marginal in hydrogels of about 300 kPa due to the small pore size [70].

When porous systems are used, pore size changes in the range of hundreds of μm when stiffness is changed [10, 11, 100, 101]. Large differences in pore sizes might influence various factors governing cellular behavior. Bigger pore sizes, as well as a higher porosity, for instance enhance diffusion of serum factors and nutrients into the hydrogel [102-104]. Increased diffusion and possibly adsorption of serum factors can enhance cellular binding, and the increased availability of nutrients and serum factors may affect cellular metabolism and catabolism [58, 105]. Additionally, pore size can influence cellular ingrowth [67] and migration [106], determine the size of cell aggregates in the matrix [107] and even influence cellular differentiation [64, 108] and matrix production [3].

While it is hardly possible to totally avoid structural changes when altering the elastic modulus, it should be kept in mind that they might have an influence on the experimental outcome as well. A good model system should minimize effects from alteration of other material properties or alternatively provide control systems to segregate different effects from each other.

2.2.3 Model systems

The following section will discuss materials that have been used to study the influence of the matrix stiffness on cellular behavior. All systems have certain advantages and disadvantages and try to overcome the above mentioned limitations.

Porous systems

Porous scaffolds with different stiffnesses can be produced through the application of different cross-linking methods [65, 100], different pore sizes [10, 11] and different porosities [109, 110]. Porous scaffolds from various synthetic and natural materials have been produced. Lee et al. [100] produced porous collagen-GAG scaffolds with compressive elastic moduli ranging from 145 to 1117 Pa by applying different chemical and physical crosslinking methods. The compressive modulus of silk scaffolds was shown to increase with decreasing pore size [10, 11] and a higher porosity of scaffolds is correlated with a decrease in stiffness [101, 109, 110]. However pore size and porosity have a high impact on cellular behavior (as described above) and crosslinking has been shown to also reduce the pore size and alter the morphology of cross-linked fibers [111].

Protein gels

Protein based ECM gels with varying stiffnesses can, for instance, be produced by physically or chemically crosslinking different concentrations of the respective protein. The elastic shear modulus of the gels is thereby estimated as proportional to the square root of protein concentration [112]. One major drawback of this approach is that an increase in protein concentration is not only accompanied by changes in the stiffness of the gels but also inevitably alters the surface texture such as fiber thickness and density and the number of available adhesion sites [74]. Semler et al. [113] used glutaraldehyde to produce matrices with different compliance from constant protein concentrations in order to partly circumvent these limitations: The group applied basal and crosslinked matrigel to study differentiation and growth behavior of hepatocytes on protein gels with different mechanical properties. A different approach was applied by Wang et al. [114] for his work with Madin-Darby canine kidney cells. To investigate whether cells responded to the elastic modulus of collagen and matrigel gels rather than to the increase in available adhesion sites, the group additionally used a control system where thin layers of the proteins were layered on top of agarose and plastic culture dishes, mimicking substrates with different mechanical properties. In order to examine the influence of mechanical properties in the nanoscale range without altering integrin recognition and topography, hydrated and dehydrated collagen fibrils have also been applied [115].

Inert natural matrices

As mentioned earlier matrix stiffness, often measured as Young's modulus, should be altered independently of other substrate properties in an optimal system. A material that does not directly interact with the cells might be applied to achieve this. Among others, the polysaccharides alginate and agarose and the GAG hyaluronic acid have been used to produce hydrogels with different elastic moduli [116, 117] and all of these materials can theoretically be modified with adhesion sites [92, 118, 119]. Only alginate has, so far, been applied as a model system to study cellular response to substrate mechanics.

Alginate is a linear polysaccharide copolymer of (1-4)-linked β -D-mannuronid acid (M) and α -L-guluronic acid (G) which is derived from sea algae. The M and G monomers are distributed in repeating or alternating blocks and the amount and distribution of the monomers is variable depending on the species, age and location of the seaweed [120]. The resulting batch to batch differences might be one disadvantage of alginate as a model system, making it necessary to test the hydrogels properties whenever a new batch is used. It has also been criticized that the purity of commercially available alginate is often not sufficient and may affect cellular behavior and induce immunological reactions [121]. The material is usually ionically crosslinked with the help of divalent cations (Ca^{2+} , Ba^{2+} , Mg^{2+}) but gels can also be formed by covalent crosslinking, for instance with the help of the crosslinker adipic acid hydrazide (AAD) [122].

The elastic modulus of the alginate gels is determined by the alginate concentration, the crosslinker type and concentration, and the ratio and length of M and G blocks. Stiffness of the resulting gel increases with an increase in alginate and crosslinker concentration and a decrease in M/G ratio. Different hydrogels with elastic moduli ranging from 12 kPa to 150 kPa have been produced by varying these parameters [123, 124].

Another drawback of the material can be its mechanical stability: it has been shown that ionically crosslinked alginate gels undergo slow, uncontrolled dissolution through exchange of calcium ions. This results in the loss of stiffness over time: LeRoux et al. [125] investigated the mechanical properties of alginate gels in a NaCl-CaCl_2 bath representative of the ionic environment in *in vitro* cell culture and found that the compressive modulus of the gels decreased by 63% after only 15 h in the bath. One

approach to overcome this limitation is the production of covalently crosslinked alginate gels. Covalently crosslinked gels with different elastic moduli have also been produced by increasing the concentration of the cross-linker adipic acid hydrazide at a given M/G ratio [122].

To facilitate cellular attachment, the gel can be modified with adhesion motifs such as RGD [124]. Cells suspended in the gel do not directly adhere to the polysaccharide and proteins are not readily absorbed due its hydrophilic character. This makes a segregation of material mechanics and cellular adhesion possible. Modified alginate has been used to study the influence of matrix mechanics on stem cells, preosteoblastic cells [126] and chondrocytes [124].

Synthetic matrices - 2D

Hydrogels made from synthetic polymers are an attractive alternative materials for TE applications as their chemical and mechanical properties are well defined and reproducible [120]. Different systems, suitable for the investigation of elasticity effects, have been developed, some of them valuable for 3D applications, some limited to applications in 2D systems.

Silicone membranes are a model system to study the influence of substrate elasticity and also determine the force exerted by a cell to probe its surrounding in a 2D environment. A silicone membrane can be crosslinked by passing it through a Bunsen flame. Silicone substrates with different degrees of mechanical resistance were produced by modulating the flaming time. One disadvantage is that, to quantify resistance, each substrate has to be tested separately with calibrated microneedles. Visualization of the degree of substrate wrinkling together with a given resistance of the substrate provides information about the force created by the cell. This system has been used to study contractile forces exhibited by myofibroblasts [127, 128].

Polyacrylamide (PA) gels are another, very widely used, system for cell studies in a 2D setting. They can be coated with different adhesion molecules and the elastic modulus of the gels can be tuned by altering the linker concentration of the bis-acrylamide while keeping the total polymer concentration constant [129]. Adhesion proteins like collagen

and fibronectin can be covalently bound to the gel with the help of a heterobifunctional crosslinker. Due to the antiadhesive surface of PA gels no serum proteins and cell receptors can bind directly to the surface [6]. The number of adhesive molecules is independent of the substrate stiffness and can be controlled by coupling different concentrations of adhesive molecules to the gel [129]. Thus, it is possible to alter the substrate stiffness by an order of magnitude while leaving the other properties of the substrate constant. This system has been applied to investigate cytoskeleton formation, proliferation and differentiation behavior in studies that involve fibroblasts, endothelial cells, neutrophils [75], neuronal cells [77], myoblasts [6] and MSCs [76]. The main drawback of PA gels is the neurotoxicity of unpolymerized acrylamide, that impairs incorporation of cells into the gel [70], rendering it unsuitable as 3D-culture system.

Synthetic matrices - 3D

PEG is a synthetic bioinert polymer that can not only be used in 2D but also in 3D systems. To encapsulate cells in this material it can be crosslinked by introducing acrylates or methacrylates at each end of the polymer. Addition of a UV initiator to PEG acrylate and PEG methacrylate derivatives and short exposure to long wave UV-irradiation then leads to photopolymerization of the material. Other methods for cell encapsulation include enzymatic crosslinking of a precursor solution in the presence of cells [130] and the application of PEG-dithiol monomers [131].

The mechanical properties of the hydrogel are determined by the derivative concentration, the structure of the PEG monomers and the crosslinking density. Differently concentrated macromer solutions from 10% to 30% could, for instance, produce hydrogels with moduli from 30 kPa to 960 kPa [57] [3]. Different structures of PEG macromers have also been shown to significantly affect the mechanical properties of the hydrogel. The modulus was shown to increase with higher PEG chain length [132] and an increased number of PEG arms in star shaped PEG derivatives [131]. The crosslinking density of photopolymerizable hydrogels can for instance be changed by mixing different amounts of PEG diacrylate (PEGDA) with non-acrylated PEG [93, 133]. Due to the bioinert properties, PEG can serve as a blank that can be altered in many ways to obtain the desired functionality. Different cell adhesion motifs have been incorporated

onto the polymer backbone to mediate attachment to the hydrogel surface [93] and degradability has been altered, for instance, by the introduction of enzyme cleavage sites [134]. PEG hydrogels have been used as 2D and 3D systems together with many different cell types [57, 93, 133, 135-137].

Other synthetic materials as poly(vinyl alcohol) have also tunable mechanical properties and can be modified to provide adhesion [120] but have not been applied as model systems so far.

2.2.4 Cellular response to matrix elasticity

The following section will focus on research relevant for tissue engineering in the musculoskeletal system. Findings that might be of importance for the development of functional tissue from stem cells, progenitor cells or primary cells will be discussed with a focus on how elasticity influences on cellular differentiation and matrix formation. For additional information please refer to reviews from [74] and [70].

Bone

Studies about the influence of mechanical stimuli on bone formation have so far been mainly focused on external mechanical stimulation, such as the application of fluid and shear stress [138]. The general susceptibility of these cells towards mechanical stimuli, however, indicates the potential responsiveness towards the elastic modulus as an intrinsic mechanical property of the scaffold.

One possibility to generate bone-like-tissue from autologous cells is the isolation, expansion and osteogenic differentiation of MSCs. The microenvironment seems to play an important role in governing cell lineage specification, in this context with extreme sensitivity of the cells towards tissue-like elasticity: Engler et al. showed that, even without the addition of additional external factors, MSCs developed an osteogenic morphology when cultured on PA gels with a stiffness similar to the one of osteoid (25 to 40 kPa), the crosslinked collagen precursor of bone. Specification into an osteogenic lineage was further confirmed by ribonucleic acid (RNA) profiles of osteogenic markers,

immunostaining of osteogenic cytoskeletal marker proteins, and of transcriptional factors. The influence of the appropriate matrix elasticity on the expression of osteogenic marker proteins was even more pronounced than that produced by the application of osteogenic induction medium. Combining osteogenic induction medium and the right substrate compliance led to the highest level of osteogenic markers, indicating a synergistic action of ECM mechanics and soluble factors [7]. It also needs to be emphasized in this context that after several weeks in culture, on substrates with the respective elasticity, cells committed to the phenotype specified by the matrix compliance and could not be reprogrammed by soluble factors. This implies that it is not only possible to positively influence cellular differentiation with the right matrix compliance, but that the choice of the wrong compliance could also vastly limit the differentiation capacity of stem cells. However, there are no studies about the relevance of these results in a 3D environment. Hsiong et al. [126], furthermore, recently questioned these results and suggested that a predifferentiation of cells is necessary to facilitate a response to differences in matrix elasticity. The group used differently crosslinked alginate hydrogels to study the importance of the differentiation stage on cellular responsiveness towards matrix elasticity. They investigated matrix elasticity dependent changes in the proliferation rate as a measure for cellular responsiveness. Proliferation of a clonally derived stem cell line (D1), preosteoblasts (MC3T3-E1), and MSCs, cultured on alginate substrates with different stiffnesses were compared. The proliferation rate of MC3T3-E1 cells increased with increasing substrate stiffness, while proliferation of uncommitted D1 cells was not influenced by elasticity changes. Predifferentiation of the same cell line into osteogenic progenitor cells clearly increased their responsiveness to this matrix cue. The proliferation rate of MSCs also increased with increasing substrate stiffness with a magnitude intermediate to that of MC3T3-E1 cells and uncommitted D1 cells [126]. The authors, therefore, suggest that a predifferentiation of cells might be necessary in order to facilitate response to matrix mechanics. Nevertheless, the experimental setup might not be sufficient to link the differentiation stage to the changes in responsiveness, since the use of a particular cell line might be associated with some restrictions, and only osteogenic predifferentiation was analyzed. Additionally, no investigation of matrix production was performed which would be crucial for successful bone tissue formation.

Some general concerns remain regarding the investigation of elasticity sensing in primary stem cells since each isolation might also contain minorities of different other cell types. Therefore, it is important to note that in the case of primary MSCs, it is hardly possible to discriminate, whether the change in elasticity causes a commitment of the stem cells, or a selection and enhanced proliferation of specific progenitor cells already present in the isolation.

Not only proliferation but also differentiation of preosteoblastic cells seems to be influenced by matrix compliance: In a first study, Khatiwalla et al. cultured MC3T3-E1 cells on collagen type I coated PA gels with different elastic moduli (11.78 kPa, 21.6 kPa and 38.98 kPa) using polystyrene as the stiffest substrate. Stiffer substrates led to an increase in the assembly of actin stress fibers, and FAs, and higher proliferation rates of the cells [139]. Additionally, mineralization increased with increasing substrate stiffness with the highest degree of mineralization found on the polystyrene substrates, when cultured in the presence of osteogenic supplements.

These results were confirmed with the help of RGD-modified PEG-hydrogels. Cells cultured on stiff PEG hydrogels (423,9 kPa) or rigid tissue culture polystyrene showed increased alkaline phosphatase (ALP) levels, osteocalcin and bone sialoprotein expression, when compared to cells grown on softer PEG gels (13.7kPa) [133]. This response to ECM elasticity seems to be mediated through a mitogen-activated protein kinase (MAPK) dependent pathway. MAPK expression was significantly higher on stiffer substrates and inhibiting its activity pharmacologically with PD98059 led to a decrease of ALP, osteocalcin and bone sialoprotein gene expression [140].

Combined, these findings indicate a supportive role of stiff substrates during osteogenic maturation in 2D culture systems, in a MAPK dependent manner. It has to be also noted, in this context, that the specific elastic modulus that enhanced osteogenic differentiation was different for MSCs and MC3T3-E1. While MSCs only specified into the osteogenic lineage upon culture on substrates of ~ 40 kPa, and not on stiffer substrates or glass, osteogenic maturation of preosteoblastic cells was enhanced on very stiff substrates and polystyrene. Whether these differences have a physiological background such as, for instance, the change of elasticity the cell experiences during bone calcification [141], or if

they are derived from different experimental setups, remains unclear.

All of these results also still lack a confirmation in 3D settings to show their relevance for tissue engineering applications. The finding that osteoblasts contract hydrated collagen to half of its size within 24h [142] might hint towards a preference for a dense, and therefore stiff, microenvironment. Buxton et al. [4] just recently applied compressed, and thus dense, collagen type I to investigate whether the dense material, with a stiffness mimicking the one of osteoid, can facilitate the maturation of primary preosteoblasts. Cells cultured in the dense collagen matrices showed enhanced survival and differentiation, in comparison to hydrated collagen, indicating that the denser osteoid like matrix supports osteogenic differentiation.

One possible explanation for a positive effect of stiff matrices on osteogenesis might be the higher cytoskeletal tension built up on stiffer substrates. The important role of intracellular tension for osteogenesis was stressed in an experimental setting where cellular fate was determined by the shape the cell was allowed to adopt. Cells were cultured in mixed media containing both, adipogenic and osteogenic differentiation factors and on micropatterned substrates that allowed either a round or a spread shape. Cells that were allowed to spread underwent osteogenesis; those that were restricted to a round shape underwent adipogenesis. Increasing intracellular tension through constitutive expression of Rho A, however, induced osteogenic differentiation even when cells were restricted to the round shape. Agents that disrupted actin mediated contractility in turn inhibited osteogenesis [98]. Increasing the number of available adhesion sites, as another possibility to increase cellular spreading and intracellular tension, also significantly increased osteogenic differentiation of MSCs in a 3D environment as shown in RGD-modified PEG hydrogels [143]. Taken together, these findings might confirm a role of intracellular tension.

Muscle

ECM mechanics are likely to play an important role in the development of contractile cells, such as muscle cells, as the ability of myocytes to contract the underlying matrix depends on the stiffness of the matrix and the cells attached to it. Additionally, as many muscular disorders are associated with an abnormal compliance of the tissue, it has been

repeatedly hypothesized, that this mechanical property might be of high importance for the accurate differentiation of muscle cells.

Two different types of muscle are part of the musculoskeletal system: smooth muscles and striated muscles. One problem that arises during TE of smooth muscle is that SMCs undergo a transition from their differentiated, contractile phenotype into a synthetic phenotype upon expansion on rigid tissue culture plastic [144]. The synthetic phenotype is characterized by a fibroblast-like appearance, an increased proliferation rate, and enhanced collagen production. The cells lose their ability to contract, and excessive collagen production can lead to the formation of functionally limited scar tissue [80]. Matrix chemistry [145] and mechanical properties [93, 146] seem to vastly influence the phenotype of SMCs, rendering them valuable tools for inhibiting dedifferentiation of the contractile phenotype, in order to create functional tissue.

Different studies, indeed, indicate that myogenesis of MSCs [7], as well as the behavior of smooth and also skeletal muscle cells, is affected by this matrix property. SMCs were shown to adapt their cytoskeletal organization, morphology, and adhesion sites to the stiffness of collagen type I coated PA gels. They remained round with monomeric actin and without observable FAs on soft substrates, but showed a well spread morphology with typically well-ordered stress fibers and clearly observable FAs on stiffer substrates and rigid glass [90]. Differences in proliferation and spreading of aortic SMCs were also observed when cells were cultured on either hydrated or dehydrated collagen fibers, that appeared to be similar in topology, but not in their mechanical properties. SMCs seem to spread and proliferate extensively on dehydrated, and, therefore, stiffer collagen fibers, which contrasts their behavior on fully hydrated fibers [115].

Peyton et al. [93] applied functionalized PEG hydrogels to show that the increased cytoskeletal organization and higher proliferation rate is accompanied by a decrease in the expression of contractile markers, as shown by the extent of smooth muscle α -actin bundling, and the degree of calponin and caldesmon association with actin fibers. Taken together, these findings could be interpreted as a transition into the synthetic phenotype upon culture on stiffer substrate and a supportive effect of the compliant substrates (13.7 kPa) on the differentiated phenotype.

The influence of substrate mechanics, and a favorable influence of this elasticity range on the differentiated phenotype, could also be confirmed in an independent study with skeletal muscle cells [6]. Culturing C2C12 skeletal myoblasts on collagen strips attached to PA gels of varying elasticity, or glass, showed that striation of the cells is highly dependent on tissue-like substrate elasticity. In this study, the elastic modulus of myotubes was measured to be about 12 kPa. Growing cells on top of a layer of myotubes or on substrates with an elasticity equivalent to the myotube elasticity (~ 12 kPa), led to accurate cellular differentiation and striation [6]. Cells cultured on very soft or stiff substrates, in contrast, fused into myotubes, but they did not develop myosin/actin striations.

Matrix elasticity seems to be of equal importance during the early stages of myogenic differentiation. As mentioned earlier, osteogenesis could be induced by growing MSCs on PA substrates with elasticity comparable to the one of osteoid. Accordingly, culturing the MSCs on PA gels, mimicking the modulus of striated muscle (~ 8 - 17 kPa) induced differentiation into myogenic precursor cells even in the absence of soluble myogenic factors. This effect could not be reversed by the addition of soluble factors after 3 weeks of culture on the corresponding substrate. The highest expression of myogenic marker proteins was achieved with a combination of the right substrate elasticity and soluble myogenic factors [7].

Experiments in a 3D environment have so far mainly been performed in modified PEG hydrogels. As mentioned earlier, the range of elastic moduli that can be produced is very limited through the small pore size of these gels that impairs cellular spreading and vastly reduces viability in stiffer gels. Studies with matrix-metalloproteinase (MMP) degradable PEG hydrogels of varying stiffness showed that although MSCs and SMCs were viable in stiffer gels, cellular spreading and proliferation was only possible in very soft hydrogels with a high density of RGD adhesion. Nevertheless, culturing SMCs and MSCs in these soft hydrogels led to an upregulation of markers associated with a less synthetic SMC phenotype, when compared to cells cultured on cell culture plastic [146].

In a similar setting, with SMCs incorporated in RGD-modified PEG hydrogels with compressive moduli of ~ 86 kPa and ~ 386.5 kPa cells expressed low levels of contractile markers but viability was only marginal, and cellular spreading not observable under any

of the conditions [93].

In a subsequent study less dense PEG-conjugated fibrinogen based hydrogels with a much softer range of ~ 0.5 kPa to ~ 5 kPa were investigated [80]. Viability was significantly higher than in RGD-modified PEG hydrogels and a relatively small influence of substrate mechanics on cellular spreading and F-actin bundling could be observed after prolonged culture of the cells. However, in contrast to findings from experiments in 2D, cells were not significantly spread in soft or stiff hydrogels after 24 hours, and vinculin expression and assembly into focal adhesions was not seen under any of the 3D conditions. Increasing intracellular tension by constitutively overexpressing the active form of Rho A increased the sensitivity to substrate mechanics in this 3D system: Vinculin expression levels increased with increasing substrate stiffness, and a possible transition from a synthetic to a contractile phenotype was observed. Overexpression of Rho A alone was enough to increase the expression of markers of a contractile phenotype (α -actin and calmodulin) and to reduce cellular proliferation in all hydrogels. Increasing the stiffness of the substrate additionally led to a significant increase in the expression of α -actin and calmodulin. A possible explanation for the necessity of Rho A overexpression to induce a response to matrix compliance could be the restriction to a significantly softer range of elastic moduli than applied in 2D. The induction of an additional increase in intracellular tension through the overexpression of Rho A, might then enable the formation of stress fibers, and focal adhesions necessary for a cellular response towards matrix compliance. Taken together, the myogenic phenotype seems to be supported by muscle-like elasticity in 2D culture systems. However, so far, these findings could not be directly transferred into 3D culture systems.

Cartilage

As described in the first section of this chapter, cartilage substitutes can be formed with the help of MSCs or chondrocytes. Only few studies about chondrocyte stiffness sensing exist and most of them are restricted to 2D culture systems.

Genes et al. crosslinked RGD modified alginate with different concentrations of CaCl_2 and BaCl_2 in order to produce gels with different degrees of stiffness [124]. They found that chondrocytes, cultured on alginate discs with higher stiffness, showed an increased

attachment rate, a flattened morphology, and enhanced actin organization, when compared to chondrocytes cultured on softer substrates. Culture of canine chondrocytes, on chitosan crosslinked with different concentrations of a functional diepoxide (1,4-butanediol diglycidyl ether) to obtain compressive moduli from 3.8 to 19.9 kPa confirmed an increased spreading and proliferation on stiff substrates [147].

Investigation of the influence of matrix elasticity on chondrogenic differentiation and ECM production in 3D systems has not been very comprehensive so far. Chondrocyte culture in tunable hydrogels has so far been limited to hydrogels, in which adhesion was not enabled. Two studies with differently crosslinked PEG hydrogels hereby showed that the crosslinking density has an effect on chondrocyte matrix deposition with a more homogeneous distribution and higher amounts of collagen type II in loosely crosslinked gels [3, 131]. Both approaches did not involve the incorporation of any adhesion sites into the material. As PEG is an inert material, this implies that the observed differences were not caused by adhesion-mediated elasticity sensing.

Studies with porous collagen GAG scaffolds revealed that chondrocytes express the gene for the contractile protein α -smooth-muscle actin. They were shown to actively pull at the scaffold and even contract it to a visible extent. Loosely crosslinked sponges that could be contracted by the cells led to higher cell densities and collagen type II densities, when compared to tightly crosslinked scaffolds [65]. Although these findings could be interpreted as elasticity effects, homogeneity and the segregation of substrate mechanics and adhesion sites is not given in protein sponges. This makes a contribution of the observed effects to elasticity sensing difficult [65]. Although first indications for an influence of substrate mechanics on chondrocyte behavior can be found, comprehensive studies about the influence of this property on the chondrogenic phenotype are still lacking.

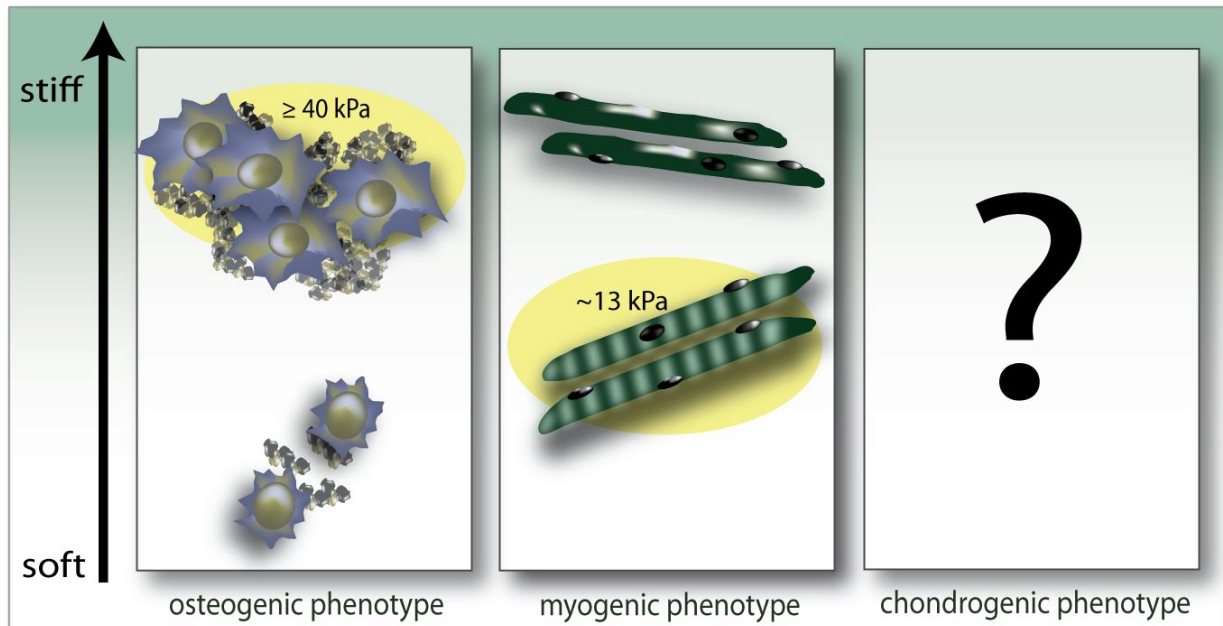


Figure 2.7: Response to substrate stiffness of cells from the musculoskeletal system. Advantageous elasticities are highlighted in yellow. Substrate stiffness that supports the differentiated phenotype differs between the cell types. The osteogenic phenotype is supported by stiff (≥ 40 kPa) substrates. The myogenic phenotype is supported by tissue like elasticity of about 13 kPa. The optimal stiffness for supporting the chondrogenic phenotype is not known.

2.2.5 Conclusions

Matrix elasticity plays an important role in the context of tissue engineering in the musculoskeletal system, in a very tissue specific way. Studies in 2D culture systems showed that stiffer substrates seem to promote the osteogenic phenotype while substrates with an elasticity of muscle tissue (~ 13 kPa) promote the myogenic phenotype. Studies on which elasticity supports the chondrogenic phenotype are still lacking (Figure 2.7). Most experimental evidence about cellular response to matrix elasticity is derived from 2D culture systems, thus, from systems where cells are cultured in monolayer on top of substrates with different elasticities. It is now of high importance to see how far experimental evidence from 2D systems can be transferred into a 3D environment to clearly assess the consequences for the generation of functional tissue from primary or precursor cells.

3 Chondrocyte response to matrix elasticity in 2D

3.1 Adaptation of a validated 2D PA system

3.1.1 Introduction

While interest in the investigation of the effect of substrate elasticity on cellular behavior is constantly increasing, the applicability of the different systems that can be used for this investigation is still under discussion. When changing the mechanics of a substrate, other properties such as pore size, permeability, and adhesion site density are likely to be affected as well. These changes might, in turn, contribute to the observed effects. One advantage of PA gels, produced according to the method described by Pelham and Wang [129], is that they have been widely applied, and have been very well characterized during numerous other studies that investigated the influence of matrix mechanics on cellular behavior [6, 71, 129, 148]. As it is a 2D culture system, pore size and permeability are not likely to influence cellular behavior, as cells are not incorporated into the material.

The elastic modulus can be tuned independently of adhesion sites by the controlled coupling of adhesion molecules to the polymerized gels [129], and due to the antiadhesive surface of PA gels, no serum proteins and cell receptors can bind directly to the surface [6].

To examine if I can produce substrates with different elasticities with this method, PA gels with different cross-linking densities were produced and their mechanical properties were determined.

3.1.2 Materials and Methods

Production of PA gels

PA gels with tunable elasticity were produced under sterile conditions according to a protocol published by Pelham and Wang [129]. Briefly, 50 μ l acrylamide/bis-acrylamide mixtures containing 10% acrylamide and 0.01% to 0.55% bis-acrylamide (both from Sigma, München, Germany) were polymerized on aminosilanized glass coverslips (45x50

mm rectangular, HASSA, Lübeck, Germany) using 1/250 volume of 10% ammonium persulfate and 1/500 volume of *N,N,N',N'*-tetramethyl-ethane-1,2-diamine (both Roth, Wiesbaden, Germany). Aminosiliconized coverslips were placed on the solution to produce a smooth gel surface; the coverslips were then removed after polymerization. Gels were briefly washed in 50 mM HEPES (Roth, Wiesbaden, Germany), placed in rectangular cell culture dishes (Nunc, Wiesbaden, Germany), and 300 μ l of 50 mM sulfosuccinimidyl 6 (4'-azido-2'-nitrophenyl-amino) hexanoate (sulfo-SANPAH; Pierce, Rockford USA) in 50 mM 2-[4-(2-hydroxyethyl)piperazin-1-yl]ethanesulfonic acid (HEPES) was layered on top. Dishes were placed under UV light (15 W and 312 nm) under a sterile bench at a distance of 10 cm for 8 minutes to activate the crosslinker.

The photoactivation procedure was repeated; gels were quickly washed with 50 mM HEPES, and incubated in a 0.2 mg/ml solution of collagen type I (BD Biosciences, Heidelberg, Germany) overnight at 4°C on a shaker. Matrices were washed and stored at 4°C in phosphate buffered saline (PBS) for up to three days.

Characterization of the PA gels

Twelve different compositions of PA gels with 10% acrylamide and 0.01% to 0.55% bis-acrylamide were produced.

To determine the Young's modulus of the gels, atomic force microscopy (MFP 3D, Asylum Research, Santa Barbara, CA, USA) was applied [149]. CSG-11 B cantilevers (NT-MDT, Moscow, Russia) were used for all experiments. The spring constants were determined using the thermal fluctuation method, leading to spring constants of about 60 mN/m. The diameters of the cantilever tips were determined by scanning a calibration sample (Nioprobe, Aurora NanoDevices Inc., Edmonton, AB, Canada). Assuming a spherical tip, the radius can be determined [150] as approximately 15 nm for the used cantilevers. Force maps with 15 x 15 points in an area of 10 x 10 μ m² were recorded with a pulling velocity of 1 μ m/s. The Young's modulus was determined for each curve using the Hertz model [151] of a paraboloid with a Poisson ratio of 0.34 [152]. The mean values and the standard deviation were calculated from the histograms of the respective values for the Young's modulus.

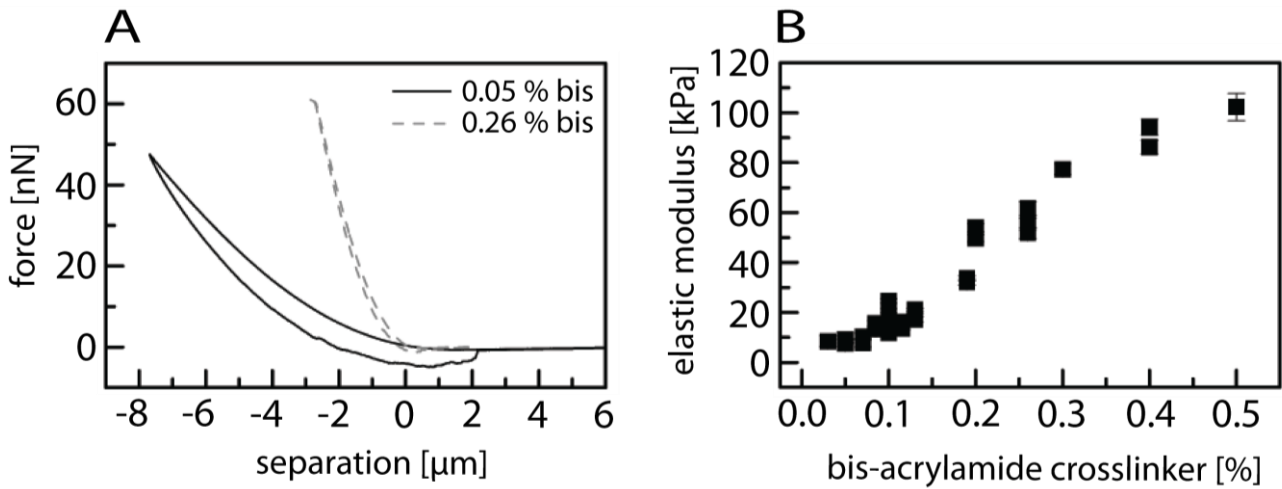


Figure 3.1: AFM measurements of PA-gels. A: Two representative force curves obtained from gels with 10% acrylamide and 0.05% or 0.26% bis-acrylamide-crosslinker. B: The elastic modulus of PA-gels with different amounts of bis-acrylamide crosslinker and a constant 10% of acrylamide.

3.1.3 Results

Collagen coated PA matrices were produced according to a previously published protocol [129] and the mechanical properties were determined by atomic force microscopy (AFM).

Gels with twelve bis-acrylamide concentrations between 0.01% and 0.5% were tested, while leaving the acrylamide (AA) concentration at a constant concentration of 10%. Figure 2.1 representatively shows two force curves (Figure 3.1A) and the values for the Young's modulus of the respective gels used in this study (Figure 3.1B). There was an almost linear correlation between the amount of bis-acrylamide in the gel and the Young's modulus with a slope of 200 ± 17 kPa/% bis and substrates with Young's moduli ranging from about 4 to 100 kPa could be produced.

3.1.4 Discussion

PA gels with Young's moduli of 4 to 100 kPa were produced by using different cross-linker concentrations. PA gels provide a well characterized model system to study cellular stiffness sensing in a 2D environment. Many different groups have repeatedly investigated

whether differences of collagen type I concentration and accessibility are observed on PA gels with different bis-acrylamide crosslinking densities. In theory, cross-linking density might affect ligand binding and maintenance on the gel. Additionally, a variation in gel porosity, due to different crosslinking densities, might also cause migration of adhesion proteins into the softer gels, thereby affecting accessibility of the ligand.

Pelham and Wang determined the relative amount of collagen type I with the use of collagen type I antibodies [71] to demonstrate that the amount of coupled ligand is not affected by differences in crosslinking densities. Other research groups showed independently that ligand accessibility is not influenced: Lo et al. applied secondary antibodies coupled to micron sized beads, much bigger than the pores of the gels. Binding of the secondary antibody to collagen type I antibody was not affected by the crosslinking density demonstrating that accessibility of the ligand is not influenced by the amount of bis-acrylamide in the gel [148]. Additionally, collagen type I antibodies were used to show that collagen type I concentration does not change with time in cell culture, neither on very soft, nor on very stiff substrates [129].

Since the response of different cell types to matrix elasticity has been studied using this system, it additionally allows a direct evaluation of differences and similarities in cellular response to matrix elasticity. The following section will apply this system to study chondrocyte response to matrix elasticity in 2D.

3.2 Chondrocyte response to matrix elasticity in 2D

3.2.1 Introduction

Studies on cytoskeleton formation, proliferation and differentiation that involve many different cell types, including fibroblasts, neutrophils [75], neuronal cells [77] and mesenchymal stem cells [76], showed that cellular response towards differences in elasticity is highly cell type dependent.

Investigations of stiffness sensing in chondrocytes has so far been limited to studies with ionically crosslinked, RGD modified alginate [124] and differently crosslinked chitosan [147]. On alginate cells showed an increased cellular attachment rate, spreading, and actin organization on stiffer substrates. The study with chitosan confirmed these results and also found that after seven days in culture, the deoxyribonucleic acid (DNA) yield and therefore cellular number, was higher on stiffer substrates.

While the authors of the latter publication imply that the stiffer substrates are advantageous for TE applications, as the overall cell number is increased, the effect of the mechanical properties on the chondrogenic phenotype was not investigated in either of the studies. Because an increase in proliferation and an altered morphology are thought to be associated with a phenotypical change of the chondrocyte, [153] the aim was to

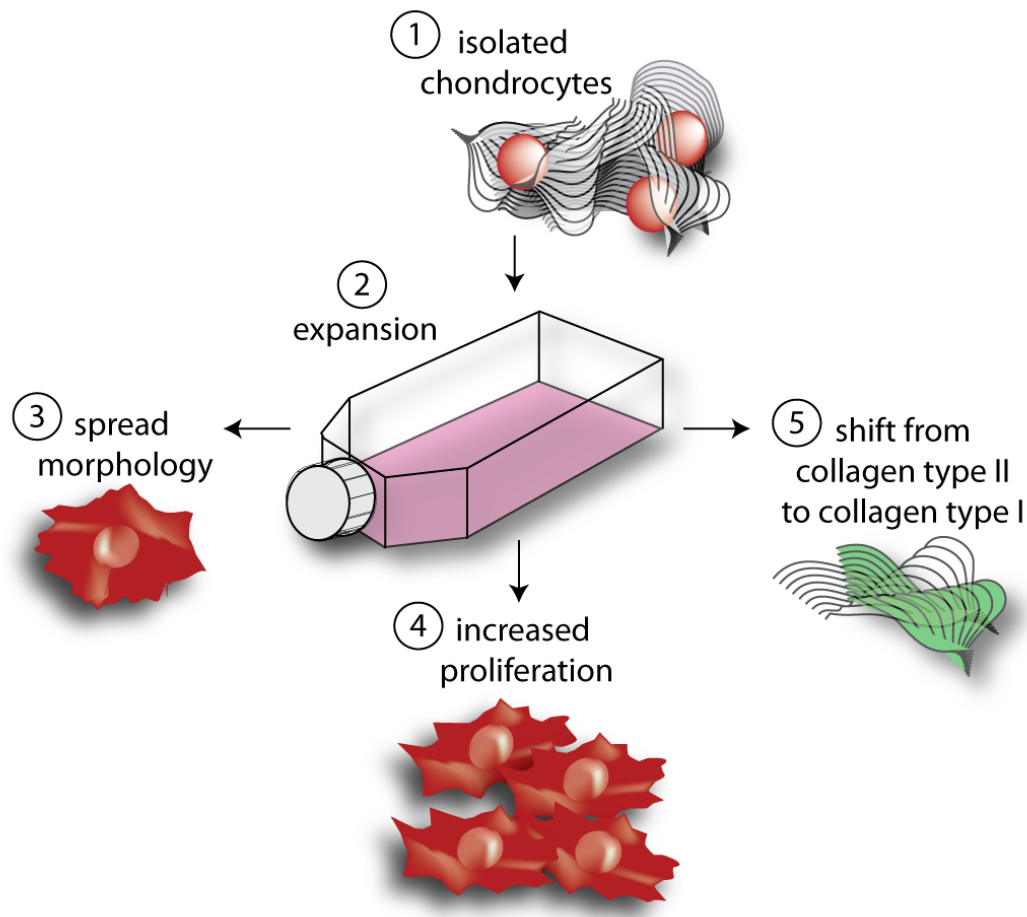


Figure 3.2: Dedifferentiation of chondrocytes. After isolation (1) chondrocytes need to be expanded (2). They, hereby, change their phenotype indicated by a spread morphology (3), an increase in proliferation (4) and an altered ECM production (5).

investigate the influence of matrix stiffness, not only on proliferation and morphology, but also on the differentiation state of chondrocytes.

Upon expansion in an adherent monolayer, for instance prior to autologous implantation in tissue engineering applications, chondrocytes progressively lose their chondrogenic phenotype and develop a fibroblast-like phenotype over time [50].

This process, typically described as dedifferentiation, is accompanied by changes in gene expression and protein synthesis, for example an increase of collagen type I and a decrease of collagen type II and aggrecan expression [154] (Figure 3.2).

In contrast to differentiated chondrocytes [155], the cytoskeleton of cells with a dedifferentiated phenotype is highly organized and characterized by the development of stress fibers [156]. Conditions that encourage cytoskeleton enforcement and cell flattening are therefore supposed to enhance chondrocyte dedifferentiation [155]. The success of autologous transplants, however, seems to depend on the ability of the cells to produce a hyaline matrix containing collagen type II [9]. Thus, it depends on maintaining the matrix production associated with the fully differentiated chondrogenic phenotype.

I hypothesized that substrates with a lower elastic modulus can help to maintain the chondrogenic phenotype, possibly by supporting the round morphology. The well-characterized PA gel system [6, 7, 71, 90, 129] was applied to investigate the morphology, proliferation and differentiation of chondrocytes cultured on substrates with different elastic moduli.

3.2.2 Materials and Methods

PA gels

PA gels were prepared and characterized as described in the previous section of the chapter. Out of the twelve compositions tested, four different bis-acrylamide crosslinker concentrations 0.01%, 0.07%, 0.2% bis and 0.5% bis were chosen for cell culture experiments, yielding Young's moduli of approximately 4 kPa, 10 kPa, 40 kPa and 100 kPa, representative for a range of elastic moduli.

Prior to plating, culture dishes with matrices were sterilized under the UV light of a sterile bench for 20 min and subsequently soaked in complete culture medium at 37°C for one hour.

Cell Culture

Porcine chondrocytes were isolated from the condyles of three to six month old pigs obtained from a local slaughterhouse. An average of five condyles was used for each isolation. The articular cartilage was excised from the condyles under aseptic conditions, washed with PBS, and digested using 30 ml of a mix of hyaluronidase (33.34 u/ml, Roche, Mannheim, Germany), collagenase type II (333.34 u/ml, Roche, Mannheim, Germany) and collagenase P (1 u/ml, Worthington, Lakewood, USA) in culture medium RPMI 1640 culture medium (2.0 g/l NaHCO₃, 25 mM HEPES, 5.5 g/l NaCl), supplemented with 10% fetal calf serum (FCS), penicillin/streptomycin 100 u/ml (all from Biochrom, Berlin, Germany)] per 10 g of cartilage. Enzymatic digestion was performed overnight in spinner flasks (Wheaton, Atlanta, USA) at 37°C and 5% CO₂.

The solution was filtered through a 100 µm cell strainer (BD Bioscience, Heidelberg, Germany) and centrifuged at 1400 rpm for 10 minutes. The supernatant was disposed; the pellet was resuspended in PBS and centrifuged for another 10 minutes at 1400 rpm. After repeating the washing step twice, cells were resuspended in culture medium. The cell viability was determined by trypan blue dye (Biochrom, Berlin, Germany) exclusion and cells were counted with the aid of a Thoma counting chamber. Cells were plated at 30 x 10⁶ per 150 cm² cell culture flask (TPP, Trasadingen, Switzerland) and allowed to attach overnight to maintain only viable cells. After 24 hours they were detached by trypsinization, centrifuged at 1400 rpm, counted and assessed for viability by trypan blue dye exclusion, resuspended in RPMI media supplemented with 20% FCS and 10% dimethylsulfoxide (Roth, Karlsruhe, Germany) at 10x10⁶ cells/ml, and frozen in liquid nitrogen for storage. Viability was between 97% and 99% for all isolations used.

Upon thawing, 20 x 10⁶ chondrocytes were plated overnight in a 75 cm² cell culture flask (Biochrom, Berlin, Germany). Additional cells were plated overnight on cell culture Petri dishes with the same density for further characterization. Cells on the Petri dishes were stained for collagen type II, to confirm that they were fully differentiated before seeding

on the matrices. Cells from the 75 cm² cell culture flask were seeded on matrices with a density of 5000 cells/cm² after trypsinization (Trypsin/EDTA, PAA, Cölbe, Germany), viability assessment (97%-99% viability), and counting.

All the samples for one experiment were seeded with cells from the same isolation. Chondrocytes were cultured on PA gels for up to seven days in culture medium supplemented with 35 mM ascorbic acid-2P (Sigma, Karlsruhe, Germany) to facilitate ECM production [157, 158].

Immunofluorescence staining

All samples were analyzed with the microscope Axioskop (ZEISS, Oberkochen, Germany) using the acquisition software Axiovision (ZEISS, Oberkochen, Germany).

Collagen type II

Chondrocyte seeded matrices were rinsed with PBS, fixed for 5 minutes with pre cooled (-20 °C) methanol-acetone (7:3, Sigma, Karlsruhe, Germany) and washed with PBS. Non-specific binding was blocked with 7.5% bovine serum albumin in PBS. Specimens were incubated with the primary antibody for 1 hour at 37°C in a humidified chamber, washed extensively, and incubated with the secondary antibody under the same conditions. The primary antibody against collagen type II (II-II-6B3, Developmental Studies Hybridoma Bank, University of Iowa, USA) was applied in PBS with a dilution of 1:50. Negative controls were incubated in PBS only. Detection in samples, as well as in negative controls, was performed with Fluoresceinisothiocyanat (FITC)-conjugated goat anti-mouse IgG (DIANOVA, Hamburg, Germany) diluted 1:200 in PBS. Nuclei were counterstained with 4',6-Diamidino-2-phenylindol (DAPI, Sigma, München, Germany) diluted in PBS 1:1000, washed extensively with PBS, embedded in Vectashield mounting medium (Alexis, Grünfeld, Germany) and sealed with clear nail polish solution.

F-actin staining

Chondrocyte seeded matrices were washed with PBST (PBS with 0.1 v/v% Triton-X-100) and fixed for 1 hour at 37°C with 100 mM HEPES (Sigma, Karlsruhe, Germany) 50 mM Ethylene glycol-bis(2-aminoethylether)-N,N,N',N'-tetraacetic acid (EGTA, Sigma, Karlsruhe, Germany), 10 mM MgSO₄, 2 v/v% Formaldehyde, and 0.2 v/v % Triton X-100. Samples were washed with PBST three times for ten minutes, and actin was stained

with Alexa-488 labeled phalloidin (Invitrogen, Karlsruhe, Germany) 1:200 in PBS, 3% bovine serum albumine (BSA), and 0.1% Triton X-100 at 37° for 1 hour. Nuclei were stained with DAPI, 1:1000 in PBS for ten minutes at 37°C. After washing three times for ten minutes in PBS, samples were embedded in Vectashield mounting medium and sealed with clear nail polish solution.

Ten images at tenfold magnification were obtained at random positions of each sample, and the cell number and fraction of round cells was counted.

Proliferation tests

Proliferation was assessed at subconfluency after 3 days in culture using a 5-Bromo-2'-deoxy-uridine (BrdU) labeling and detection kit (Roche, Mannheim, Germany). The kit detects BrdU-labeled DNA with an anti-BrdU antibody, which is then visualized with a fluorescein-labeled secondary antibody. Immunofluorescence staining for BrdU was performed according to the manufacturers' instructions. Briefly, chondrocyte seeded

Table 3.1: PCR primers

Gene	Primer (forward & reverse)	concentration [nm]	fragment length [bp]	tm [°C]
18S	5'-CGC GGT TCT ATT TTG TTG GT-3'	100	219	55.3
	5'-AGT CGG CAT CGT TTA TGG TC-3'	300		57.3
Collagen type I	5'-AAT CAC CTG CGT ACA GAA CGG-3'	100	120	61.3
	5'-TCG TCA CAG ATC ACG TCA TCG-3'	100		61.3
Collagen type II	5'-CTC CTG GAG CAT CTG GAG AC-3'	50	152	61.4
	5'-ACC ACG ATC ACC CTT GAC TC-3'	50		59.4
Aggrecan	5'-GCA TCT GGG TCT CCT GAC AT-3'	300	224	59.4
	5'-ACG CCA GAA AGA ACT CCT GA-3'	50		57.3

Sequences, applied concentrations, product fragment length, and melting temperatures (tm) of applied primers.

matrices were cultured in BrdU supplemented medium for one hour, washed, fixed and incubated with an anti-BrdU antibody at 37°C for 30 minutes. After washing with PBS, specimens were incubated with an FITC-conjugated secondary antibody (1:20) for 30 minutes at 37°C, washed, embedded in Vectashield mounting medium and sealed with clear nail polish solution.

For each sample ten images at tenfold magnification were obtained, and BrdU-positive cells were counted against DAPI positive cells to obtain the fraction of proliferating versus non-proliferating cells. To normalize for differences between donor animals, values were displayed as percentage of maximal proliferation in the respective experiment.

Detection of gene expression by semi-quantitative reverse transcriptase polymerase chain reaction (RT-PCR)

RNA was isolated using an RNA isolation kit (Macherey & Nagel, Düren, Germany). The manufacturers' protocol was slightly altered to obtain RNA from the PA matrices. Samples were washed with PBS and 300µl RNA Lysis buffer with 0.1% β-mercaptoethanol was added to the sample. After 30 seconds incubation time, lysed cells were transferred to a 1.5 ml Eppendorf tube and processed according to the manufacturers' protocol. RNA concentration was measured using an RNA assay kit (Quant-iT™ RNA Assay Kit, Invitrogen, Karlsruhe, Germany) and determined in the Qubit™ fluorometer (Invitrogen, Karlsruhe, Germany).

150 ng RNA per sample were reverse transcribed using oligo-dT primer and Superscript II reverse transcriptase (Invitrogen, Karlsruhe, Germany) following the manufacturer's recommendations. Optimal primer concentrations were determined by titration according to the published recommendations for PCR optimization [159]. Aliquots of 2 µl from the reverse transcriptase reactions were used for amplification of transcripts using primers specific for the analyzed genes and Taq polymerase according to the manufacturer's instructions (Invitrogen, Karlsruhe, Germany). Reverse transcriptase reactions were denatured for 2 minutes at 95 °C, followed by amplification for 38 cycles of 40-s denaturation at 95 °C, 40-s annealing at 60°C and 50-s elongation at 72 °C. Primer sequences, applied concentrations, and melting temperatures are provided in Table 3.1. Electrophoretic separation of PCR products was carried out on 2% agarose gels. Distilled

water was included as a negative control. The fragments were analyzed in relation to *18S* gene expression by computer-assisted densitometry with the Image J software (National Institute of Health, Rockville, USA). Values are displayed as a percentage of the maximum gene expression of the respective gene in the experiment to normalize for differences between donor animals.

Statistical analyses

All statistical analyses were performed with the SPSS 16.0 software (SPSS inc., Chicago, USA). Statistical significance was determined by analysis of variance (ANOVA) followed by Fisher's least significant difference (LSD) with a significance level of $p < 0.05$. All results are displayed as mean \pm standard error of the mean (SE). All experiments were repeated three to six times.

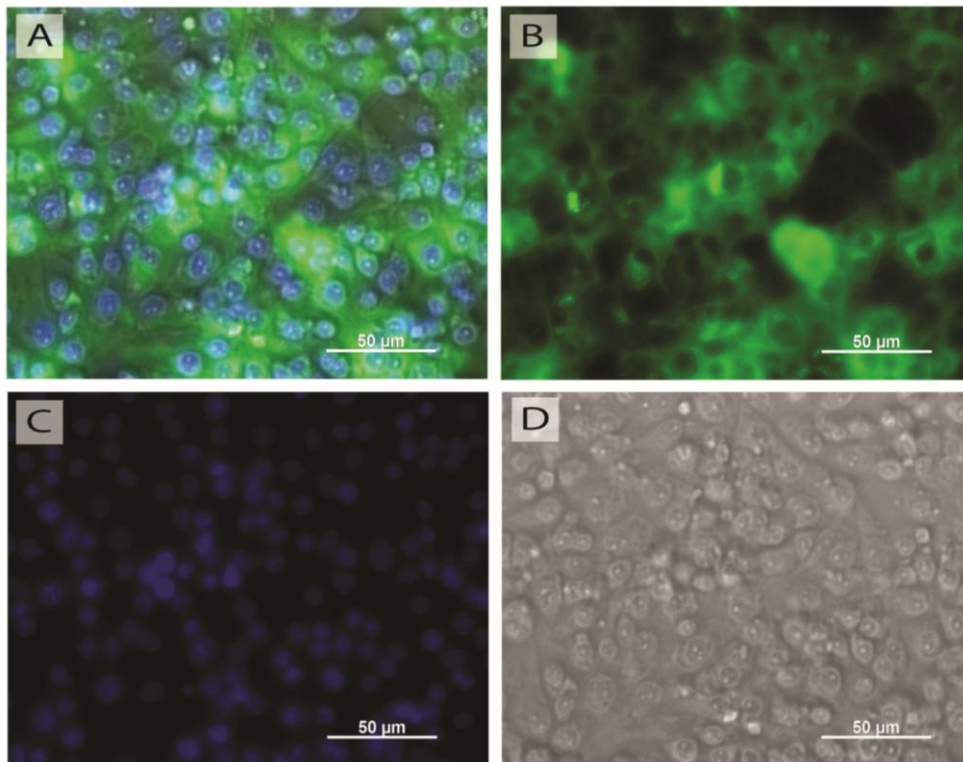


Figure 3.3: Fully differentiated chondrocytes. Immunohistochemistry (IHC) of collagen type II produced by chondrocytes prior to plating. A: Overlay of nuclear stain, collagen type II IHC and brightfield image. B: IHC of collagen type II (green). C: Nuclei stained with DAPI (blue). D: Brightfield image of chondrocytes.

3.2.3 Results

Chondrocyte isolation led to an average of 40×10^6 cells per gram of cartilage, and cellular viability was between 97% and 99 % for all isolations. Prior to plating, cells were fully differentiated, produced collagen type II, and had a round morphology (Figure 3.3), as confirmed by immunofluorescent staining and light microscopy. RT-PCR also confirmed high levels of collagen type II (102.2 ± 11.5 % of 18S) and aggrecan (95.9 ± 5.8 % of 18S) and the complete absence of collagen type I expression.

Chondrocyte actin organization is influenced by matrix stiffness

Cells were grown on the PA substrates at low density monolayer for up to seven days. A low density of 5000 cells/cm² was used to avoid that cells cultured on the stiffest matrices reach confluency before the end of the experiment.

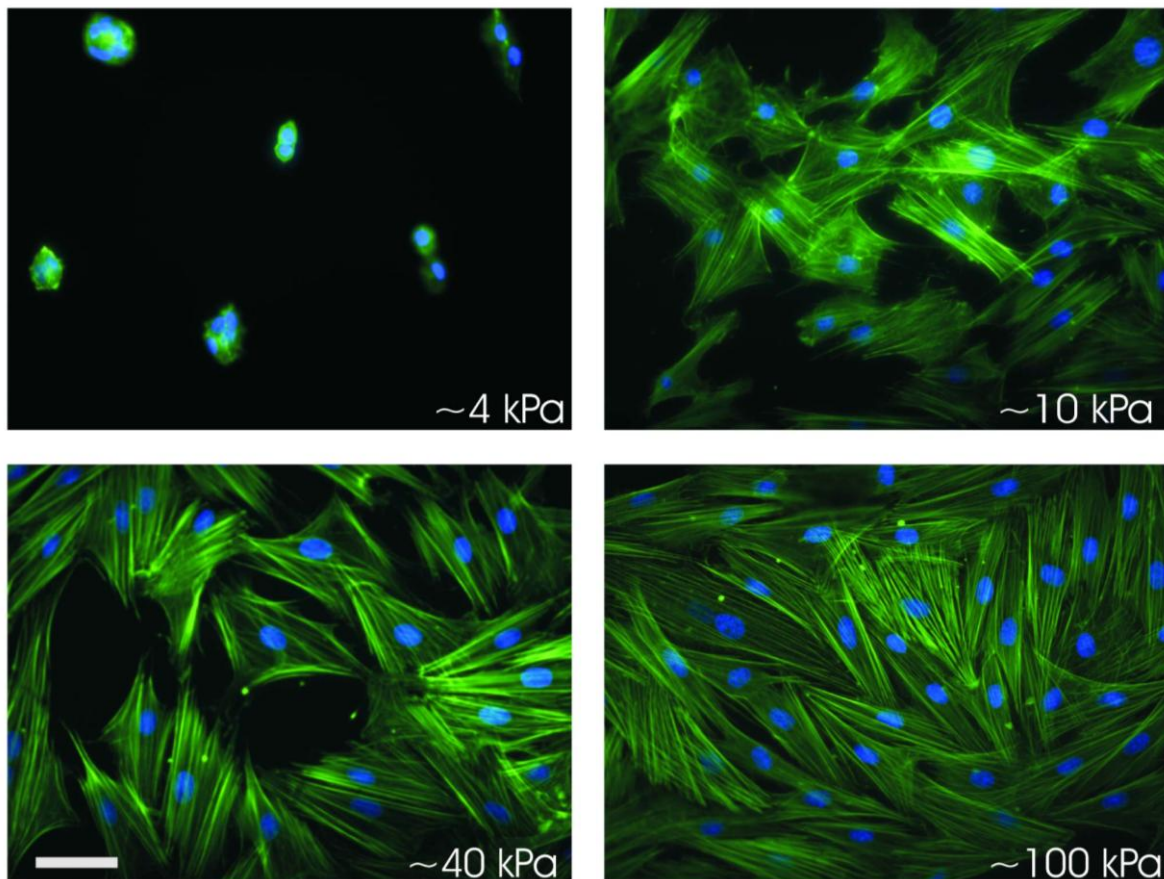


Figure 3.4: Actin staining of chondrocytes cultured for seven days on matrices with different elastic moduli. Staining with FITC-conjugated phalloidin revealed that an increase in matrix stiffness leads to an increase in actin organisation in chondrocytes. Nuclei were stained with DAPI. Scale bar = 50 μ m.

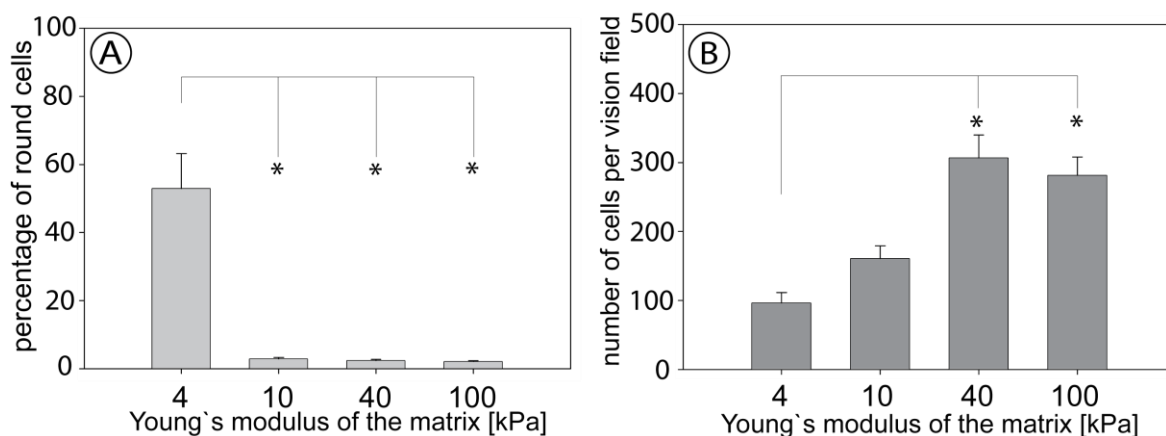


Figure 3.5: Quantitative analysis of phalloidin stains. Cells were divided into spread and round morphology (A). The average percentage of round cells was significantly higher on very soft PA-gels. The average cell number per vision field (B) was significantly higher after seven days of culture on stiffer gels (40 kPa and 100 kPa). Values are displayed as mean + SE; * $p < 0.05$ between groups.

Phalloidin staining for actin filaments was performed to investigate whether cellular morphology and cytoskeleton organization was altered by cultivation on substrates with different elastic moduli. Cells grown on stiffer gels (100 kPa and 40 kPa) spread to a larger extent, showed a flattened morphology and developed highly organized stress fibers after seven days of cultivation. In contrast, chondrocytes cultured on soft 4 kPa gels showed a spherical cell shape and diffuse actin organization (Figure 3.4).

For quantification, ten random microscopy images at 10-fold magnification were obtained per sample, and cells were classified according to the clearly distinguishable phenotypes: round with diffuse actin, or spread with organized stress fibers (Figure 3.5). On 4 kPa substrates 52.9 % \pm 10 of the cells maintained their round morphology, which is significantly ($p < 0.001$) more than on stiffer gels, where the percentage of round cells is 2.9% \pm 0.5 on 10 kPa matrices, 2.4% \pm 0.4 on 40 kPa, and 2.1% \pm 0.4 on 100 kPa matrices.

Although stress fiber formation seemed to be slightly less distinct on 10 kPa substrates when compared to stiffer substrates, no significant difference in the fraction of round cells was observed ($p = 0.433$ and $p = 0.77$).

After seven days in culture, a significant ($p < 0.01$) difference between the number of cells on 4 kPa substrates (96 \pm 15.2 cells / vision field) and the number of cells on 40 kPa and

100 kPa substrates (300 ± 33 and 280 ± 27 cells /vision field) was observed (Figure 3.5). The number of cells on 10 kPa (160.4 ± 18.6) was not significantly ($p = 0.1$) higher than on 4 kPa substrates.

Proliferation on substrates with different elastic moduli

To investigate whether differences in cellular proliferation, in contrast to increased attachment, contributed to the higher cell number on day seven, a BrdU incorporation assay was performed on day three, when cells on all matrices were still in subconfluency and cellular numbers were not yet significantly different. The number of BrdU positive cells was counted, calculated as the fraction of total cells in the respective vision field, and normalized to the maximal proliferation in the assay (Figure 3.6).

Normalized proliferation was $16.52 \% \pm 2.9$ for the 4 kPa substrate, $30.84 \% \pm 3.32$ for the 10 kPa, $50.92 \% \pm 4.6$ for the 40 kPa, and $50.12 \% \pm 5.2$ for the 100 kPa substrate. Increasing the matrix stiffness from 4 to 40 kPa thus led to a threefold enhancement of the proliferation rate. The percentage of proliferating cells increased significantly from 4 kPa to 10 kPa, and then to 40 kPa, where a plateau was reached without any additional measurable effect of even stiffer substrates.

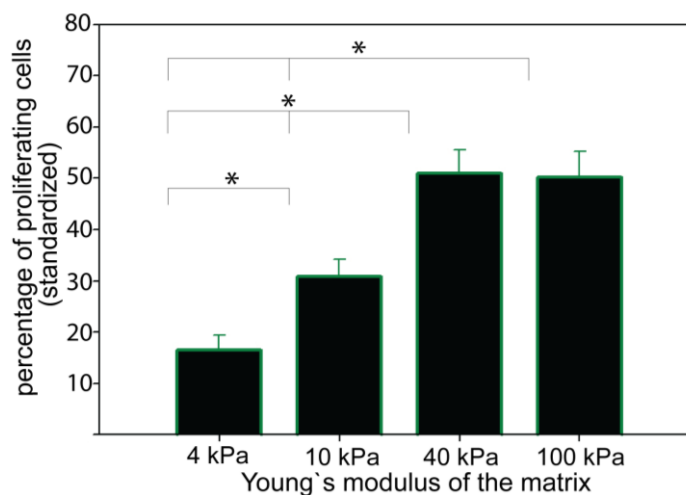


Figure 3.6: Proliferation of chondrocytes at subconfluence, at day 3. Cells were stained for BrdU by indirect immunofluorescence staining and BrdU-positive, proliferating cells were determined in percentage of total cell number. Proliferation is displayed as percentage of maximal proliferation in the assay (mean +SE). * $p < 0.05$ between groups.

Maintaining the chondrogenic phenotype on matrices with variable stiffness

Total RNA from chondrocytes cultured at low density on PA gels with varying stiffness for seven days was isolated, and the expression of collagen type II, aggrecan, and collagen type I was analyzed by RT-PCR (Figure 3.7). The differentiated chondrogenic phenotype is characterized by a high expression of collagen type II (A) and aggrecan (B), and a low expression of collagen type I (C).

On the softest substrates, 18 S normalized collagen type II expression remained at $90.25\% \pm 11.1$ in comparison to cells cultured on the stiffest substrates, where expression was as low as $47.77\% \pm 11.9$. Aggrecan expression was $82.1\% \pm 2.9$ on the softest but only $62.8\% \pm 10.1$ on the stiffest substrates. Collagen type I expression, in turn, was slightly higher on stiff ($89.6\% \pm 10.422$), in comparison to the softest substrate ($71.49\% \pm 17.3$).

Chondrocytes cultured on the softest matrices (4 kPa) thus maintained a significantly

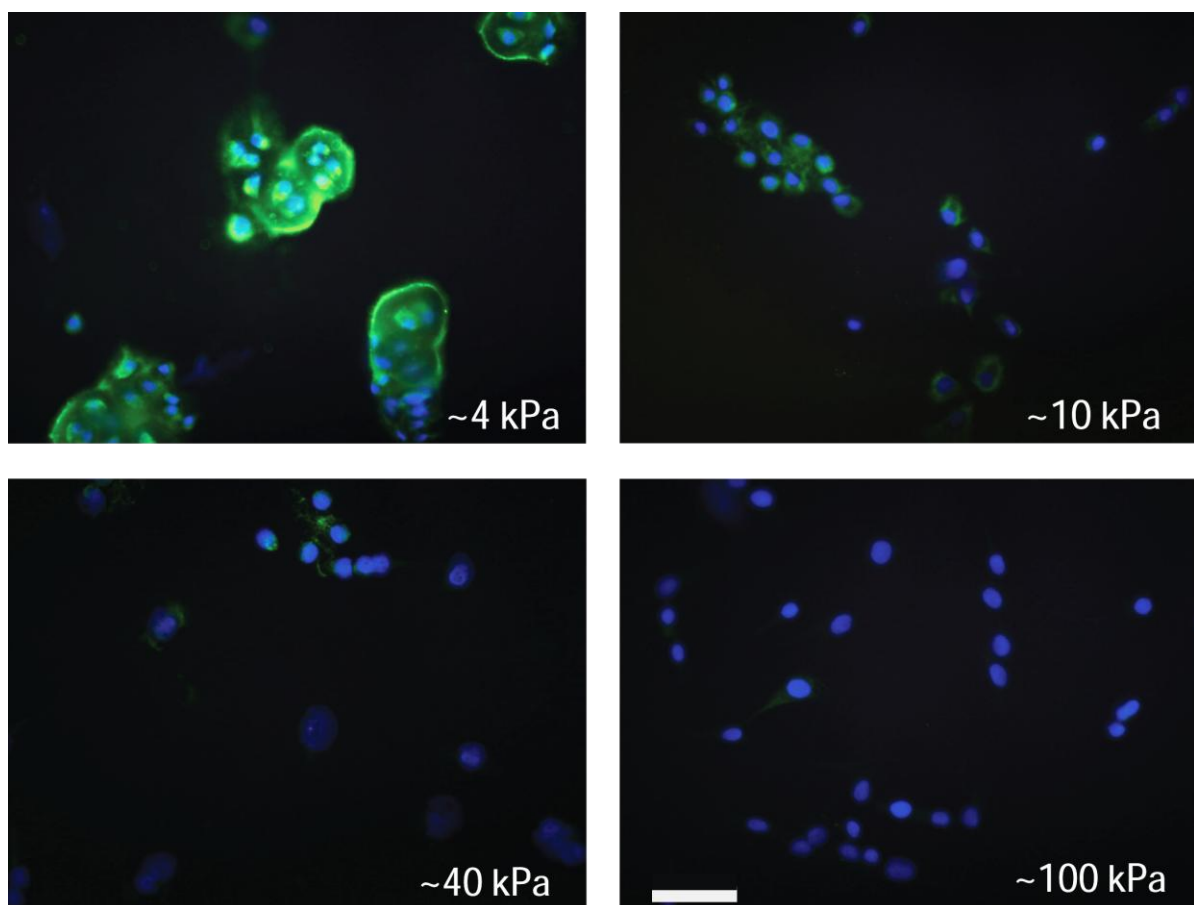


Figure 3.8 IHC for collagen type II (green). Collagen type II expression remained higher in cells grown on softer matrices (4 kPa) when compared to cells grown on stiffer matrices. Nuclei were stained with DAPI (blue). Scale bar = 50 μ m.

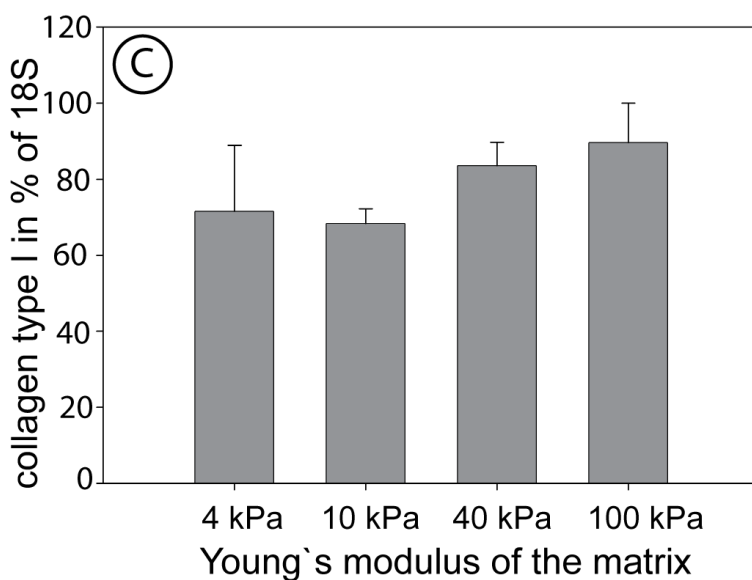
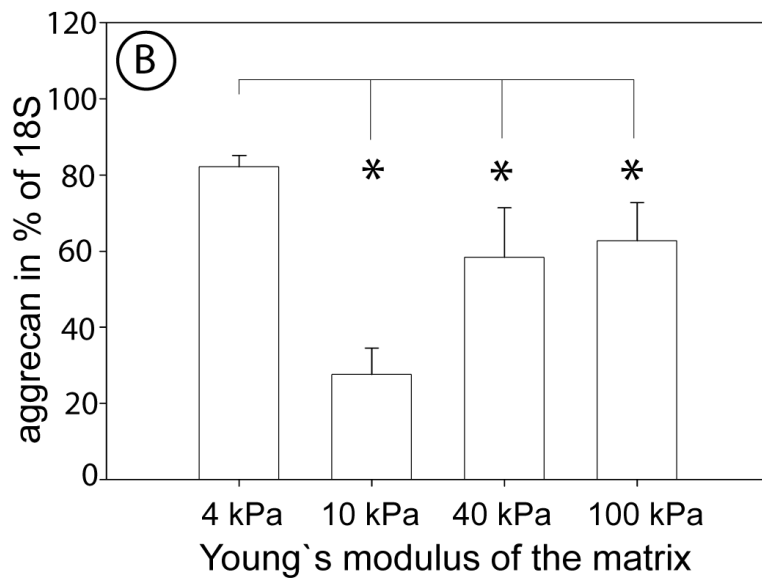
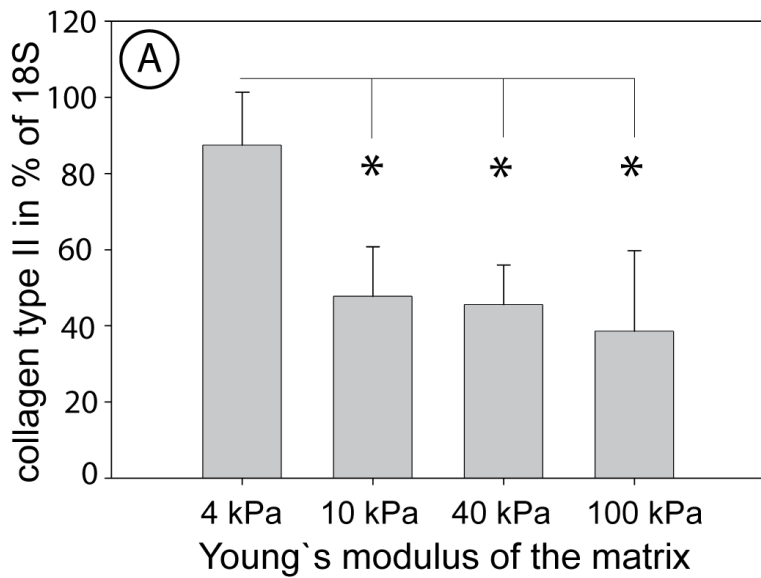


Figure 3.7: Gene expression of chondrocytes on different matrices. Collagen type II (A), aggrecan (B) and collagen type I (C) expression (mean + S.E.M) of chondrocytes cultured for seven days in low density culture on matrices with different Young's moduli. RT-PCR results were normalized for 18S rRNA and displayed in percentage of maximal expression in the respective experiment. Collagen type II and aggrecan expression were significantly higher on soft PA-gels (4 kPa) $*p < 0.05$ compared to cells on stiffer matrices. There were slight but not significant differences in collagen type I expression with a trend towards higher expression levels on stiffer matrices.

higher level of collagen type II and aggrecan production when compared to cells grown on stiffer substrates, while collagen type I expression seemed to be slightly, but not significantly, lower.

To confirm RT-PCR results, collagen type II was visualized by immunofluorescence staining (Figure 2.8). On very soft substrates (4 kPa) the majority of chondrocytes was still surrounded by collagen type II after seven days, while its production was clearly diminished on stiffer substrates, confirming the assumption that substrate stiffness has a significant influence on ECM production.

3.2.4 Discussion

Collagen coated PA gels were applied as a model system to investigate the influence of substrate stiffness, not only on morphology, but also on the proliferation and ECM production of chondrocytes.

The softest substrate promoted the maintenance of the chondrogenic phenotype as indicated by a diffuse orientation of the actin in the cytoskeleton, low proliferation, high collagen type II and aggrecan, and slightly lower collagen type I expression.

Chondrocytes cultured on stiff substrates developed spread morphology and organized actin fibers, when compared to cells cultured on soft substrates. This increased cytoskeleton organization on stiffer substrates resembles the response observed in different other cell types, such as fibroblasts, endothelial cells [75] and MSCs [7].

Different studies also showed that spread morphology and organized actin cytoskeleton, rather than adhesion per se, promotes the entry into the cell cycle [160-163]. As an increase in stiffness seems to enhance stress fiber formation in chondrocytes, a measurable effect on the proliferation rate should also be observable. My experiments confirmed these assumptions, as a stiffer matrix led to cytoskeleton organization and an increased proliferation rate. These results are consistent with findings in other differentiated cell types, where matrix stiffness was able to induce a switch between cellular differentiation and proliferation by variably inducing entrance into the cell cycle [6, 72, 126, 129, 164, 165].

I hypothesized that this transition into a proliferative state, through stimulation of the cell

cycle entry, might be associated with a loss of the differentiated phenotype.

The results confirm an accelerated loss of the differentiated phenotype on stiffer substrates, while the maintenance of the chondrogenic phenotype is prolonged on softer matrices. This is supported by the significant decrease of collagen type II and aggrecan production on stiff matrices in comparison to cells cultured on soft substrates. It is not yet clear why the aggrecan expression is lowest on the 10 kPa matrices; however, the favorable effect of the softest 4 kPa matrix, in comparison to all other matrices tested, is also clearly observable for this matrix molecule. After seven days of culture, a certain collagen type I expression is measurable on stiff, as well as on soft, matrices on which cells are round and produce collagen type II. Thus, the soft matrix seemingly slows down dedifferentiation, but is not able to completely prevent it. Immunofluorescence staining of collagen type I could not be performed in this context due to the collagen type I coating of the matrix.

As mentioned earlier, previous studies investigating the influence of matrix elasticity [6, 75-77] revealed that different cell types often show a preference for a distinct modulus. In this context, it was shown by several groups that cells differentiate optimally on tissue level elasticity. Mesenchymal stem cells differentiate into neurogenic, myogenic and osteogenic precursor cells through cultivation on substrates with the respective elasticity [166]; studies with neurons [77], preosteoblasts [139, 140] and myoblasts [6] additionally showed that tissue level elasticity is optimal for the growth and differentiation of further developed cells.

However, it is not entirely clear, what determines the mechanical properties in the direct cellular environment *in vivo*. Engler et al. measured the elasticity of freshly formed osteoid and found that this elasticity induces an osteogenic response [7]. In the case of muscle, they measured the elasticity of other muscle cells and found that this elasticity supports myogenic differentiation [6].

The immediate mechanical environment of a chondrocyte may be regarded as being determined by the PCM, which differs by orders of magnitudes from the mechanical properties of the extracellular matrix [15], but also by other chondrocytes, as in isogenous groups of chondrocytes, where cells are separated only by a thin partition of matrix.

The elasticity of freshly isolated chondrocytes was reported to be in the range of 0.7 - 4 kPa [167-169], which would roughly match the mechanical properties of the matrix, favorable for the prolonged maintenance of the chondrogenic phenotype in this study.

AFM based measurements of the stiffness of freshly developed PCM led to similar values of 1- 4 kPa [170], which would again be in the range of the Young's modulus of the softest substrate tested here.

According to the tensegrity hypothesis, cells adapt their cytoskeletal tension to the stiffness of the substrate in order to create a homeostatic balance [84, 85]. In chondrocytes, this could mean that they need to increase their cellular stiffness on the stiffer substrates in order to match the stiffness of the substrate, which could result in an alteration of their physiological, differentiated phenotype. However, reports about the elasticity of mature PCM, obtained with different measurement techniques, contain a wide range of elastic moduli (1.5 - 69 kPa, [15, 171, 172]), which complicates a true contribution of my results to the effects of tissue level elasticity.

Thus, further investigations are needed to identify the mechanical conditions a chondrocyte would feel *in vivo*. The results of this study support the studies that found lower elastic moduli. My findings stress the importance of matrix elasticity for the design of novel scaffolds for tissue engineering of cartilage. As mechanical properties of cartilage *in vivo* are mainly determined by the composition and quality of the matrix synthesized by the chondrocytes, the chondrogenic phenotype needs to be tightly controlled. By tuning the elastic properties of the substrate, it might be possible to control cellular matrix production and proliferation to obtain the optimal behavior for transplant formation.

Based on these results, stiff materials could be applied for the expansion of cells *in vitro*, to obtain high proliferation rates. In turn, softer materials could be used for implant formation, to support the chondrogenic phenotype. However, since tissue engineered cartilage needs to provide certain mechanical properties for the patient, transplants of mixed materials might be a promising alternative. Chondrocytes could, for instance, be embedded in a softer material to optimize the immediate cellular environment. The whole construct could then be further enforced with a network of a stiffer material, in order to provide initial stability of the transplant.

While the aim of this study was the systematic investigation of the influence of matrix mechanics on the maintenance of the chondrogenic state, additional research may also focus on the influence of substrate mechanics on chondrogenic differentiation in a 2D culture system. This research should investigate the influence of the mechanical properties on the redifferentiation potential of expanded, dedifferentiated chondrocytes, but possibly also on the chondrogenic potential of stem cells, since these have been shown to strongly respond to matrix mechanics [7]. Knowledge obtained in this 2D model system may then aid in specifically tailoring biomaterials to optimally support the chondrogenic phenotype and ECM production. To further confirm the relevance of these findings for TE applications according studies in 3D systems would be very valuable.

4 Chondrocyte response to matrix elasticity in 3D: evaluation of a porous system

4.1 Characterization of a porous silk-based system

4.1.1 Introduction

While cells naturally find themselves in a complex, 3D environment *in vivo*, most of the research about cellular stiffness sensing is still limited to studies in 2D environments [173]. However, since cellular morphology and cell matrix interactions are known to be very different in 2D when compared to 3D [88], 2D monolayer systems always represent a suboptimal setting to study cellular mechanosensing.

Besides hydrogels, porous scaffolds of various materials are widely applied for cartilage TE approaches [1, 109]. The mechanical properties of porous scaffolds can, for instance, be changed by altering the overall porosity [101, 109, 110] or by altering the pore size [11, 110, 174]. 3D studies about cellular stiffness sensing are still often performed in porous systems [4, 65] although these are not likely to provide the controlled environment needed for this purpose.

Silk has been extensively used as a suture material [175] and gained increasing interest as a material for TE applications, within the last few years. Porous, silk-based scaffolds have, hereby, been shown to also be suitable for the fabrication of cartilage tissue substitutes with mesenchymal stem cells [44, 176] and autologous chondrocytes [48]. The most commonly commercially available type of silk is derived from the cocoon of the silk worm *Bombyx Mori*. Silk fibers from this source consist of fibroin, the core structural protein which is held together by the glue-like protein sericin [177]. Since sericin has been found to be responsible for most of the immunogenic response against silk sutures [175, 178] it is removed in the scaffold production process. A solution of the purified silk is prepared and porous scaffolds can be formed through the salt leaching procedure [44]. Silk scaffolds with different pore sizes can be produced through the application of differently sized NaCl particles [179]. Different pore sizes, in turn, have been shown to result in different mechanical properties of silk scaffolds with higher compressive moduli found in scaffolds with small pores when compared to scaffolds with large pores [11,

174]. This section characterizes porous silk scaffolds, representative for other porous culture systems, that may be used to study cellular stiffness sensing in 3D. I hypothesized that silk scaffolds with different pore sizes can be produced through the application of differently sized porogens and that different pore sizes result in different mechanical properties.

To investigate this hypothesis, porous silk scaffolds with three different pore sizes were produced. Pore size and distribution was analyzed by micro-computed tomography (micro-CT) measurements and the mechanical properties of different scaffold types were determined by stepwise, indentation stress-relaxation testing. Additionally, metabolic activity of cells cultured on the different scaffold types was determined.

4.1.2 Materials and Methods

Reagents were obtained from Sigma-Aldrich (Buchs, Switzerland) and of pharmaceutical grade, unless stated otherwise.

Production of porous silk scaffolds

Silk cocoons from *Bombyx Mori* (Trudel Inc, Zurich, Switzerland) were cleaned from larvae and boiled in a 0.02 M Na₂CO₃ solution two times for 1 h. Silk was thoroughly washed in ultrapure water (UPW) and left to dry over night. Dry silk was dissolved in 9 M LiBr (Fluka, Buchs, Switzerland) for 1 h at 55°C to produce a 10% (w/v) silk solution. The solution was dialyzed (3500 g/mol cutoff, Pierce, Woburn, USA) against UPW with frequent changes for 36 h, filtered with a 5 µm pore size syringe filter (Sartorius, Dietikon, Switzerland), frozen and lyophilized.

Table 4.1: Amounts of NaCl used

NaCl particle diameter [µm]	Amount of NaCl [g] per 1 ml silk
112-224	1.87
315-400	2.59
500-600	2.5

NaCl grains (Retsch, Arlesheim, Switzerland) with three different diameters were used to produce scaffolds with different pore sizes (Table 4.1). Lyophilized silk was dissolved in hexafluoro-2-propanol (HFIP, Fluka, Buchs, Switzerland) to obtain a 17% (w/v) silk solution. The amount of NaCl crystals was, hereby, adjusted in order to obtain a constant overall volume of the silk/HFIP and NaCl mix (Table 4.1). The appropriate amount of NaCl was weighted into Teflon containers and 1 ml silk solution was added into each Teflon container. HFIP was allowed to evaporate for 3 days and silk/NaCl constructs were immersed in 90% (v/v) methanol (EGT Chemie AG, Trägerig, Switzerland) for 30 min to induce a conformational change of the silk into the water-insoluble β -sheet structure. Constructs were dried and NaCl was leached out for 2 days in UPW (5 changes of UPW). Constructs were cut into sections of ~ 3 mm thickness and disc shaped scaffolds with a diameter of 5 mm were punched (dermal punch, Miltey, Lake Success, USA) out of the sections. Scaffolds were placed into PBS and autoclaved.

Micro-CT

Autoclaved scaffolds were dried and measured in air with a micro-CT imaging system (μ CT 40, Scanco Medical AG, Brüttisellen, Switzerland). The X-ray tube was operated at 40 kVp and 180 μ A with an integration time set to 200 ms and all projection frames were recorded 4 times and then averaged. Scans were performed at an isotropic, nominal resolution of 6 μ m (high resolution mode). A cylindrical volume of interest was then placed in the digital image data for quantitative morphometry and visual assessment. A Gaussian filter, with a filter width of 0.8, and a filter support of 1 was applied to reduce the noise in the image and a threshold of 4.5% of the maximal grey value was used to segment the scaffold from the background. For the morphometric analysis the same morphometric parameters as used for human bone biopsy analysis were applied. For the transcription of the 3D morphometry of the porous scaffolds, quantitative analyses of pore diameter, scaffold porosity, scaffold wall number and scaffold wall thickness were performed [180]. 3D visualizations were generated with the software μ CT Ray V3.8 (Scanco Medical AG, Brüttisellen, Switzerland). To plot the pore size distribution, curves were fitted with a Weibull non-linear regression method [181].

Mechanical testing

Mechanical testing was performed according to a previously published, modified protocol [182] on a Zwick materials testing machine (Zwick Z005, Ulm, Germany) equipped with a calibrated 10 N load cell, built-in displacement control, and a cylindrical, flat, stainless steel indenter tip with a diameter of 1.2 mm. To exclude an influence of scaffold thickness on the mechanical testing results, thickness of hand-cut scaffolds was measured. Feasible indenter size was determined according to [183], to assure that $R_{\text{spec}} / R_{\text{ind}} > 4$ where R_{spec} denominates the radius of the specimen tested and R_{ind} being the radius of the indenter.

To detect the sample position, and measure sample thickness, a preload of 2 mN was applied. Stepwise, stress-relaxation indentation was then carried out in three strain steps of 5%, 15% and 25% of the measured sample thickness. At each indentation step, specimens were left to relax for 45 min to reach equilibrium. Force, displacement, and time data were recorded throughout the whole testing period. A force-smoothing

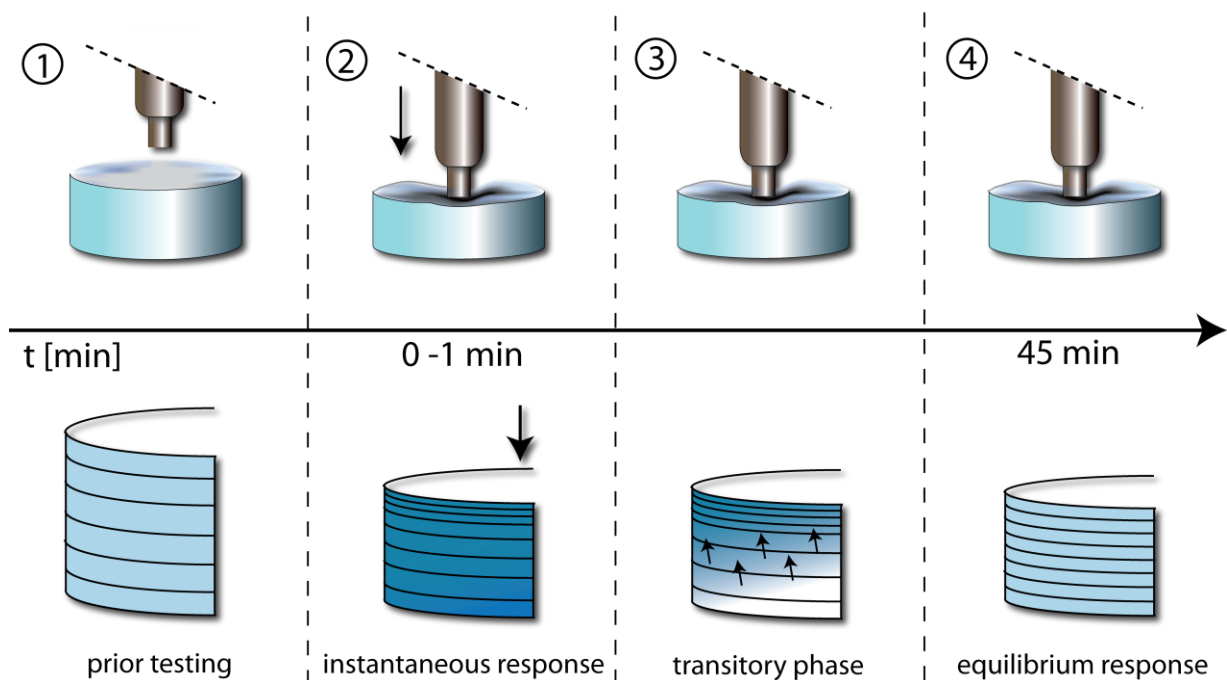


Figure 4.1: 1: Water in the scaffold is equally distributed prior to testing. 2: In an initial response the load is carried by the fluid and solid phase of the material. 3: In the transitory phase the water is redistributing and flowing out of the gel. 4: At equilibrium, fluid flow ceased and the load is carried by the solid phase of the material.

LOWESS (locally weighted scatterplot smoothing) algorithm was applied to the data, and force and displacement data were converted to stress (σ) and strain (ϵ) values. The instantaneous modulus (E_{inst}) was determined from the slope of the stress-strain curve obtained during the first step, at a constant strain rate of 100 mm/min. It was calculated according to the equation: $E_{inst} = \sigma_{inst}/\epsilon_{inst}$, with σ_{inst} being the stress at this indentation step and ϵ_{inst} , being the strain during the first indentation (0 to 0.05). The equilibrium modulus (E_{eq}) was determined from the three indentation steps according to the following equation: $E_{eq} = \sigma_{eq}/\epsilon_{eq}$, with σ_{eq} being the stress measured at equilibrium at the respective step and ϵ_{eq} being the corresponding strain for this step.

The instantaneous modulus is strain rate dependent and reflects the initial response of the bulk material, thus, of both the liquid and solid phase of the material. In the transitory phase the fluid phase redistributes, and flows out of the gel and at equilibrium, fluid no longer flows and the load is only carried by the material [117]. The equilibrium modulus, thus, reflects the properties of the solid phase of the material (Figure 4.1).

Cell seeding and culture

Porcine chondrocytes from the condyles of three to six month old pigs were isolated and characterized as described previously [184]. Viability was between 97% and 99% for all isolations used. Basal culture medium was composed of RPMI 1640 Medium, with GlutaMAX™ and 25 mM HEPES, supplemented with 10% FCS, 1% antibiotic/antimycotic solution (all from Invitrogen, Basel, Germany).

After isolation, cells were resuspended in RPMI media supplemented with 20% FCS and 10% dimethylsulfoxide (Roth, Karlsruhe, Germany) at 10×10^6 cells/ml, and frozen in liquid nitrogen for storage. Upon thawing, 20×10^6 chondrocytes were plated overnight in a 75 cm² cell culture flask (Biochrom, Berlin, Germany), detached by trypsinization and counted for seeding on the scaffolds.

Sterile 96-well plates were covered with thin layers of agarose to prevent cellular attachment. One scaffold was placed into each well and 1×10^6 cells dissolved in 20 μ l culture medium were pipetted on each scaffold. Cells were allowed to attach for 3 h at 37°C and 5% CO₂. 100 μ l medium was added into each well and constructs were incubated for another 21 h before they were transferred into 24-well plates for the rest of

the culture period. Cells were cultured in basal culture medium supplemented with ascorbic acid 2-phosphate (50 µg/ml) for 14 days. Medium was changed three times per week.

AlamarBlue® assay:

The alamarBlue® assay was performed according to manufacturer's instructions, with a 1:10 dilution of alamarBlue® reagent (Invitrogen, Basel, Switzerland) in basal culture medium and an incubation time of 4h at 37°C. Absorption was read with an excitation of 560 nm and emission at 590 nm (590 nm cutoff).

Each sample was then digested for 16 h with 0.6 ml papain solution (2.375 U/ml; Worthington, Lakewood, USA) in buffer (0.1 M disodium hydrogen phosphate, 0.01 MEDTA disodium salt, 14.4 mM L-cysteine), at 60°C.

DNA content was measured fluorometrically from a 96-well black flat-bottom microtiter plate, by using the PicoGreen assay (Molecular Probes, Basel, Switzerland), according to manufacturer's instructions (excitation wavelength, 480 nm; emission wavelength, 528 nm).

Statistical analysis

All statistical analyses were performed with the SPSS 17.0 software (SPSS inc., Chicago, USA). Statistical significance was determined by an ANOVA followed by post hoc comparisons using Fisher's LSD. $P < 0.05$ is considered statistically significant.

4.1.3 Results

NaCl grains with a diameter of 112-224 µm, 315-400 µm and 500-600 µm were applied to produce scaffolds with different pore sizes and dry scaffolds were analyzed by micro-CT. Pore sizes were visibly different for the different particle sizes (Figure 4.2). The average pore size was 98.5 ± 1.5 µm (small pores) for the smallest NaCl particle size, 142.0 ± 11.5 µm (medium pores) for medium particle sizes and 196.9 ± 20.2 µm (large pores) for the largest particle size and was significantly different for the three preparations used (Table

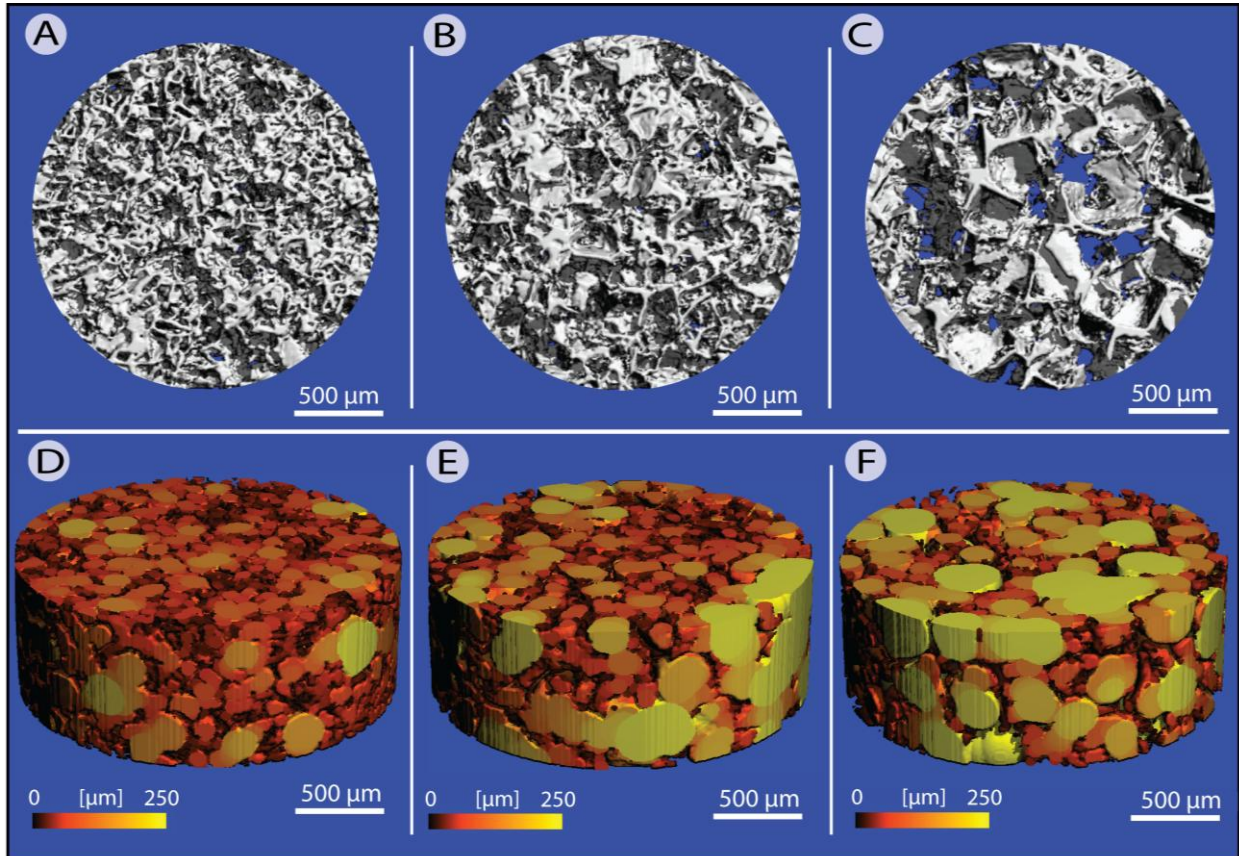


Figure 4.2: Micro-CT image of silk scaffolds. **A-C:** micro-CT top view of reconstructed images of silk scaffolds produced with NaCl particles of different grain sizes of **A:** 112-224 μm ; **B:** 315-400 μm and **C:** 500-600 μm . **D-F:** 3D-visualization of the different scaffolds (**D:** 112-224 μm ; **E:** 315-400 μm and **F:** 500-600 μm) fitted with spheres to determine the pore sizes. The colormap visualizes the diameter of the pores from 0 to 250 μm .

Table 4.2: Micro-CT analysis of porous silk scaffolds

	Small pores	Medium pores	Large pores
NaCl particle diameter [μm]	112-224	315-400	500-600
Average pore diameter [μm]	$98.5 \pm 1.5^*$	$142.0 \pm 11.5^*$	$196.9 \pm 20.2^*$
Scaffold surface [mm^2]	$97.4 \pm 3.1^*$	$72.8 \pm 5.7^*$	$56.6 \pm 8.1^*$
Porosity [%]	80.3 ± 1.8	81.2 ± 3.3	80.0 ± 7.0
Wall number [mm^{-1}]	$10.5 \pm 0.2^*$	$7.5 \pm 0.6^*$	$5.7 \pm 0.9^*$
Wall thickness [μm]	$23.8 \pm 1.2^*$	$29.7 \pm 3.3^*$	$38.0 \pm 10.5^*$

* $p < 0.05$ between the indicated and both other scaffold types

4.2). Pore sizes measured in the dry scaffolds were, hereby, smaller than NaCl particle sizes and scaffold volumes noticeably increased upon rehydration. Scaffold surface was inversely correlated with the particle size and differed significantly between the preparations with different particle sizes. Overall porosity remained constant and was about 80% for all preparations (Table 4.2). Plotting of the pore size distribution in the different scaffold types shows that the applied NaCl particles produce a range of different pore sizes. The curves of the pore size distributions are therefore overlapping. Porous scaffolds produced with the smallest grain size show the highest homogeneity in pore size, as indicated by the narrow peak of the curve (Figure 4.3).

To determine the influence of different pore sizes on the mechanical properties of silk scaffolds stepwise, stress-relaxation indentation testing was performed (Figure 4.4). The average equilibrium modulus was 30.8 ± 5.2 kPa for scaffolds with small, 38.4 ± 22.6 kPa for scaffolds with medium and 48.2 ± 14.9 kPa for scaffolds with large pores (Figure 3.4A). The instantaneous modulus was 69.2 ± 21.0 kPa for scaffolds with small, 68.0 ± 30.3 kPa for scaffolds with medium and 86.5 ± 26.3 kPa for scaffolds with large pores (Figure 3.4B). Both equilibrium and instantaneous modulus had a high standard deviation and were not significantly different for the different scaffold types. Thickness was

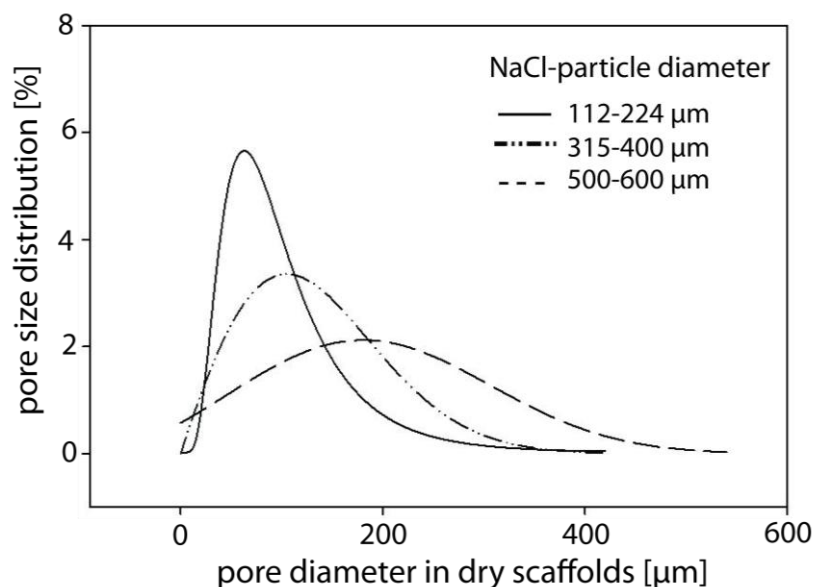


Figure 4.3: Pore size distribution measured in dry silk scaffolds produced with small (112-224 μm), medium (315-400 μm) and large (500-600 μm) NaCl particles. $N = 6$.

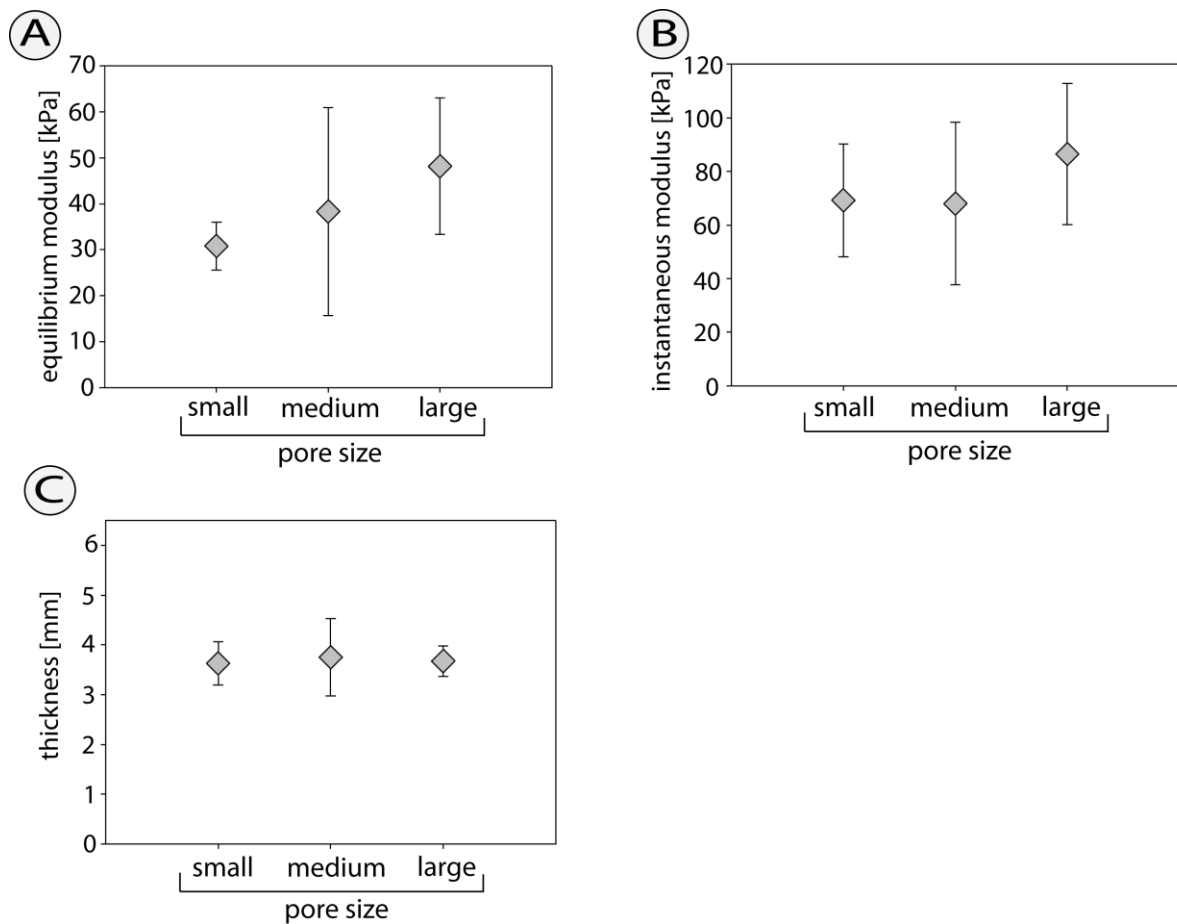


Figure 4.4: Mechanical properties of silk scaffolds. **A:** Equilibrium modulus and **B:** instantaneous modulus of silk scaffolds with small, medium and large pores. **C:** Thickness of scaffolds with different pore sizes. Values displayed as mean \pm S.D., $n = 6$.

determined to be approximately 3.7 mm and was not significantly different between the scaffold types (Figure 4.4C).

After 14 days of culture, an alamarBlue® assay was performed to measure metabolic activity of cells as an indicator of cellular viability. Absorption was normalized to DNA content to account for possible different cell numbers on the scaffolds. Pore size had no effect on the metabolic activity of cells cultured on the different scaffolds (Figure 4.5).

4.1.4 Discussion

Silk scaffolds with different pore sizes and a constant porosity were produced as confirmed by micro-CT measurements. However, although mean pore diameters differed significantly some heterogeneity in the pore sizes was observed.

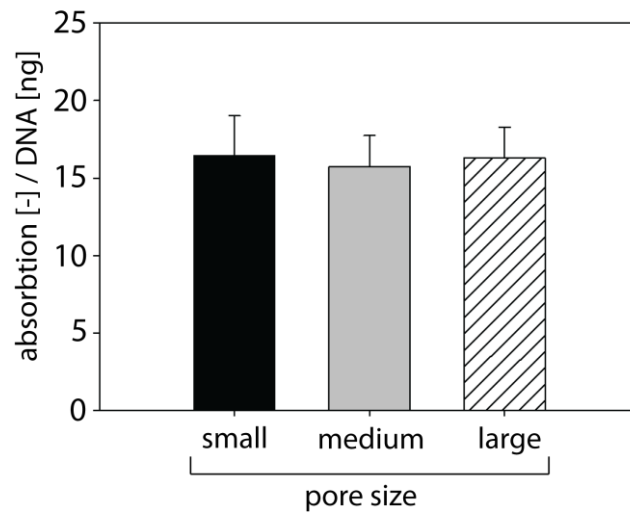


Figure 4.5: Metabolic activity of cells cultured on scaffolds with different pore sizes as determined by an alamarBlue® assay. Values displayed as mean + S.D., $n = 6$.

The average pore diameter was hereby markedly below the diameter of the porogens. Due to the low X-ray absorbance of silk, the scaffolds had to be dried and measured in air. Pore sizes are likely to be larger, and therefore more similar to the size of the porogens, in the hydrated state they adopt under cell culture conditions. In contrast to findings of other groups [11, 174], no increase in stiffness with decreasing pore size was observed. However, an indentation test was applied for the mechanical testing of the scaffolds in this study while the respective studies applied confined compression tests. Indentation tests determine the stiffness more locally, thus, where the sample is indented. In compression tests, these local differences are not detected since only the average mechanical properties of the whole scaffold are determined. Cells will, however, sense the local mechanical properties. Porous scaffolds are not likely to display a homogeneous architecture and consequently no homogeneous mechanical properties. The high standard deviations of the mechanical properties reflect this. Another deviation might be derived from different scaffold processing methods. In contrast to other studies, I performed mechanical testing on autoclaved scaffolds to resemble the mechanical properties of the scaffolds under cell culture conditions. The autoclaving process might additionally influence the mechanical properties and also decrease the stiffness of the scaffolds.

In conclusion, the porous system might be used to study the effect of pore size on the

chondrogenic phenotype and cellular behavior, since cellular viability was not decreased in any of the scaffold types and pore sizes were significantly different. However, the mechanical characterization of the porous system indicates that porous scaffolds do not provide a suitable setting to study cellular stiffness sensing, due to their heterogeneous architecture and, thus, the lack of significant differences in the elastic moduli of the different scaffold types.

4.2 Chondrocyte response to pore size

4.2.1 Introduction

Although porous systems do not seem to provide an optimal setting to study cellular stiffness sensing, they may be used to gain further insight into a possible contribution of the scaffold architecture on chondrocyte behavior. Pore size is likely to be changed in a certain, although possibly very small, range in most systems used to study cellular response to matrix elasticity. The influence of pore size on chondrocyte behavior should, therefore, be investigated in order to later on separate effects from different pore sizes from effects of the substrate elasticity. Besides the investigation of the influence of pore size on cellular behavior, this study should also help to obtain further knowledge about possible pitfalls that should be avoided when designing a system to study the influence of physical matrix properties on cellular behavior. I hypothesized that pore size would influence chondrocyte distribution, proliferation and differentiation stage.

To investigate this hypothesis, primary chondrocytes were cultured on silk scaffolds with different pore sizes for up to 28 days. Cellular distribution and proliferation in the different scaffolds as well as ECM quantity and quality was assessed during and after the culture period.

4.2.2 Materials and Methods

All chemicals were obtained from Sigma-Aldrich (Buchs, Switzerland) and of pharmaceutical grade, unless stated otherwise.

Scaffold production

Scaffolds were produced and characterized as described in **Chapter 4 Section 1**.

Cell culture

Porcine chondrocytes from the condyles of three to six month old pigs were isolated and characterized as described previously [184]. Viability was between 97% and 99% for all isolations used. Basal culture medium was composed of RPMI 1640 Medium, with GlutaMAX™ and 25 mM HEPES, supplemented with 10% fetal calf serum (FCS), 1% antibiotic/antimycotic solution (all from Invitrogen, Basel, Germany). After isolation, cells were resuspended in RPMI media supplemented with 20% FCS and 10% dimethylsulfoxide (Roth, Karlsruhe, Germany) at 10×10^6 cells/ml, and frozen in liquid nitrogen for storage. Upon thawing, 20×10^6 chondrocytes were plated overnight in a 75 cm² cell culture flask (Biochrom, Berlin, Germany), detached by trypsinization and counted for seeding on the scaffolds.

Sterile 96-well plates were covered with thin layers of agarose to prevent cellular attachment. One scaffold was placed into each well and 1×10^6 cells dissolved in 20 μ l culture medium were pipetted on each scaffold. Cells were allowed to attach for 3 h at 37°C and 5% CO₂. 100 μ l medium was added into each well and constructs were incubated for another 21 h before they were transferred into 24-well plates for the rest of the culture period. Cells were cultured in basal culture medium supplemented with ascorbic acid 2-phosphate (50 μ g/ml) for up to 28 days. Medium was changed three times per week.

Quantitative assays

Specimens for quantitative assays were lyophilized and the dry weight was determined. Each sample was then digested for 16 h with 0.6 ml papain solution (2.375 U/ml; Worthington, Lakewood, USA) in buffer (0.1 M disodium hydrogen phosphate, 0.01 MEDTA disodium salt, 14.4 mM L-cysteine), at 60°C. One part of the digest was directly used to determine the GAG content; one part was frozen at -20°C, to subsequently determine the DNA content.

Glycosaminoglycan content was determined in triplicates, spectrophotometrically at 525 nm,

following binding to the dimethylmethylene blue dye (AxonLab, Baden Dättwil, Switzerland) dissolved at 16 mg/l in 0.01 M HCl with 40.5 mM Glycine and 40.5 mM NaCl. Chondroitin sulfate was used as a standard.

DNA content was measured fluorometrically from a 96-well black flat-bottom microtiter plate, by using the PicoGreen assay (Molecular Probes, Basel, Switzerland), according to manufacturer's instructions (excitation wavelength, 480 nm; emission wavelength, 528 nm).

Histology

All samples were analyzed with the microscope Axioskop (ZEISS, Oberkochen, Germany) using the acquisition software Axiovision (Release 4.7, ZEISS, Oberkochen, Germany).

Cryosection preparation

Upon removal, samples for histology were placed into plastic molds, immersed in embedding solution (Cryomold® Biopsy Tissue-Tek® and O.C.T. compound® Tissue-Tek® both Sakura Finetek Europe, Zoeterwoude, Netherlands), snap frozen in liquid nitrogen, and stored at -20°C . Cryosections of 12 μm thickness were prepared, using the Cryo-Star HM 560 cryostat (Microm International AG Schweiz; Volketswill, Switzerland), transferred to SuperFrost® Plus glass slides (Menzel, Braunschweig, Germany) and allowed to dry at room temperature (RT) for at least one day.

Immunohistochemistry (IHC)

For collagen type II IHC, cryosections were fixed for 5 minutes with pre cooled (-20°C) methanol-acetone (7:3). Non-specific binding was blocked with 2% BSA in PBS for 30 min at RT. Specimens were incubated with the primary antibody for 1 h at 37°C , washed extensively, and incubated with the secondary antibody under the same conditions. The primary antibody against collagen type II (II-II-6B3, Developmental Studies Hybridoma Bank, University of Iowa, USA) was applied in PBS with a dilution of 1:50. Negative controls were incubated in PBS only.

Detection in all samples, and negative controls, was performed with FITC-conjugated goat anti-mouse IgG (Invitrogen, Basel, Switzerland) diluted 1:500 in PBS. DNA was

stained with Hoechst 33258 in UPW (1 μ g/ml) for 15 min at 37°C; samples were washed extensively with PBS, and embedded.

Histological stains

For Haematoxylin and Eosin (H&E) stain, sections were fixed in 5% formaldehyde, washed in PBS, stained in Haematoxylin solution, stained in Eosin solution (Eosin Y solution), dehydrated and cleared in graded ethanol solutions and xylene, and mounted. For Alcian blue staining for proteoglycans, Alcian blue working solution was prepared by dissolving 0.025 % (w/v) Alcian blue (Alcian blue 8GX) in 3% (v/v) acetic acid (Carlo Erba, Rodano, Italy) containing 0.15 M sodium chloride, and 0.06 M magnesium chloride (Hänseler AG, Herisau, Switzerland). The solution was stirred for 3 h, filtered, and stored at RT. Cryosections were washed with PBS, fixed in 5% formaldehyde for 30 min at RT and incubated in Alcian blue working solution overnight. Sections were washed in PBS, nuclei were stained in Haematoxylin solution (Haematoxylin solution according to Delafield) for 2 min, blued in tap water, washed in PBS and embedded.

Scanning electron microscopy (SEM)

For SEM analysis, specimens were removed after 28 days of culture, fixed for 4 h at 4°C in 2.5% glutaraldehyde in 0.1M sodium cacodylate buffer, washed thoroughly and incubated in 0.04% osmium tetroxide in 0.1M sodium-cacodylate buffer for 90 min at RT in the dark. Specimens were washed, dehydrated in graded ethanol solutions, and lyophilized. Dry specimens were sputtered with gold and analyzed by SEM (Zeiss Leo Gemini 1530, Cambridge, UK).

Statistical analyses

All statistical analyses were performed with the SPSS 17.0 software (SPSS inc., Chicago, USA). Statistical significance was determined by an ANOVA followed by post hoc comparisons using Fisher's LSD. $P < 0.05$ is considered statistically significant. DNA content, GAG content and GAG/DNA were analyzed separately with time of culture and NaCl grain size as fixed factors.

All results are displayed as mean \pm standard deviation (SD). Sample size is $n = 6$ unless stated otherwise.

4.2.3 Results

DNA content increased significantly over the whole culture period and was similar on the three different scaffold types used (Figure 4.6A). However, over the course of the culture period, neither DNA nor GAG content differed significantly on the three scaffold types.

Cell and ECM distribution was further visualized by histological staining. H&E stained sections (Figure 4.7) show that cells were not evenly distributed on the scaffold: A thick layer of tissue was formed at the rim and cell numbers visibly decreased towards the center of the scaffolds. The same trend was observed on Alcian blue stained sections (Figure 4.8) with thick layers of ECM at the rim and less ECM in the center of the scaffold. Scaffolds with small pores showed a seemingly better distribution of cells in the scaffolds compared to scaffolds with medium and large pores. The ECM, formed during the 28 days of culture, was rich in GAGs (Figure 4.8) and collagen type II (Figure 4.9), a marker for the differentiated phenotype of chondrocytes. Collagen type II was found independently of the pore size and was generally found in higher density at the rim when compared to the center of the scaffolds.

SEM images of the tissue engineered constructs after 28 days of culture (Figure 4.10) additionally showed that most cells exhibited a round morphology, typical for the differentiated, chondrogenic phenotype and that the major part of the scaffold surface was covered with a layer of cells and ECM.

4.2.4 Discussion

None of the tested pores sizes diminished or favorably increased cellular viability or growth and DNA content increased over the whole culture period. All scaffold types showed a thick layer of cells and ECM at the rim of the scaffold and visibly diminished amounts of cells and ECM in the center. This is in agreement with a study from Wang et al. [48] in which chondrocytes were redifferentiated on silk scaffolds. Chondrocytes were found in high density in a thin outer layer and a lower density in the center of the scaffolds. However, cell numbers in the scaffold centers were still visibly denser than in

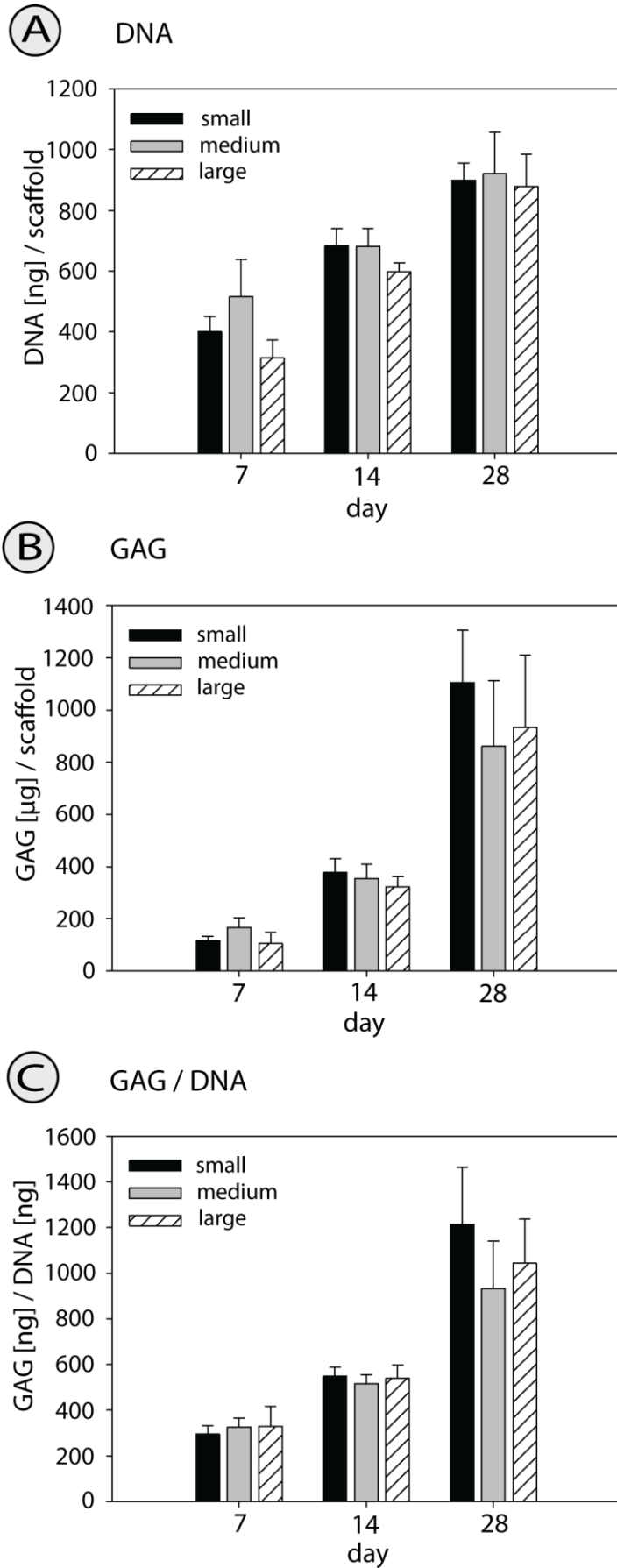


Figure 4.6: Quantitative assays of **A:** DNA content, **B:** GAG content and **C:** GAG/DNA in scaffolds with small, medium and large pores. Neither DNA nor GAG or GAG/DNA differed significantly between the different scaffold types over the time of culture. Values displayed as mean + S.D., n = 6.

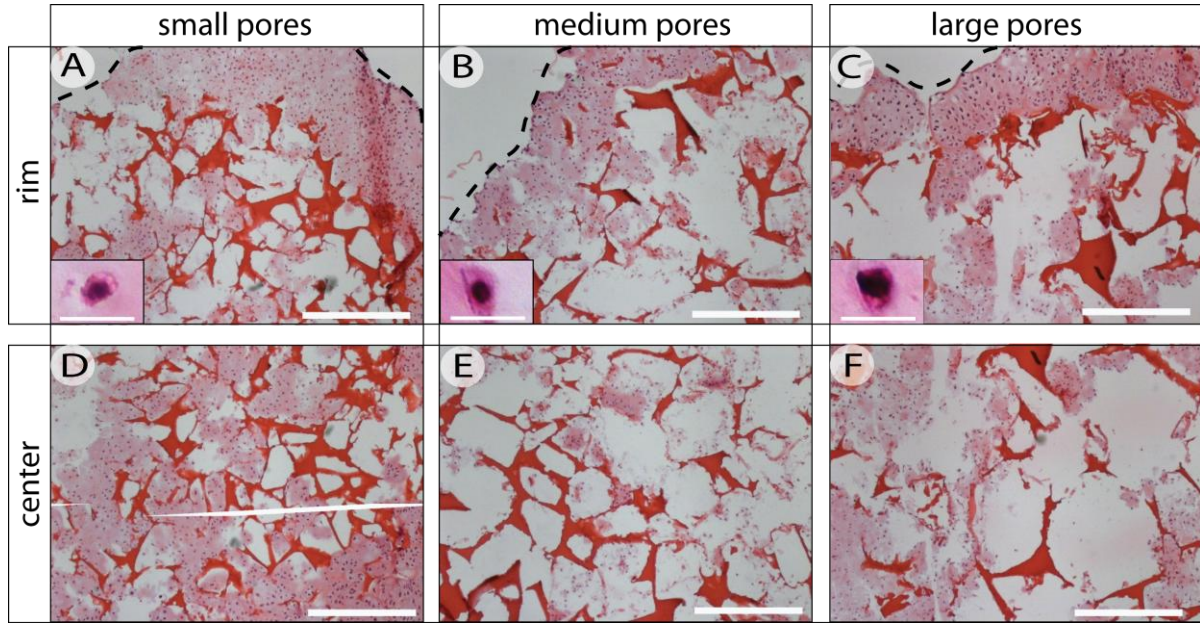


Figure 4.7: H&E stain after 28 days of culture on scaffolds with **A, D** small pores; **B, E:** medium pores and **C, F:** large pores. Top row: images taken from the rim (indicated by the black, dashed line) of the scaffolds. Bottom row: images taken from the center of the scaffold. Cell density is higher at the rim of the scaffolds independent of the pore size. Scale bar: 500 μm . Scale bar in close-up insertions: 20 μm .

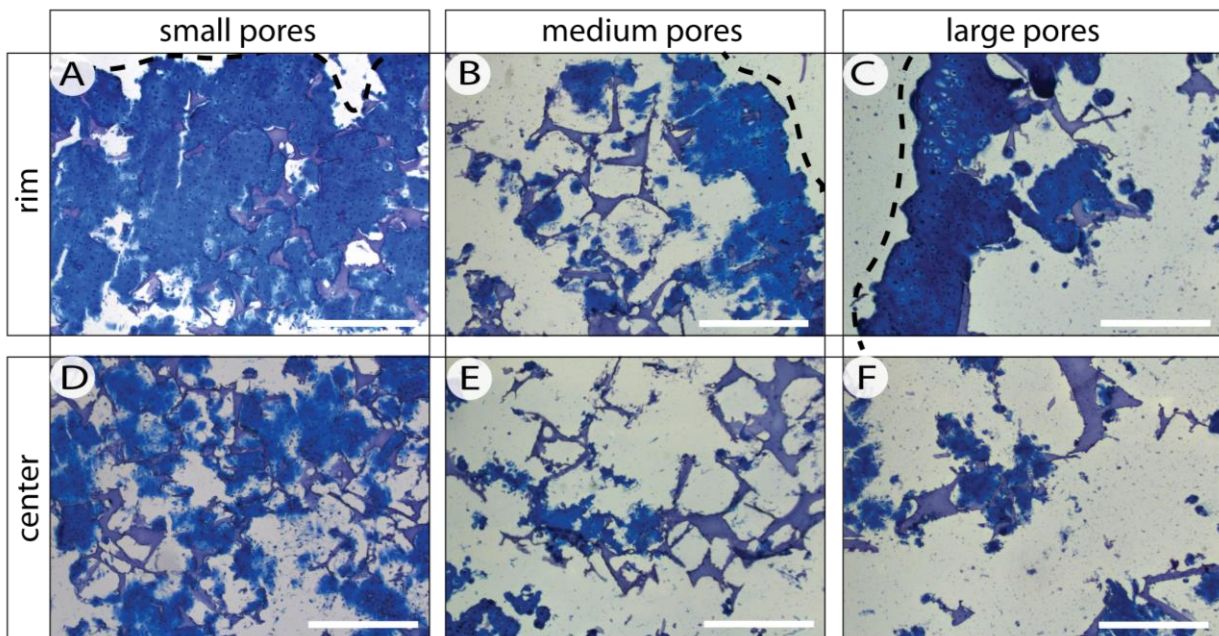


Figure 4.8: Alcian blue staining for GAGs after 28 days of culture on scaffolds with **A, D** small pores; **B, E:** medium pores and **C, F:** large pores. Top row: images taken from the rim (indicated by the black, dashed line) of the scaffolds. Bottom row: images taken from the center of the scaffold. Distribution of GAGs reflects cellular distribution seen on H&E stained sections. Scale bar: 500 μm .

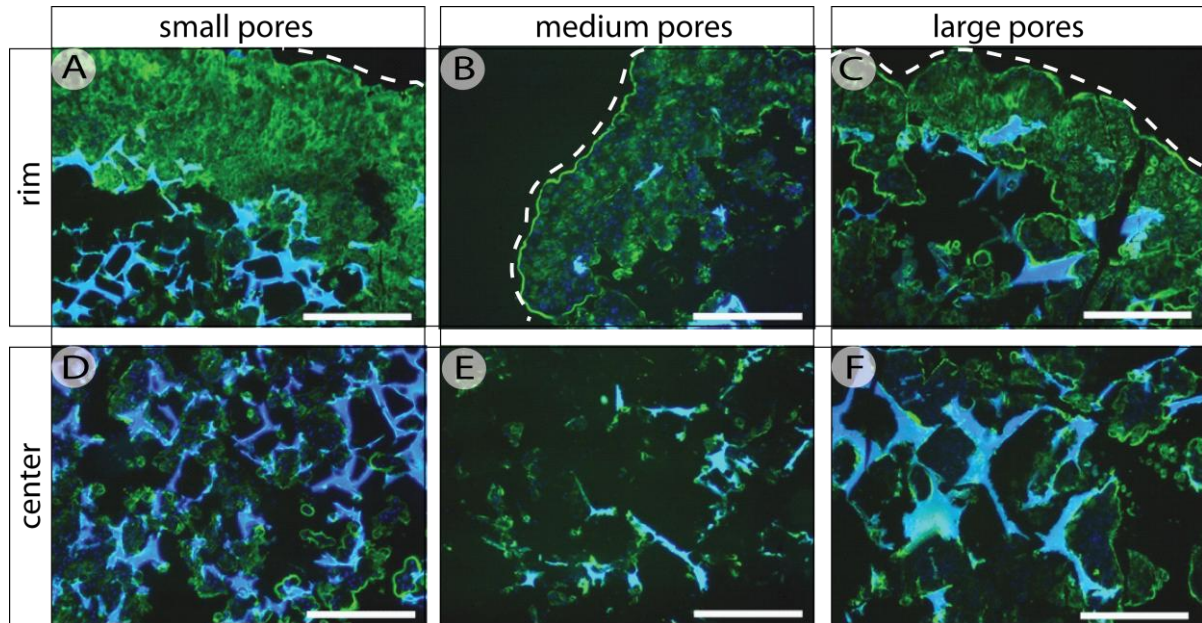


Figure 4.9: IHC for collagen type II after 28 days of culture on scaffolds with **A, D** small pores; **B, E**: medium pores and **C, F**: large pores. Top row: images taken from the rim (indicated by the white, dashed line) of the scaffolds. Bottom row: images taken from the center of the scaffold. Scale bar: 500 μm .

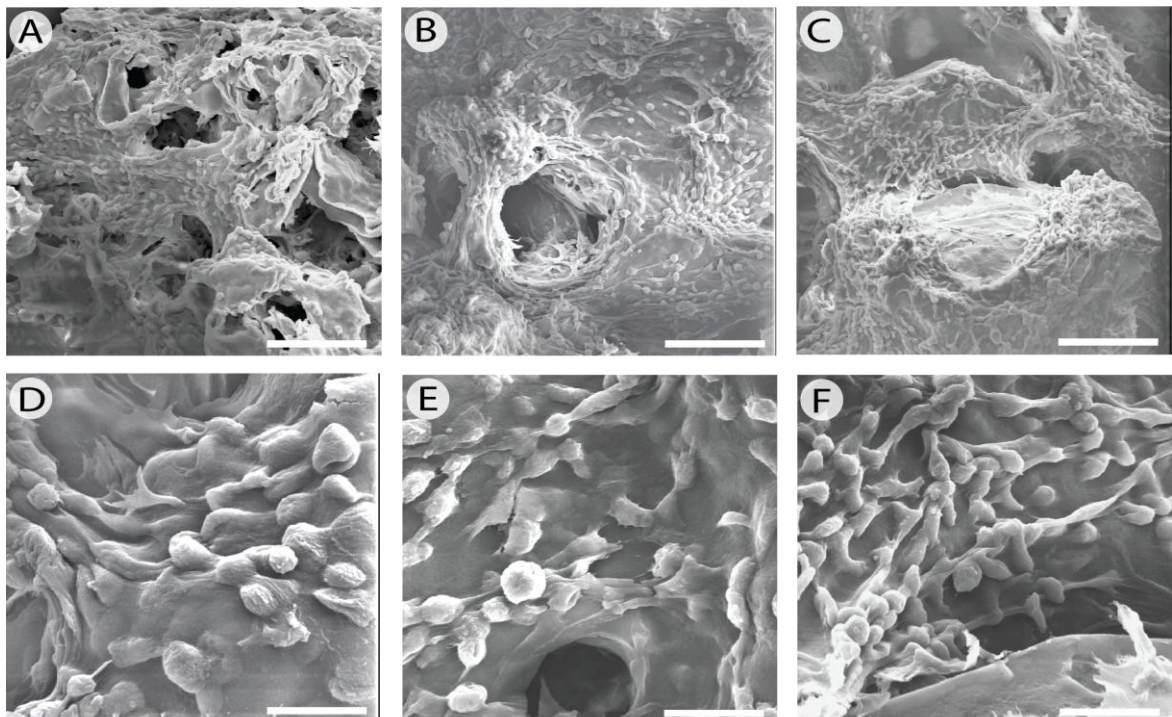


Figure 4.10: SEM images of chondrocytes cultured on porous silk scaffolds with **A, D**: small pores; **B, E**: medium pores and **C, F**: large pores. Scale bar **A-C** = 130 μm . Scale bar **D-F** = 30 μm . Independent of the pore size, thick layers of cells and ECM are formed and the majority of cells displays a round morphology.

the study presented here.

Surprisingly, scaffolds with small pores showed a slightly better distribution of cells and ECM compared to scaffolds with medium and large pores. It also has to be noted that the cells formed large ECM-clusters in all scaffolds types, leading to limited contact to the silk substrate. A significant effect of pore sizes on ECM deposition and cellular proliferation and attachment could not be found. The tested silk scaffolds seemed to support the maintenance of the chondrogenic phenotype, as shown by the round morphology of cells and the high amount of collagen type II that was produced. Maintenance of the chondrogenic phenotype was, however, also independent of the pore size. While a better cell distribution was found in scaffolds with the smallest pore size, no significant influence of pore size on cellular behavior as proliferation, ECM production and maintenance of the chondrogenic phenotype was observed.

It might, therefore, be cautiously concluded that studies about stiffness sensing in other systems (that can control the cell distribution) would not have to account for a possible effect of pore size on the above mentioned aspects of cellular behavior. However, summing up findings from this and the previous section, several main issues render this porous system unsuitable to study stiffness sensing. While some of them might only be valid for the system presented here others generally reflect the limitations of porous systems for this application. 1: porous systems are likely to display heterogeneous mechanical properties, 2: due to the large size of the pores in relation to the cell size, cells form aggregates which in turn vastly limits the contact of cells with the material 3: cells are not equally distributed. Taken together, the local environment of single cells within one scaffold can be very different depending on where in the scaffold the cell is located. The environment of the cells is, furthermore, not mainly determined by the material properties due to the formation of aggregates.

The following chapter takes into account the findings from this, and the previous, section and aims to design a controlled environment that is suitable to study stiffness sensing in a 3D environment.

5 Chondrocyte response to matrix elasticity in a 3D hydrogel system

5.1 Development of a tunable 3D hydrogel system

5.1.1 Introduction

The previous chapter identified certain pitfalls that should be avoided in a suitable model system. Based on these, requirements can be identified that the system should fulfill. It should 1: provide homogeneous mechanical properties 2: allow an alteration of the mechanical properties without changing the architecture or the microstructure of the material and 3: allow an equal distribution of the cells in the material. The first aim in this chapter was the development of a model system that fulfills these requirements and, therefore, provides a suitable environment to transfer previous research from the 2D PA setting into a 3D system, more closely mimicking *in vivo* conditions.

As in 2D, hydrogels seem to be a good choice to achieve this aim, due to their relatively high homogeneity. An additional advantage is the range of stiffnesses that can be produced, which is very similar to the range of stiffnesses seen in soft tissues [74]. Cells also have direct contact to the substrate and, as described in the second chapter, pore sizes of hydrogels only change in the nanometer range when the mechanical properties are altered.

One remaining challenge of hydrogel systems is a separation of mechanical properties and adhesion site densities. An alteration of adhesion site density has been shown to induce similar effects to an alteration of mechanical properties [89, 90, 139, 185]. This side effect is very likely in protein based systems where different elasticities are often achieved by changing the protein concentration. As in the 2D PA system presented in Chapter 3, one possibility to overcome this problem is the application of an inert bulk material with tunable mechanical properties that can then be modified with a controlled number of adhesion sites. However, PA cannot be used as a material for 3D studies since cells cannot be incorporated into the material due to the toxicity of unpolymerized PA monomers [173]. Another synthetic material, PEG, has been applied as an inert 3D system with tunable elastic properties to culture different cell types [2, 58, 80, 134, 186,

187]. Respective studies with chondrocytes, however, did not facilitate active stiffness sensing since no adhesion sites were incorporated [3, 131].

I chose to develop an agarose-based model system since agarose was shown to be highly compatible with chondrocytes in various studies over the last few decades [188, 189]. Agarose is a marine algal polysaccharide, consisting of alternating D-galactose and 3,6-anhydro-L-galactose units, that forms thermally reversible gels [190]. It is soluble in water at temperatures between 45°C and 65°C and gels in a range of 17-40° C depending on the degree of hydroxyethyl substitutions on its side chains [5]. Cells can therefore be incorporated into the material in its liquid form and the material can then be gelled at lower temperature to facilitate hydrogel formation. Agarose does not contain any moieties associated with cellular adhesion or absorption of cell adhesive proteins [60]. Several papers about the correlation between molecular weight, the molar concentration of the agarose and the mechanical properties of the gel have been published [5, 123, 191]. Agarose discs with elastic moduli ranging from less than 1 up to 300 kPa have been produced [189, 192] allowing to cover a significant range of stiffnesses.

To facilitate cellular attachment, one type of agarose, Seaprep® agarose, has been modified with RGD, the minimal amino acid sequence known to provide cellular adhesion. [193] It was coupled to the agarose with the commercially available, heterobifunctional crosslinker Sulfo-SANPAH (Pierce, Rockford USA) that was also applied in the 2D model system. The crosslinker forms stable amide bonds with amino groups and can be reacted with a variety of proteins and subsequently coupled to the agarose through UV exposure.

I hypothesized, that RGD-modified agarose can be used to produce an improved 3D culture system that can be used to study chondrocyte response to matrix elasticity. To test this hypothesis, I aimed to examine if (1) hydrogels with stable and tunable mechanical properties can be produced with the help of agarose, if (2) a controlled number of adhesion sites can be coupled to agarose and if (3) chondrocytes interact with the adhesion sites and remain viable in the modified hydrogels. For this purpose, two different types of low gelling agarose: Type VII and Seaprep® agarose were tested for their suitability for the development of a model system with tunable mechanical properties. The modification

process of agarose with adhesion sites was optimized and cellular interaction with the moieties and maintenance of chondrocyte viability was verified.

5.1.2 Material and Methods

Reagents were obtained from Sigma-Aldrich (Buchs, Switzerland) and of pharmaceutical grade, unless stated otherwise.

Hydrogel modification

Low gelling agarose (Type VII) was dissolved in Ca^{2+} - and Mg^{2+} -free PBS and autoclaved. The amount of solution evaporated during autoclaving was determined by weighing, and replaced accordingly.

The synthetic peptide GRGDSP (Bachem AG, Bubendorf, Switzerland) was conjugated to agarose hydrogels with the help of the heterobifunctional, UV-activatable crosslinker sulfo-SANPAH (Pierce, Rockford, USA), according to a modified protocol adapted from [119, 193]. Briefly a reaction was performed with the crosslinker and the respective peptides in ten molar excess for 4 h at room temperature (RT) in the dark. Agarose hydrogels were melted for 5 minutes at 65°C and cooled to 37°C. One part crosslinker-peptide mix was then thoroughly mixed with an equal volume of a 3% agarose solution under sterile conditions to obtain a 1.5% solution.

Based on manufacturer's recommendations, three different conditions were chosen and tested to obtain optimal activation of the crosslinker: (1) Activation with a 308 nm, 8 W UV-handlamp for eight minutes; (2) activation with a 300 W medium-pressure mercury arc lamp for five minutes; (3) activation with a 450 W medium-pressure mercury arc lamp for three minutes, the latter two both equipped with a filter to exclude excitation below 302 nm.

The solutions were gelled at 4°C and washed in PBS for seven days, with frequent changes of the solution, to remove unbound peptide and crosslinker.

The amount of coupled protein was determined with a Bradford assay (Bradford Reagent), according to the manufacturer's instructions. One part of a 1.5% agarose-

hydrogel, modified with 400 μM of RGD or RGE, was then mixed with one part 5.5% agarose to obtain gels with 200 μm protein and 3.5% plain agarose, or with one part PBS to obtain 0.75% agarose-hydrogels.

Mechanical testing of the gels

A preliminary test was performed to determine the stability of mechanical properties under cell culture conditions and choose the type of agarose suitable for a model system.

Solutions of 5% Seaprep agarose (Lonza, Basel, Switzerland) and 5% Type VII agarose were prepared in UPW and autoclaved. The amount of water evaporated during autoclaving was determined and replaced accordingly. Agarose hydrogels were melted in the water bath at 65°C for 5 min. Eight samples of each agarose type were prepared by gelling the solutions between two glass slides, in custom made spacers, to obtain disc shaped samples, with a diameter of 5 mm and a height of 2 mm. Gels were allowed to gel at 4°C for 15 min. Four Samples of each agarose type were stored in PBS at 4°C for 7 days while another 4 samples of each type were stored at 37°C for the same time period.

Solutions for specimens of different percentage of plain and modified agarose were prepared and gelled to obtain disc shaped specimens as described above. Gels were stored in PBS at 4°C until testing. Prior to testing, gels were allowed to equilibrate to RT, placed into a custom built, confined, testing chamber and covered with PBS. Mechanical testing of scaffolds was performed with a Zwick materials testing machine (Zwick Z005, Ulm, Germany) at RT in PBS as described in Chapter 4, Section 1 and adapted for the hydrogels. A preload of 2 mN was applied, and stepwise, stress-relaxation indentation was carried out in three strain steps of 5%, 15% and 25% of the measured sample thickness. After each indentation step, the relaxation response was measured for 30 min, when equilibrium was reached.

The instantaneous modulus was determined from the slope of the stress-strain curve obtained during the first step, at a constant strain rate of 100 mm/min. The equilibrium modulus was determined from the equilibrium phase of the three indentation steps as presented earlier.

Cell culture

Porcine chondrocytes from the condyles of three to six month old pigs were isolated and characterized as described previously [184]. Viability for all isolations was between 97% and 99%. Culture medium was composed of RPMI 1640 Medium, with GlutaMAX™ and 25 mM HEPES, supplemented with 10% fetal bovine serum (FBS), 1% antibiotic/antimycotic solution (all from Invitrogen, Basel, Switzerland) and ascorbic acid 2-phosphate (50 µg/ml). Upon thawing, 20×10^6 chondrocytes were plated overnight in a 75 cm² cell culture flask (TPP, Trasadingen, Switzerland) to maintain only viable cells, and thus precise cell numbers for seeding.

For cell incorporation into hydrogels, modified agarose was melted for 5 min at 60°C and allowed to cool to 37°C. Cells were detached from the flask by trypsinization and counted with the help of a Neubauer counting chamber (Neubauer improved, Assistant, Sondheim, Germany). Cells were incorporated into the hydrogels with a density of 4.5×10^6 cells/ml. An according volume of cell suspension was centrifuged for 10 minutes at 300 g, the supernatant was removed and the cell pellet was thoroughly mixed with the agarose. For each sample, 25 µl of cell-agarose suspension was pipetted into spacers between two glass slides to obtain discs with a diameter of 4 mm and a height of 2 mm. Cell-hydrogel constructs were allowed to gel at 4°C for 15 minutes and removed from the spacers. Random samples were taken in all experiments to assure constant seeding densities in the different preparations. Constructs were cultured in free-floating conditions in 24-well plates (TPP, Trasadingen, Switzerland) in the culture medium described above.

Cellular viability and attachment

LIVE/DEAD® assay:

Specimens were stained with a LIVE/DEAD® Viability/Cytotoxicity Kit (Invitrogen, Basel, Switzerland) according to manufacturer's instructions, with a 4 µM EthD-1 and 2 µM calcein AM solution, after three days of culture. Specimens were transferred to PBS and immediately investigated under the fluorescence microscope.

AlamarBlue® assay:

The alamarBlue[®] assay was performed according to manufacturer`s instructions, with a 1:10 dilution of alamarBlue[®] reagent (Invitrogen, Basel, Switzerland) in basal culture medium and an incubation time at 37°C of 4h. Absorption was read with an excitation of 560 nm and emission at 590 nm (590 nm cutoff). Samples were then processed as described below, to determine the DNA content.

Cellular attachment

24-well plates (TPP, Trasadingen, Switzerland) were coated with thin layers of RGD-modified agarose, RGE-modified agarose, agarose from a reaction with the crosslinker only, and plain agarose, respectively. Gels were allowed to gel at 4°C for 20 minutes. Primary chondrocytes were seeded on top of the different substrates and on cell culture plastic, as a reference, with a density of 10 000 cells/cm². Cells were allowed to attach for 24 h. All wells were thoroughly washed with PBS to remove unbound cells. Attached cells were counted under a light microscope: 5 viewing fields of 10x magnification were counted per sample and averaged.

Statistical analysis

All statistical analyses were performed with the SPSS 17.0 software (SPSS Inc., Chicago, USA). Statistical significance was determined by ANOVA followed by Fisher`s LSD with a significance level of $p < 0.05$. Instantaneous modulus and equilibrium modulus were analyzed separately with percentage of agarose as fixed factor and thickness as covariate. Linear regression fits for mechanical testing data were obtained using Microsoft Excel 2000 (Microsoft Corporation, Redmond, USA). All results were displayed as mean \pm SD. Sample number was $n = 4$ unless stated otherwise.

5.1.3 Results

Mechanical stability

The preliminary study investigated the mechanical stability of type VII and Seaprep[®] agarose. The equilibrium modulus of Type VII agarose did not significantly change with time in culture. Mechanical testing of Seaprep[®] agarose stored at 37°C did not even reach

the preload needed for sample detection, indicating that this type of agarose completely lost its mechanical properties under culture conditions (Figure 5.1). Based on these results, I chose to use agarose Type VII as material for the model system.

Incorporation of adhesion sites

RGD was covalently coupled to Type VII agarose in order to provide adhesion sites and hereby facilitate active stiffness sensing of cells. Three different conditions for coupling were tested. The highest coupling efficiency ($11.8 \% \pm 3.8$) was achieved with the 450 W UV lamp (Figure 5.2 A) in spite of a reduction of exposure time.

To test if cells attached to modified agarose in contrast to plain agarose, an adherence test was performed in 2D: chondrocytes were seeded on top of thin layers of the different substrates, with cell culture plastic as a control, known to provide adherence. Non-adherent cells were removed by thorough washing, and the number of attached cells was determined (Figure 5.2 B). The number of chondrocytes that attached to RGD-modified agarose was not significantly different from the number of cells that attached to cell culture plastic ($p = 0.561$). Cells did not adhere to agarose hydrogels modified with RGE, with the crosslinker alone, or plain agarose.

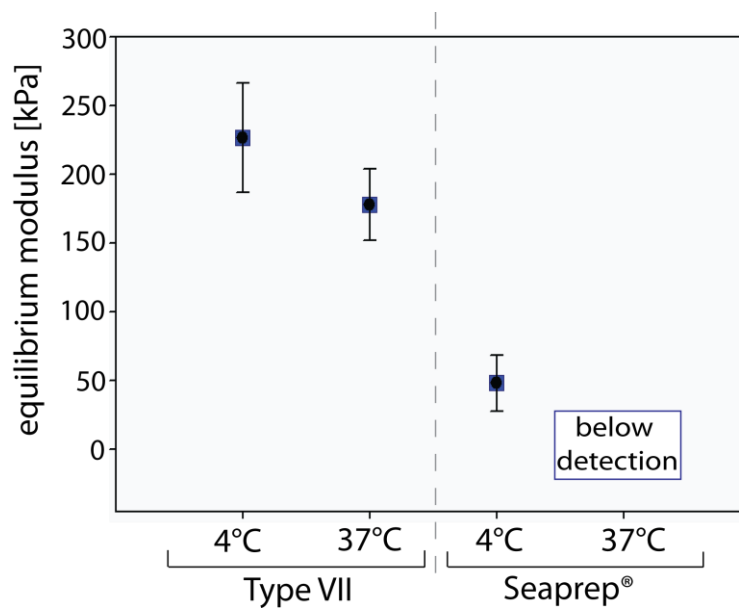


Figure 5.1: Mechanical stability of different types of agarose. Equilibrium moduli of seaprep and type VII agarose hydrogels stored at 4°C or 37°C, respectively.

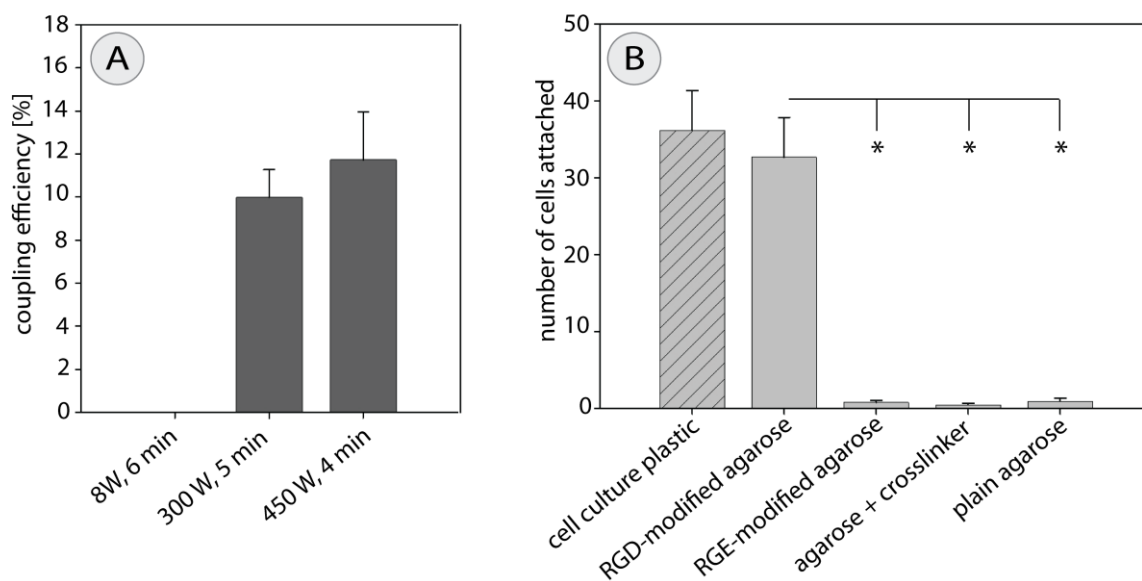


Figure 5.2: Modification with adhesion sites. **A:** Coupling efficiency of the modification process, as determined by Bradford assay. RGD was covalently coupled to agarose with a UV-activatable crosslinker. Coupling efficiency increased with increasing power of the UV lamp, despite a reduction in exposure time. **B:** Cellular attachment to thin layers of agarose. Cells adhered to RGD-modified agarose, while attachment to RGE-modified agarose, agarose with crosslinker only, or plain agarose was not observed. Values displayed as mean + SD, $n = 4$, $*p < 0.05$.

Mechanical tunability

In a next step, the tunability of the elasticity of agarose hydrogels was investigated. Stepwise, stress-relaxation indentation testing was performed to determine the mechanical properties of plain and modified agarose of different concentrations. Specimens reached equilibrium during the relaxation phase of the mechanical test (Figure 5.3 A, C, E) and the slope of the stress-strain curves increased with increasing agarose concentration (Figure 5.3 B, D, F). Equilibrium modulus increased in an almost linear manner with agarose concentration ($R^2 = 0.85$ for RGD-modified and $R^2 = 0.97$ for plain agarose) from 3.7 ± 1.9 kPa to 53.2 ± 14.6 kPa for modified, and from 2.3 ± 1.1 kPa to 36.1 ± 0.3 kPa for plain agarose (Figure 5.4 A, C). A slight stiffening of the material through the modification process was observed, but differences were only significant for the highest concentration of agarose (3.5%, $p = 0.01$). The instantaneous modulus also increased with increasing agarose concentration, from 26.2 ± 11.6 kPa to 82.9 ± 22.4 kPa for modified and from 16.7 ± 5.5 kPa to 89.2 ± 11.4 kPa for plain and agarose (Figure 5.4 B, D).

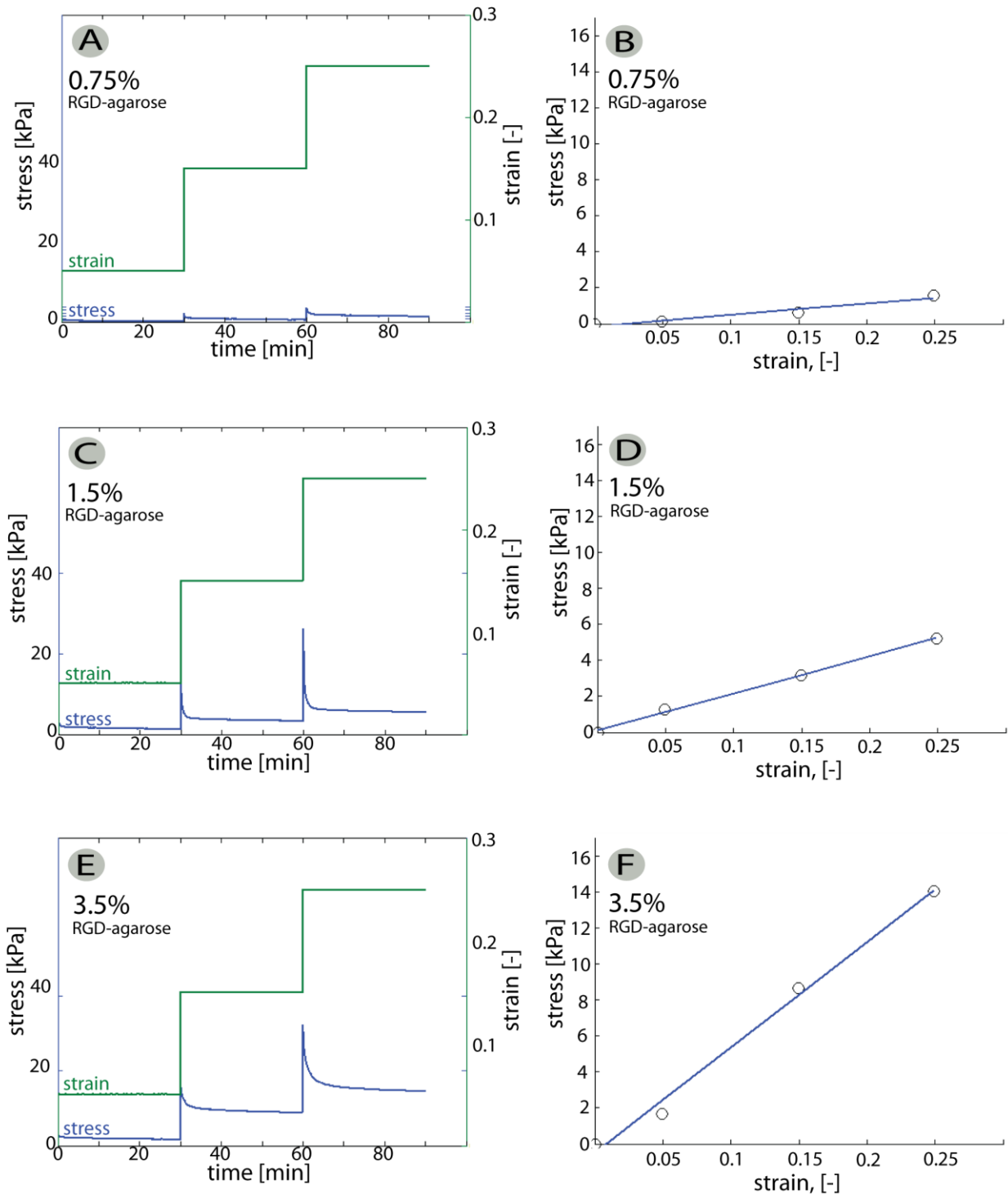
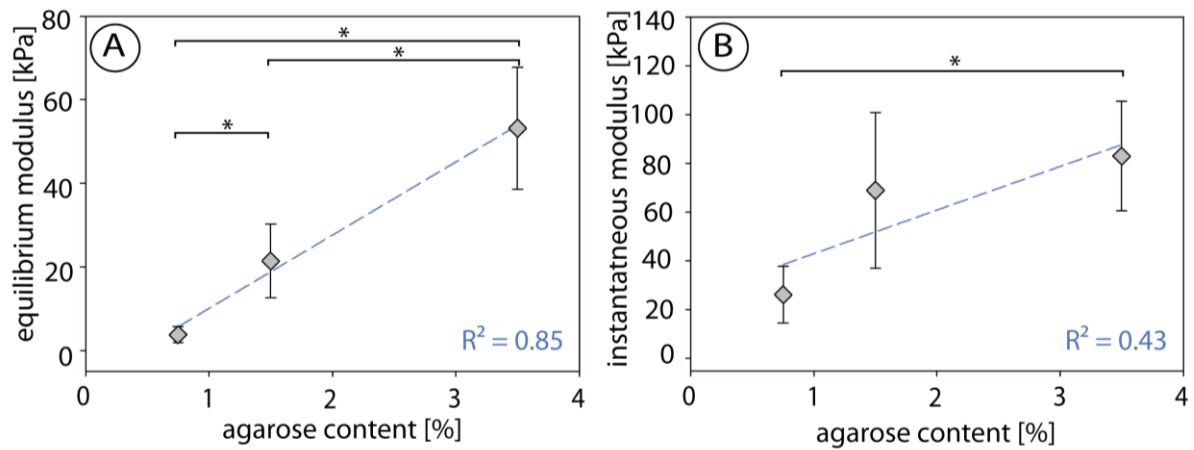


Figure 5.3: Representative stress-strain curves from the mechanical testing of different percentages of RGD-agarose. **A, C, E:** Strain steps and stress responses of hydrogels with different percentages of RGD-agarose plotted against time. Equilibrium is reached during the relaxation phase of all gels. **B, D, F:** Stress values at equilibrium plotted against strain-step values. The slope of the curve, thus the equilibrium modulus, increases with increasing agarose concentration.

RGD - agarose



plain - agarose

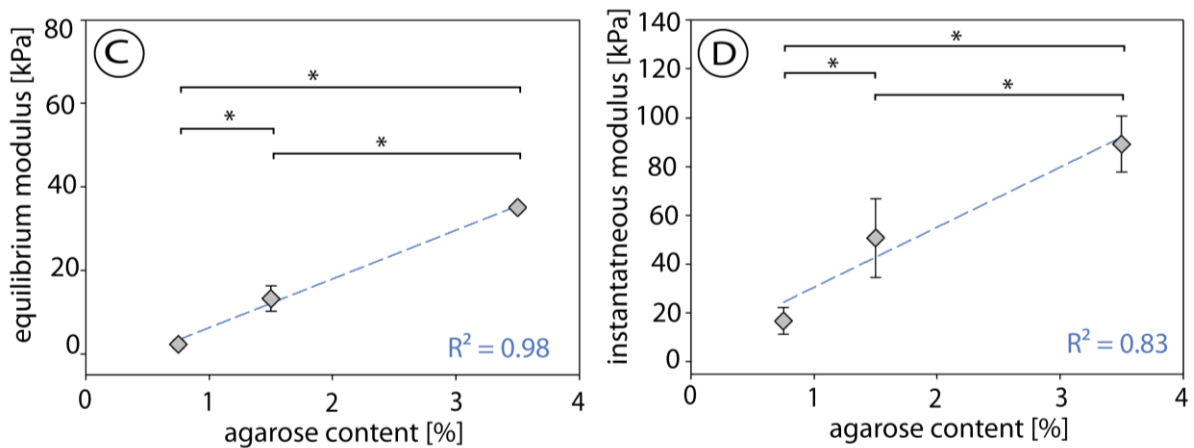


Figure 5.4: Mechanical properties of plain and modified agarose. Mechanical testing of **A, B:** RGD-modified agarose and **C, D:** plain agarose. **A, C:** Equilibrium modulus of gels increases with increasing agarose concentration. **B, E:** Instantaneous modulus of gels increases with increasing agarose concentration. Values displayed as mean \pm SD, the linear regression line was fitted on all data points. $n = 4$, $*p < 0.05$.

Chondrocyte viability in modified agarose

To investigate whether the modification process influenced the viability of chondrocytes incorporated into the material, I performed a Live-Dead assay to stain the viable and dead cells and additionally tested for metabolic activity of the incorporated cells, as a quantitative measure. Chondrocytes remained viable in both, plain, as well as RGD-modified agarose (Figure 5.5 A-C) and incorporation of RGD did not affect metabolic activity (Figure 5.5 D).

5.1.4 Discussion

I performed a preliminary study with different types of agarose and found that Type VII agarose maintained its mechanical properties over time at 37°C, in contrast to Seaprep® agarose, which has been modified with RGD by other groups [193]. Generally, hydrogels made from Type VII agarose were approximately ten times stiffer than hydrogels made with the same concentration of Seaprep® agarose.

Based on these findings, Type VII agarose was chosen for the model system. I showed that agarose without modification is inert and that cells interact with the RGD after modification. Since the choice of ligand can also significantly influence the outcome of a study [194] RGD was chosen, which has been repeatedly used as adhesion molecule in

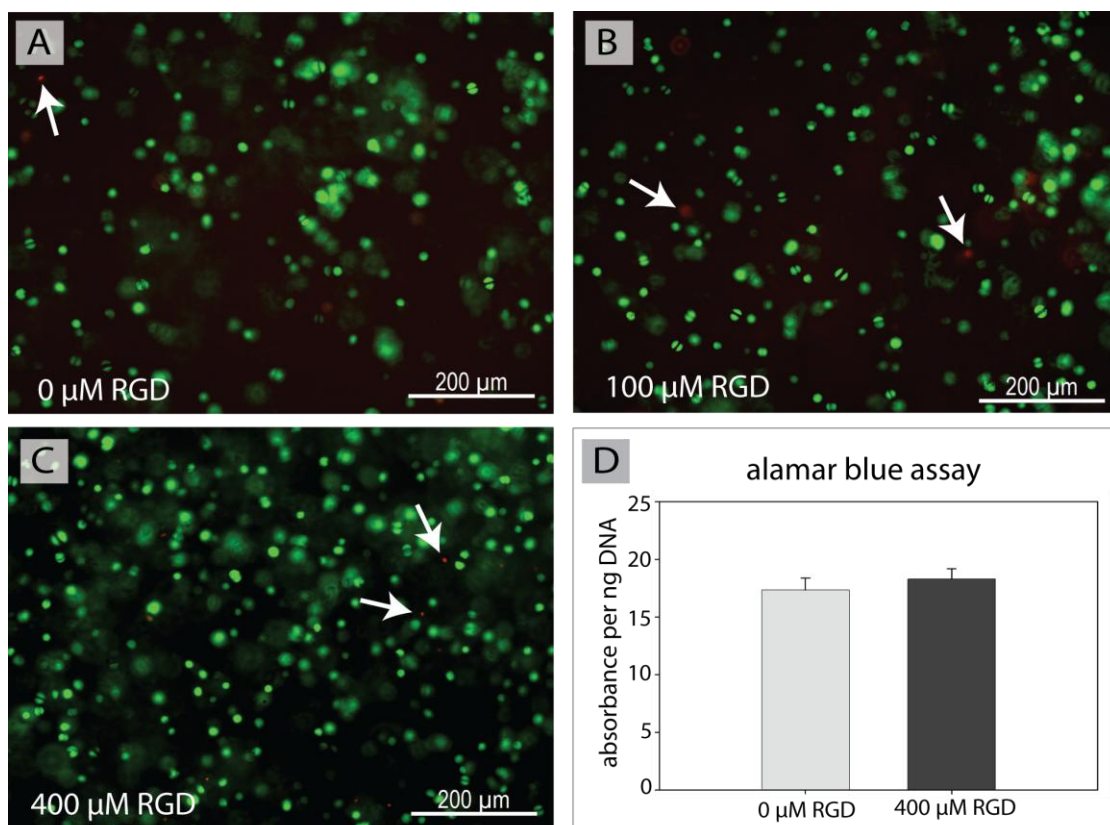


Figure 5.5: Cellular viability. **A-C:** Live-Dead assay of cells incorporated in agarose modified with, **A:** 0 μM RGD, **B:** 100 μM RGD, **C:** 400 μM RGD. Live cells are stained green, dead cells red. Cells remained viable in all compositions, with only very few dead cells as indicated by arrows. **D:** Metabolic activity of cells in modified and unmodified agarose, measured with an alamarBlue® assay and normalized to the amount of DNA in the respective gel. Cells showed no differences in metabolic activity in modified or plain agarose. Values displayed as mean + SD, n = 4, *p < 0.05.

other 3D studies in this field [126, 195].

The second experiment with type VII agarose showed that the mechanical properties of the hydrogels can be tuned by altering concentration of agarose in the gel. Both, instantaneous and equilibrium modulus increased with increasing agarose concentration. No obvious changes in the microstructure were observed, which would confirm findings from other studies where the change of pore size, with a similar change of agarose concentration, was reported to be in the nanometer range [196].

This system thus provides the possibility to segregate mechanical properties from adhesion site density in contrast to, for instance, protein based model systems, and from changes in topography, as in porous scaffolds. Since I additionally showed that chondrocyte viability was not diminished through the modification process, modified agarose seemed to be a suitable model system for our purpose. As commercially available constituents were used this system is also easily adaptable by other research groups. The flexibility of the crosslinker additionally allows an adaptation of the system for studies with other adhesion proteins.

5.2 Chondrocyte response to matrix elasticity in 3D

5.2.1 Introduction

In TE applications or *in vivo* cells mostly find themselves in complex 3D environments. Studies with other cell types showed that findings from 2D can often not be directly transferred into these 3D environments since cells behave very differently.

Boonthekul et al. [2] found that the influence of stiffness on the proliferation of myoblasts was the exact opposite in 3D when compared to 2D culture systems, with the highest proliferation found in 2D on stiff materials but in soft materials in 3D. Other studies additionally showed that adhesion site organization and composition as well as cytoskeletal components are very different in 2D- when compared to 3D settings [88,

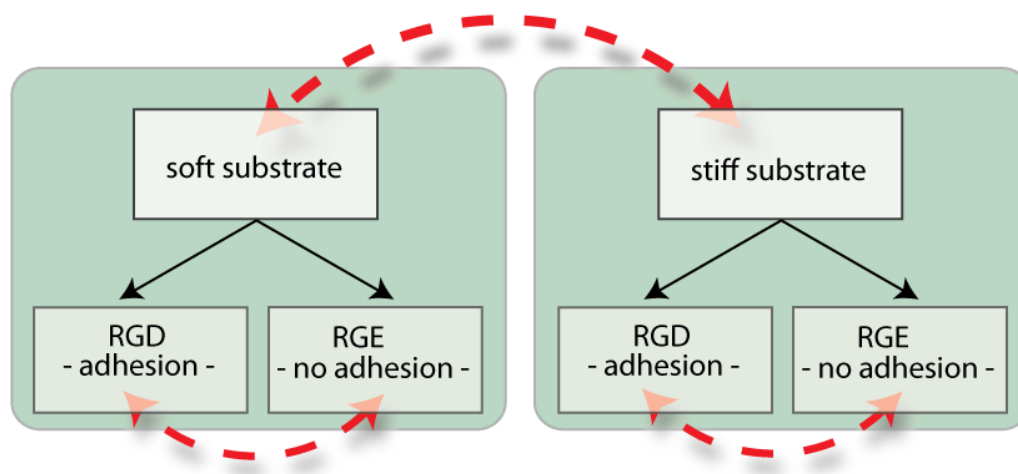


Figure 5.6: Experimental setup. Cells were incorporated into materials with different stiffnesses and modified with RGD or RGE respectively. This allowed an analysis of the impact of both, availability of adhesion sites, and stiffness of the matrix.

197].

The 3D model system developed in the previous section should now be applied to study if chondrocytes show the same response to matrix elasticity in the 3D environment as they did in 2D. Based on my findings in the 2D system [184], I hypothesized that chondrocytes change their phenotypical state, and cellular behavior, in response to matrix mechanics. And that soft hydrogels would be favorable for cell differentiation and ECM production.

In contrast to studies in 2D, where cells cannot be immobilized without adhesion sites, studies in 3D additionally allow to analyze if the availability of adhesion sites *per se* can already impact cellular behavior. With this in mind, I produced hydrogels with different mechanical properties, modified with RGD for adhesion or with RGE as a chemically similar control that does not allow adhesion. Chondrocytes were incorporated in RGD- or RGE- modified agarose gels with different mechanical properties, and the influence of matrix mechanics on the differentiated phenotype, cellular proliferation and distribution, and ECM quantity and distribution were studied (Figure 5.6).

5.2.2 Material and Methods

All chemicals were obtained from Sigma-Aldrich (Buchs, Switzerland) and of

pharmaceutical grade, unless stated otherwise.

Hydrogel modification

Low gelling agarose (Type VII) was dissolved in Ca^{2+} - and Mg^{2+} -free PBS and autoclaved. The amount of solution evaporated during autoclaving was determined by weighing, and replaced accordingly. The synthetic peptides GRGESP and GRGDSP (Bachem AG, Bubendorf, Switzerland) were conjugated to agarose hydrogels with the help of the heterobifunctional, UV-activatable crosslinker sulfo-SANPAH (Pierce, Rockford, USA), according to a modified protocol adapted from [119, 193]. Briefly a reaction was performed with the crosslinker and the respective peptides in ten molar excess for 4 h at room temperature (RT) in the dark. Agarose hydrogels were melted for 5 minutes at 65°C and cooled to 37°C . One part crosslinker-peptide mix was then thoroughly mixed with an equal volume of a 3% agarose solution under sterile conditions to obtain a 1.5% solution. The crosslinker was activated with a 450 W medium-pressure mercury arc lamp equipped with a filter to exclude excitation below 302 nm for three minutes. The solutions were gelled at 4°C and washed in PBS for seven days, with frequent changes of the solution, to remove unbound peptide and crosslinker. The amount of coupled protein was determined with a Bradford assay (Bradford Reagent), according to the manufacturer's instructions. One part of a 1.5% agarose-hydrogel, modified with $400\ \mu\text{M}$ of RGD or RGE, was then mixed with one part 5.5% agarose to obtain gels with $200\ \mu\text{m}$ protein and 3.5% plain agarose, or with one part PBS to obtain 0.75% agarose-hydrogels.

Cell culture

Porcine chondrocytes from the condyles of three to six month old pigs were isolated and characterized as described previously in Chapter 3. Viability for all isolations was between 97% and 99%. Culture medium was composed of RPMI 1640 Medium, with GlutaMAX™ and 25 mM HEPES, supplemented with 10% fetal calf serum (FCS), 1% antibiotic/antimycotic solution (all from Invitrogen, Basel, Switzerland) and ascorbic acid 2-phosphate ($50\ \mu\text{g}/\text{ml}$).

Upon thawing, 20×10^6 chondrocytes were plated overnight in a $75\ \text{cm}^2$ cell culture flask (TPP, Trasadingen, Switzerland) to maintain only viable cells, and thus precise cell

numbers for seeding.

Modified agarose was melted for 5 min at 60°C and allowed to cool to 37°C. Cells were detached from the flask by trypsinization and counted with the help of a Neubauer counting chamber (Neubauer improved, Assistent, Sondheim, Germany). Cells were incorporated into the hydrogels with a density of 4.5×10^6 cells / ml. An according volume of cell suspension was centrifuged for 10 minutes at 300 g, the supernatant was removed and the cell pellet was thoroughly mixed with the agarose. For each sample, 25 μ l of cell-agarose suspension was pipetted into spacers between two glass slides to obtain discs with a diameter of 4 mm and a height of 2 mm. Cell hydrogel constructs were allowed to gel at 4°C for 15 minutes and removed from the spacers. Random samples were taken in all experiments to assure constant seeding densities in the different preparations. Constructs were cultured in free floating conditions in 24-Well plates in the culture medium described above. Medium was changed twice a week.

Histology

All samples were analyzed with the microscope Axioscope (ZEISS, Oberkochen, Germany) using the acquisition software Axiovision (Release 4.7, ZEISS, Oberkochen, Germany).

Cryosection preparation

Upon removal, samples for histology were placed into plastic molds, immersed in embedding solution (Cryomold® Biopsy Tissue-Tek® and O.C.T. compound® Tissue-Tek® both Sakura Finetek Europe, Zoeterwoude, Netherlands), snap frozen in liquid nitrogen, and stored at -20°C. Cryosections of 12 μ m thickness were prepared using the Cryo-Star HM 560 cryostat (Microm International AG Schweiz; Volketswil, Switzerland).

Immunohistochemistry (IHC)

Collagen type II IHC was performed according to [184]. The primary antibody against collagen type II (II-II-6B3, Developmental Studies Hybridoma Bank, University of Iowa, USA) was applied in PBS with a dilution of 1:50. Negative controls were incubated in PBS only.

For collagen type I IHC, cryosections were washed in PBS, fixed for 30 min in 5%

formaldehyde at RT, permeabilized with 1% Triton-X-100 in PBS for 15 min, blocked with 2% BSA in PBS for 30 min at RT and incubated with the primary antibody against collagen type I (C2456, 1:1000 in PBS) for 12 h at 4°C. Negative controls were incubated in PBS only, additionally, positive controls were performed with dedifferentiated chondrocytes (data not shown).

Detection in all samples and in controls, was performed with FITC-conjugated goat anti-mouse IgG (Invitrogen, Basel, Switzerland) diluted 1:500 in PBS for 1 h at 37°C. DNA was stained with Hoechst 33258 (1µg/ml) for 15 min at 37°C; samples were washed extensively with PBS, and embedded.

Histological stains

Alcian blue staining for proteoglycans solution was performed according to [198]. The Alcian blue working solution was prepared by dissolving 0.025% (w/v) Alcian blue (Alcian blue 8GX) in 3% (v/v) acetic acid (Carlo Erba, Rodano, Italy) containing 0.15 M sodium chloride, and 0.06 M magnesium chloride (Hänseler AG, Herisau, Switzerland). Cryosections were washed with PBS, fixed in 5% formaldehyde for 30 min at RT and incubated in Alcian blue working solution overnight. Sections were washed in PBS, nuclei were stained with Haematoxylin solution (Haematoxylin solution according to Delafield) for 2 min, blued in tap water, washed in PBS and embedded.

For H&E stain, sections were fixed in 5% formaldehyde, washed in PBS, stained in haematoxylin solution, stained in Eosin solution (Eosin Y solution), dehydrated and cleared in graded ethanol solutions and xylene, and mounted. To quantify cell number and diameter of cell clusters, 150 cell clusters from at least 4 sections were randomly selected and captured for each sample. Evaluation was done with the help of the Axiovision Software (Release 4.7, ZEISS, Oberkochen, Germany).

Quantitative assays

Specimens for quantitative assays were lyophilized and the dry weight was determined. Each sample was digested in papain solution (2.375 U/ml; Worthington, Lakewood, USA) in buffer (0.1 M disodium hydrogen phosphate, 0.01 MEDTA disodium salt, 14.4 mM L-cysteine), for 16 h at 60°C. One part of the digest was directly used to determine

the GAG content; one part was frozen at -20°C to subsequently determine the DNA content.

GAG content was determined in triplicates, spectrophotometrically at 525 nm, following binding to the dimethylmethylene blue dye (AxonLab, Baden Dättwil, Switzerland) dissolved at 16 mg/l in 0.01 M HCl with 40.5 mM glycine and 40.5 mM NaCl. Chondroitin sulfate was used as a standard.

DNA content was measured fluorometrically using the PicoGreen assay (Molecular Probes, Basel, Switzerland) according to manufacturer`s instructions (excitation wavelength, 480 nm; emission wavelength, 528 nm).

Statistical analyses

All statistical analyses were performed with the SPSS 17.0 software (SPSS Inc., Chicago, USA). Statistical significance was determined by an ANOVA followed by post hoc comparisons using Fisher`s LSD. $P < 0.05$ is considered statistically significant. DNA content, GAG content and GAG/DNA were analyzed separately with time of culture, stiffness, and type of modification as fixed factors. Diameter of clusters and cells per cluster were analyzed separately, with stiffness and type of modification as fixed factors.

5.2.3 Results

Chondrocytes were incorporated and cultured in either soft or stiff hydrogels, modified with RGD to facilitate adhesion, or with RGE as control (Figure 5.6). Samples were taken after 3, 7 and 14 days, and the chondrogenic phenotype, cellular ECM production, and proliferation were investigated.

Maintenance of the chondrogenic phenotype

Cells in all scaffold types were already surrounded by their own ECM at the first time point of analysis (day three) (Figure 5.7.I). Cells displayed the chondrogenic phenotype over the whole culture period (Figure 4.7 I-III), as shown by a clearly positive stain for collagen type II, a complete lack of collagen type I in all samples (in contrast to the positive control, data not shown), and a round morphology. This observation was

independent of the availability of adhesion sites and the stiffness of the substrate.

Clusters of cells and ECM clearly increased in size over the whole culture period, with a more prominent increase in size of collagen type II and GAG clusters in softer hydrogels, when compared with stiffer hydrogels (Figure 5.7 I-III).

Quantification of proliferation and ECM production in different hydrogels

Quantification of DNA and GAG content confirmed that cell number and amount of ECM increased over the culture period in all types of scaffolds (Figure 5.8).

There was no significant difference in GAG content and DNA content between RGD and RGE-modified hydrogels. However, softer gels, with both, RGD- and RGE-modification contained significantly more DNA ($p < 0.01$, Figure 5.8 A and D) and GAG ($p < 0.01$, Figure 5B, E) when compared to stiffer hydrogels. The increase in DNA content in softer gels was highest between day three and day seven and slowed between day seven and 14. This trend was not observed in stiffer substrates. To determine if the higher GAG content in soft gels was only caused by the higher cell numbers or if cells were secreting more GAG, GAG was normalized to the DNA content (Figure 5.8 C, F): GAG per DNA significantly increased with time in culture ($p < 0.01$) but was neither affected by the availability of adhesion sites nor by the stiffness of the substrate (Figure 5.8 C, F).

Matrix and cell distribution in different hydrogels

Quantitative evaluation of H&E stained sections at day 14 (Figure 5.9 A) showed that the average diameter of cell-ECM clusters in softer gels was $73.6 \pm 28.2 \mu\text{m}$ in RGE- and $78.3 \pm 29.3 \mu\text{m}$ in RGD-modified hydrogels and was significantly larger than in stiffer gels, with a diameter of $57.3 \pm 21.1 \mu\text{m}$ in RGE- and $48.9 \pm 20.3 \mu\text{m}$ in RGD-modified agarose (Figure 5.9 B). Cluster in softer gels were not only bigger in size, but also contained significantly more cells, with an average of 6.9 ± 4.8 in soft, RGE- and 7.6 ± 4.5 cells in RGD-modified agarose, in comparison to 3.4 ± 1.9 in stiff, RGE- and 3.4 ± 2.2 cells in RGD-modified gels (Figure 5.9 C).

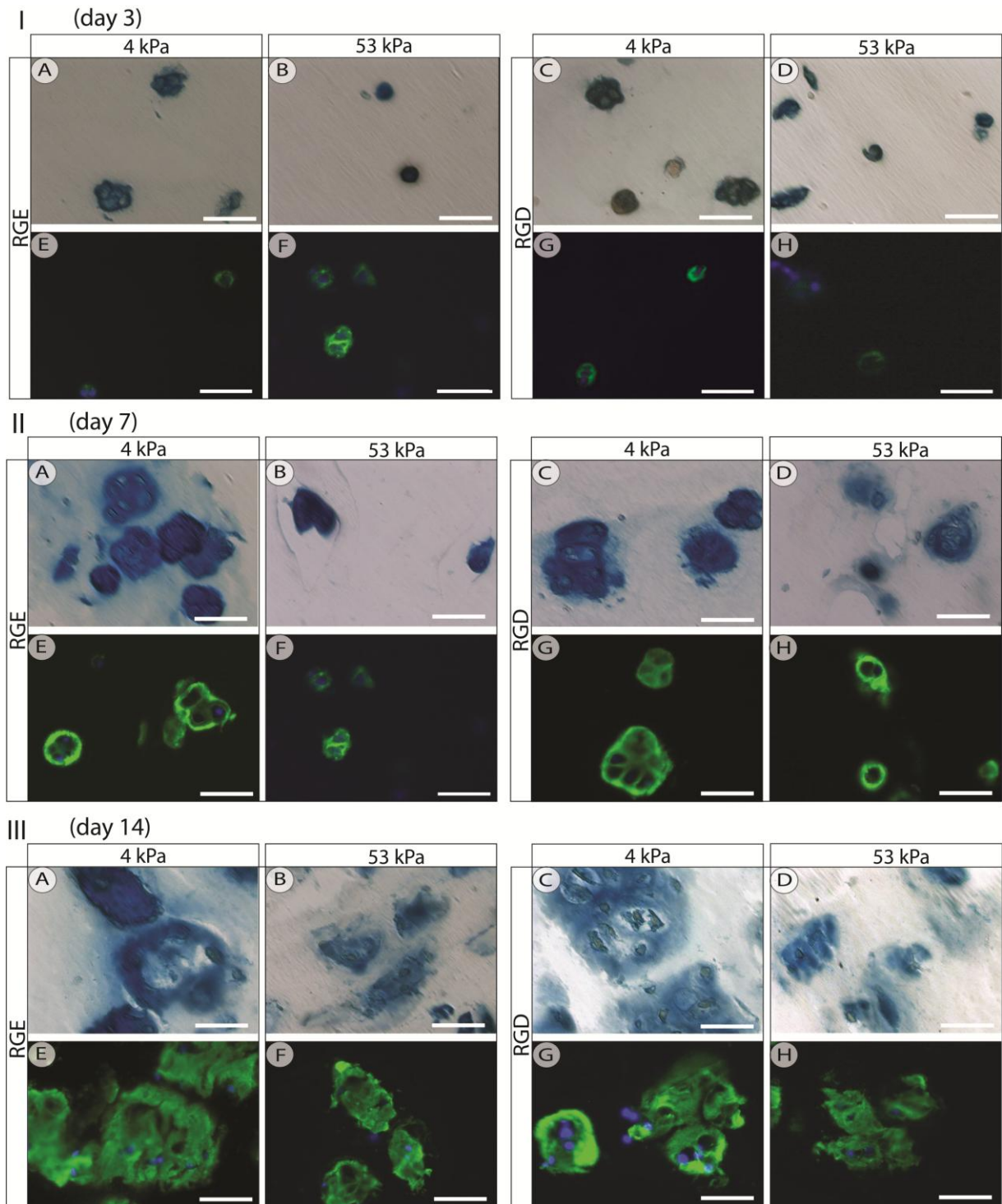


Figure 5.7: Collagen type II and GAG production in different hydrogels. I: After three days. II: After seven days. III: After 14 days. A-D: Alcian blue staining for GAGs. Nuclei were counterstained with haematoxylin. E-H: IHC for collagen type II. DNA was counterstained with Hoechst. Cells were already surrounded by their own ECM at day three, the amount of cells and ECM increased with time in culture, and cells generally formed bigger ECM cluster in soft gels independent of the type of modification. Scale bar = 50 μm .

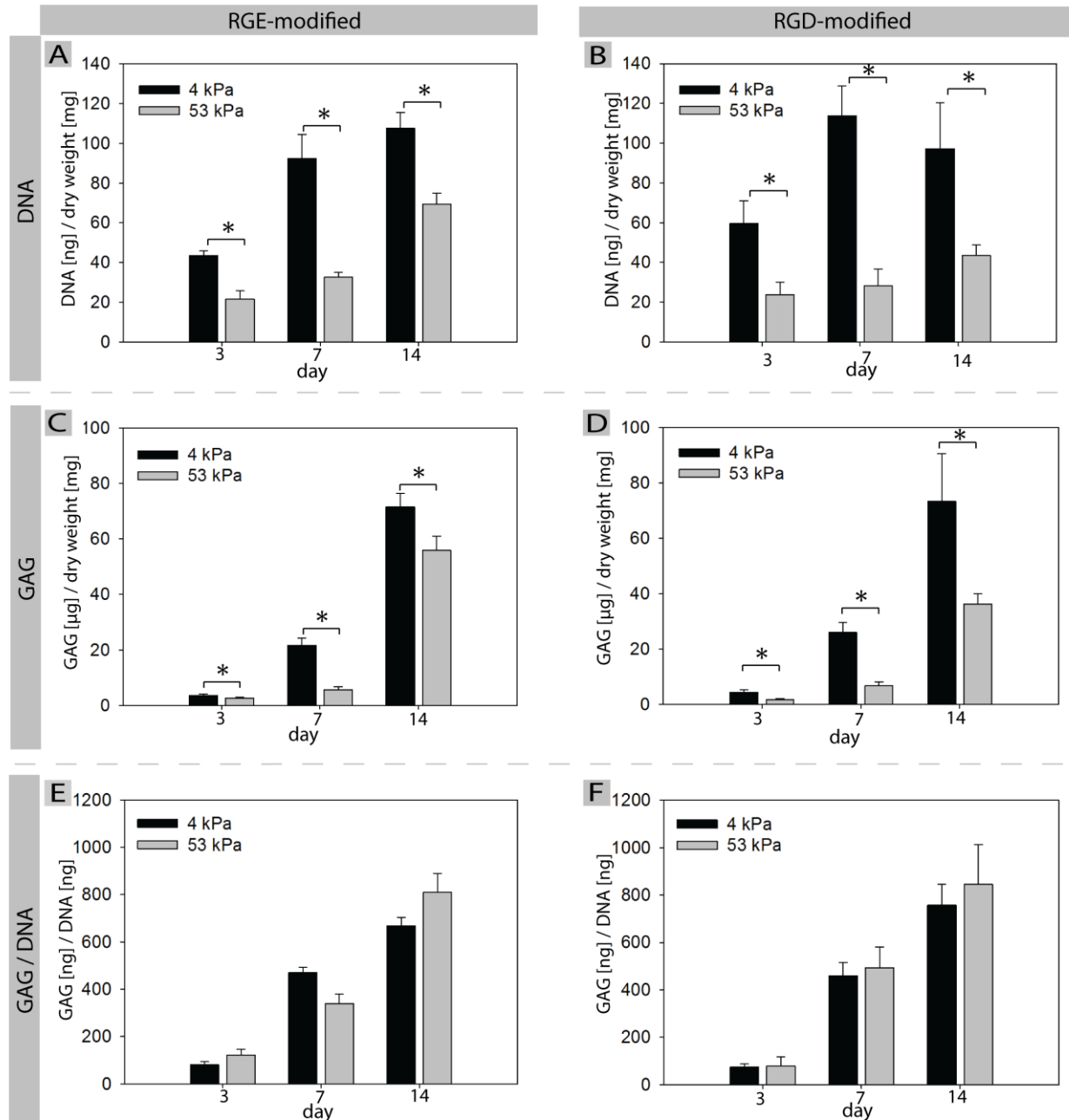


Figure 5.8: DNA and GAG quantification. **A, B:** DNA content in hydrogels with different stiffnesses, modified with **A:** RGE and **B:** RGD. **C, D:** GAG content in hydrogels with different stiffnesses modified with **C:** RGE and **D:** RGD. DNA and GAG content were significantly different between soft and stiff hydrogels (both with $p < 0.01$), but were not significantly affected by the type of modification (DNA-content: $p = 0.91$; GAG-content: $p = 0.52$). **E, F:** GAG per DNA in soft and stiff hydrogels modified with **E:** RGE and **F:** RGD. There was no significant differences between soft and stiff gels ($p = 0.099$) and RGD- or RGE- modification ($p = 0.171$). Values displayed as mean + SD, $n = 4$. * $p < 0.05$.

Additionally, a slight gradient in staining intensity of the GAG-cell clusters between the inner part of the scaffold and the outer rim was observed in all samples, with a deeper stain at the rim. This gradient was more prominent in stiff gels than in soft gels (Figure 5.10 A and B).

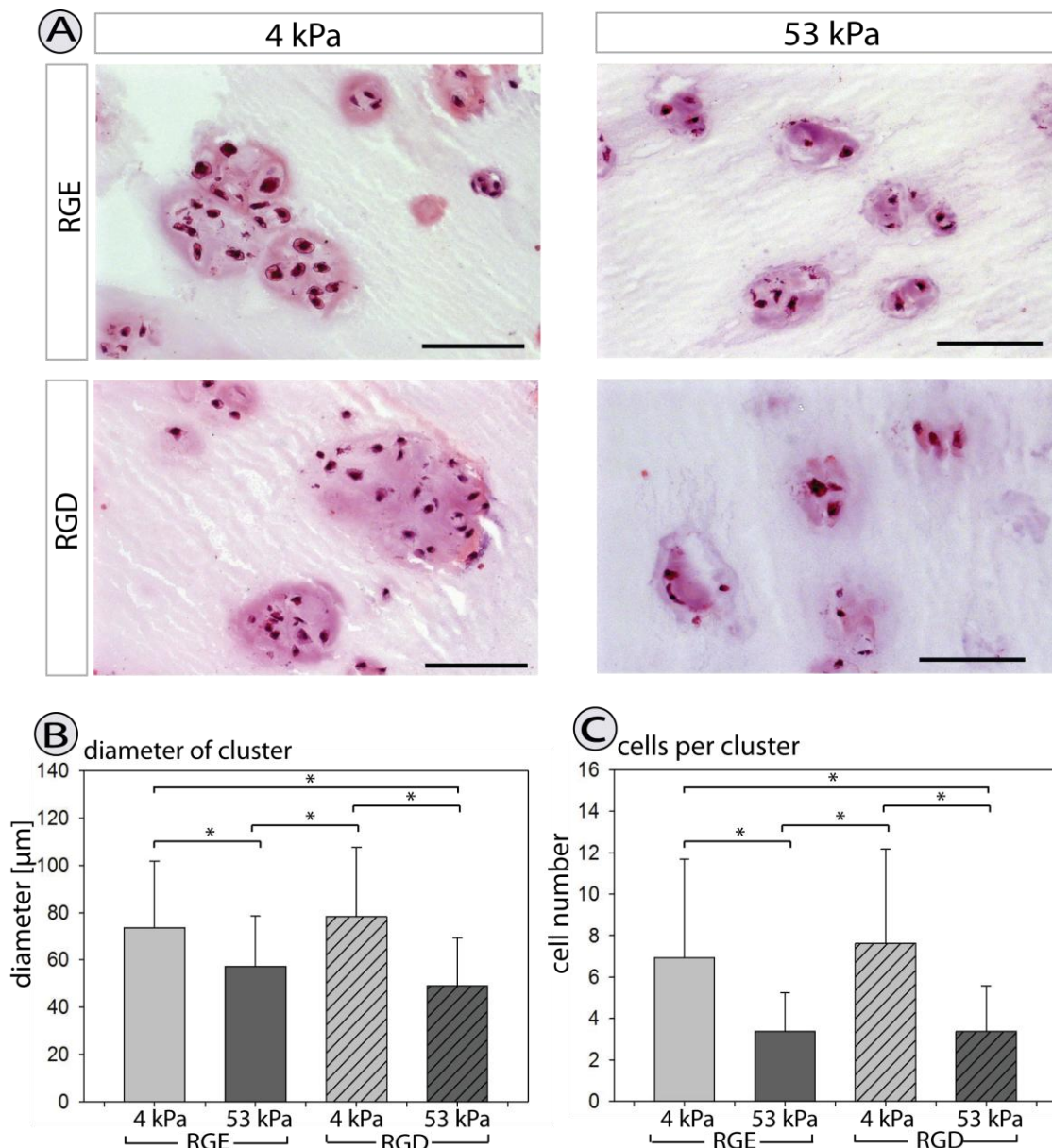


Figure 5.9: A: H&E stain of histological sections from day 14. Scale bar = 100 μm . B: Size of cell clusters in the different materials and C: number of cells per cluster. In softer gels cell clusters were bigger in size and contained more cells, when compared to stiff gels. Values displayed as mean + SD, * $p < 0.05$.

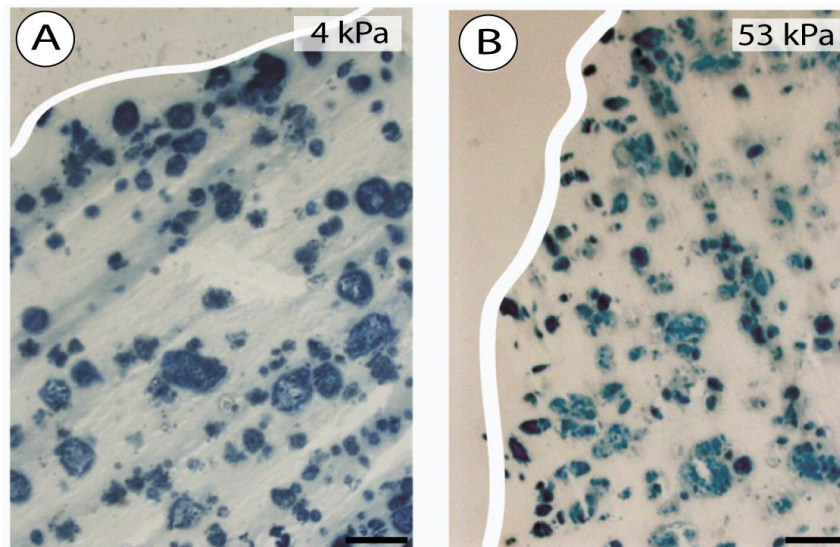


Figure 5.10: A and B: Representative Alcian blue stained sections (RGD-modified, day 14) from an A: 4 kPa hydrogel and B: 53 kPa hydrogel. The white line indicates the rim of the scaffold. A gradient in staining intensity between the outer rim and the middle of the gel seemed more prominent in stiff substrates, when compared to soft substrates. Scale bar: 200 μ m.

5.2.4 Discussion

Cell and ECM quantity and distribution

Based on the findings in 2D, I hypothesized that chondrocytes would sense and react to matrix elasticity in 3D and that soft substrates would promote the chondrogenic phenotype. In this study, a clear difference between cell behavior in soft and stiff substrates was observed. Cellular proliferation was significantly higher in softer hydrogels, but the increase in proliferation was not accompanied by a phenotypical change. Cells were also organized in larger clusters in softer hydrogels, and differences between the outer rim and the middle of the hydrogels appeared less prominent.

Based on these findings, I postulate that cells can sense the stiffness through their own ECM, thus, not as in 2D through active pulling of the substrate, but through the resistance of the surrounding substrate. Larger cell clusters could be formed against the resistance of the softer but not of the stiffer substrates (Figure 5.9) allowing higher proliferation, an observation that is also made in other systems [131]. With higher cell numbers, resistance in the softer gels increased as well, which led to a decrease in cell

proliferation in softer gels at a later time in culture.

Differences in diffusion of nutrients and serum factors into the gel might additionally contribute to these findings. Since diffusivity in agarose gels was shown to decrease with an increase in gel concentration and an increase in the size of the molecule [199] a higher stiffness of the hydrogel might decrease the availability of serum factors and nutrients. This could reduce cellular proliferation and lead to more prominent differences between the rim and centre of the hydrogel (Figure 5.10 A, B). However, diffusivity in TE constructs and hydrogels was shown to be generally higher than in native cartilage [200] and studies of a positive effect of high diffusivity come to rather contrary results [201-203]. This complicates a clear contribution.

The chondrogenic phenotype

Although hydrogel elasticity significantly influenced ECM quantity and distribution, neither the availability of adhesion sites, nor the elasticity of the hydrogels influenced the chondrogenic phenotype. Cells maintained their chondrogenic phenotype independent of the substrate properties, as shown by a complete lack of collagen type I and high production of collagen type II. GAG produced per cell, was not affected by the scaffold composition either, which confirms this finding. This is in contrast to my findings in a 2D PA system [204]. The 3D environment in the hydrogels, and the round morphology associated with it, seem to be sufficient to prevent cells from dedifferentiation. Since a round cell morphology has been shown to promote the chondrogenic phenotype [153], I postulate that the effect of stiffness on the chondrogenic phenotype in 2D was tightly linked to stiffness-induced morphological changes.

The type of modification (RGD or RGE) neither affected differentiation nor proliferation in this study. This is in contrast to findings from MSCs, where comparable concentrations of RGD inhibited chondrogenic differentiation [92].

The fully differentiated chondrocytes used here changed their immediate surroundings, from the early days of culture onwards, by depositing their own ECM molecules. It is likely that they then mostly interacted with their own ECM, comparable to attachment to their PCM *in vivo*. Although modification with other types of ECM molecules might lead

to different results, these findings show that cells not only react to the physical and chemical properties of an environment, but also actively change it, which is an important factor for TE applications.

Future studies with MSCs or expanded, dedifferentiated chondrocytes that do not directly change their environment (but have to first initiate differentiation) would, however, provide valuable additional information about the influence of substrate properties on chondrogenesis.

5.2.5 Conclusions and future work

A system was set up to study the effect of matrix elasticity on chondrocyte behavior in 3D. I have, hereby, been able to overcome some of the limitations of other 3D systems, such as the toxicity of acrylamide monomers or differences in adhesion site density, in protein based systems.

I showed that chondrocytes respond differently to matrix mechanics in 3D when compared to 2D culture: Substrate elasticity had no effect on the maintenance of the chondrogenic phenotype, but on cellular proliferation and cluster formation in 3D.

The maintenance of the chondrogenic phenotype in 3D, independent of the mechanical properties, confirms the positive effect of the 3D environment on the chondrogenic phenotype [18, 38, 52, 205], but also strengthens the assumption that findings from a 2D environment cannot be easily transferred into the third dimension. This is especially true for the effects of stiffness sensing, that are likely linked to changes in cellular morphology. On the other hand, additional effects may be seen in 3D that cannot be investigated in 2D, such as the restriction of cellular cluster sizes in stiff substrates, seen here.

The excellent maintenance of the chondrogenic phenotype in this agarose-based system and the positive outcomes from previous *in vivo* studies [206, 207] also suggest that agarose -possibly in combination with novel biomaterials- could still be an attractive material for cartilage TE applications and that cells could potentially be expanded in a suitable 3D system, without losing their differentiated phenotype.

5.3 Chondrocyte redifferentiation in 3D

5.3.1 Introduction

The last section of this chapter describes the application of the 3D model system to investigate another possible scenario in TE applications: the redifferentiation of expanded chondrocytes. To obtain sufficient cell numbers for the formation of TE constructs with primary chondrocytes, these cells are typically expanded on cell culture plastic. Upon expansion, chondrocytes lose their chondrogenic phenotype [8] in a process called dedifferentiation: The stiff, 2D environment, hereby, induces cellular spreading and actin stress fiber formation, accompanied by a change in ECM secretion as the shift from collagen type II to collagen type I production [156].

It has been shown that the cells can regain their differentiated phenotype after expansion when transferred into a 3D environment [38]. In order to produce functional cartilage tissue, this redifferentiation process needs to induce the production of substantial amounts of GAGs to enable load bearing of the developed tissue [208], and a reversal of the shift from collagen type II to collagen type I secretion, to avoid the formation of fibrocartilage [9]. While the 3D environment, as well as the cellular morphology and the cytoskeletal organization associated with it, seems to play an important role in regaining the chondrogenic phenotype [38], only very few systematic studies investigate the influence of isolated matrix properties on this process [209].

The availability of cellular adhesion sites and the mechanical properties of a scaffold are two characteristics that may be potentially tuned to optimize the redifferentiation process. Adhesion site density and substrate elasticity are assumed to increase cytoskeletal tension in a biphasic manner [70], an effect that is likely to negatively influence the chondrogenic phenotype [210]. Due to its presence in a number of different adhesion molecules, RGD is the most intensively studied sequence involved in cellular adhesion [211]. The influence of RGD on primary chondrocytes is still not completely understood, but it was shown to

be involved in the transmission of extrinsic [212] and intrinsic [124] mechanical stimuli. Its incorporation into hydrogels increased collagen type I production of freshly isolated chondrocytes *in vitro* in an initial response [212], but was also shown to have a positive influence on chondrocytes during the development of osteochondral grafts *in vivo* [213].

To my knowledge, nothing is known about the influence of RGD on the redifferentiation of expanded chondrocytes in 3D. Since Conelly et al. [119, 193] recently showed that RGD, and therefore substrate adhesiveness, inhibited chondrogenic differentiation of MSCs in a dose-dependent manner, I wanted to investigate if a similar effect on the redifferentiation process of expanded chondrocytes can be found.

The elasticity of a substrate is also, by now, well recognized to have an impact on cytoskeletal organization and differentiation [2, 5, 133, 137, 214], but the mechanisms behind these responses are, despite current advances [79, 215], still only poorly understood. Responses are highly cell type specific [7, 74, 75] but all seem to involve active probing of the substrate by the cell, upon adhesion, and force transmission over focal adhesions [216]. I showed, that chondrocytes also sense and respond to the elasticity of the substrate, when cultured in a 2D environment [184]. Soft substrates showed a

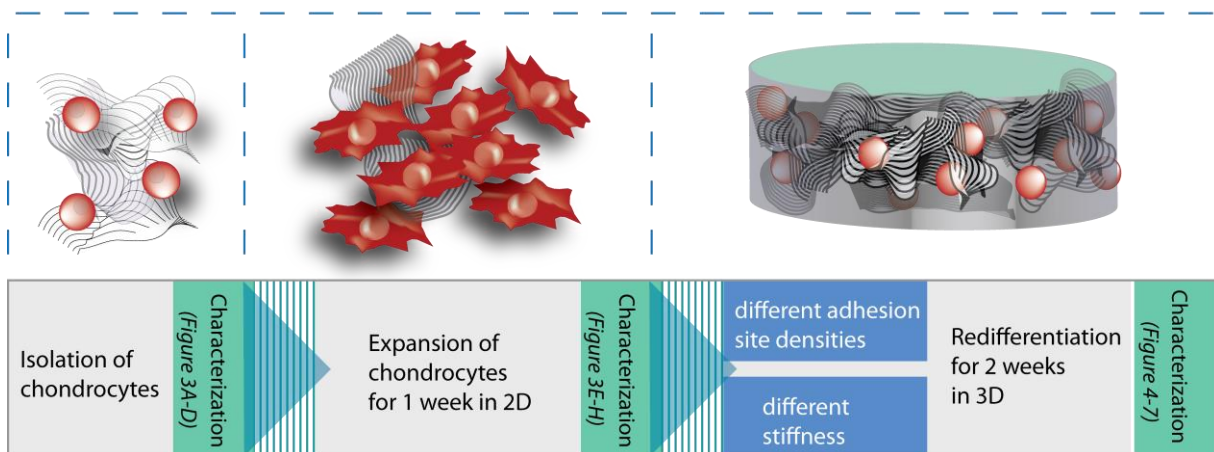


Figure 5.11: Experimental setup. Cells were expanded in 2D, on cell culture plastic after isolation and their phenotypical changes were monitored. Cells were redifferentiated in different 3D-hydrogel settings and the influence of RGD density and substrate mechanics on cellular redifferentiation was investigated.

positive effect on the maintenance of the chondrogenic phenotype, indicated by a round morphology, diminished actin stress fiber formation, and chondrogenic ECM production, while stiff substrates had a negative impact.

I therefore hypothesized that both, an increase in adhesion site density, and an increase in matrix stiffness, would have an inhibitory effect on the redifferentiation process of expanded chondrocytes in 3D.

To investigate this hypothesis, the tunable agarose hydrogel system from Chapter 5, Section 1 was applied. Chondrocytes were isolated and expanded in monolayer, and their phenotypical change was studied. Cells were then redifferentiated in hydrogels with different adhesion site densities and mechanical properties. The resulting constructs were analyzed to investigate the influence of the different substrate properties on the redifferentiation process (Figure 5.11) by looking at the reversal of the shift from collagen type II to type I production and on the amount of cells and GAG in the scaffolds.

5.3.2 Material and Methods

All chemicals were obtained from Sigma-Aldrich (Buchs, Switzerland) and of pharmaceutical grade, unless stated otherwise.

Hydrogel modification and characterization

Low melting agarose (Type VII) was dissolved in $\text{Ca}^{2+}/\text{Mg}^{2+}$ free phosphate buffered saline, pH 7.4 (PBS) to produce solutions with 0.75%, 1.5%, 3% and 6.25% (w/v) agarose. Solutions were autoclaved and the amount of water evaporated during autoclaving was determined by weighting, and replaced accordingly. The synthetic peptide GRGDSP (Bachem AG, Bubendorf, Switzerland) was conjugated to agarose hydrogels with the help of the heterobifunctional UV-activatable cross linker sulfo-SANPAH (Pierce, Rockford, USA), according to a modified protocol adapted from [119, 193]. Briefly, the crosslinker was reacted with the respective peptides in ten molar excess for 4 h at room temperature (RT) in the dark. One part crosslinker-peptide mix was then thoroughly mixed with an equal volume of a 1.5% (w/v) agarose solution, under sterile conditions, to obtain a 0.75% gel. The crosslinker was then activated with a 450 W

medium-pressure mercury arc lamp equipped with a filter to exclude excitation below 302 nm for three minutes. The reacted gels were gelled at 4°C and washed in PBS for seven days, with frequent changes of the solution, to remove unbound peptide and crosslinker. The amount of coupled protein was determined with the help of a Bradford assay (Bradford Reagent), according to manufacturer's instructions. Absorbance was read against a blank containing the same amount of plain agarose and the amount of protein was quantified with a bovine serum albumin (BSA) standard curve. After determining the amount of coupled RGD, the hydrogel solution was adjusted with a 0.75% plain agarose solution to obtain gels modified with 400 µM RGD and 200 µM RGD, respectively. To obtain 3.5% gels with 200 µM RGD, a hydrogel solution modified with 400 µM RGD was mixed with an equal part of a 6.25% agarose solution.

Cell Culture

Porcine chondrocytes from the condyles of three to six month old pigs were isolated and characterized as described previously [184]. Viability was between 97% and 99% for all isolations used. Basal culture medium was composed of RPMI 1640 Medium, with GlutaMAX™ and 25 mM N-(2-Hydroxyethyl)piperazine-N'-(2-ethanesulfonic acid) (HEPES), supplemented with 10% fetal bovine serum (FBS), 1% antibiotic/antimycotic solution (all from Invitrogen, Basel, Switzerland).

Upon thawing, 20×10^6 chondrocytes were plated in high density overnight in a 75 cm² cell culture flask (TPP, Trasadingen, Switzerland) to exclude dead cells from the freezing process. Additional cells from the same batch were seeded overnight in 24-well-plates (TPP, Trasadingen, Switzerland) with the same density. After overnight culture, cells in 24-well-plates were used for characterization of cells before expansion.

For expansion, cells from cell culture flasks were detached by trypsinization, plated in new cell culture flasks and 24-well-plates with a density of 10'000 cells per cm², and cultured at 37°C with 5% CO₂ in basal culture medium for seven days. Medium was changed twice a week. Cells plated on cell-culture wells were then used for characterization of cells after expansion. Cells from cell culture flasks were detached and incorporated into hydrogels as described below. Cellular doubling time (t_d) was calculated according to [205]: $t_d = t / (\log_2(N/N_0))$ with t being the time of culture, N_0 the number of cells before and N

the number of cells after expansion.

For cell incorporation into hydrogels, modified agarose was melted for 5 min at 60°C and allowed to cool to 37°C. Cells were detached by trypsinization, counted with the help of a Neubauer counting chamber (Neubauer improved, Assistent, Sondheim, Germany). The volume of cell suspension needed was centrifuged for 10 minutes at 300 g; the supernatant was removed and the cell pellet was thoroughly mixed with the agarose to obtain a seeding density of 6×10^5 cells/ml. For each sample, 25 μ l of cell-agarose suspension was pipetted into spacers between two glass slides to obtain discs with a diameter of 4 mm and a height of 2 mm. Cell-hydrogel constructs were allowed to gel at 4°C for 15 minutes and removed from the spacers. Constructs were cultured in free-floating conditions in 24-well-plates at 37°C and 5% CO₂ in the culture medium described above, supplemented with ascorbic acid 2-phosphate (50 μ g/ml). Medium was changed twice a week.

Histology

All samples were analyzed with the microscope Axioskop (ZEISS, Oberkochen, Germany) using the acquisition software Axiovision (Release 4.7, ZEISS, Oberkochen, Germany).

Cryosection preparation

Upon removal, samples for histology were placed into plastic molds, immersed in embedding solution (Cryomold® Biopsy Tissue-Tek® and O.C.T. compound® Tissue-Tek® both Sakura Finetek Europe, Zoeterwoude, Netherlands), snap frozen in liquid nitrogen, and stored at -20°C. Cryosections of 12 μ m thickness were prepared, using the Cryo-Star HM 560 cryostat (Microm International AG Schweiz, Volketswill, Switzerland), transferred to SuperFrost® Plus glass slides (Menzel, Braunschweig, Germany) and allowed to dry at RT for at least one day.

IHC

For collagen type II IHC, cryosections were fixed for 5 minutes with pre cooled (-20 °C) methanol-acetone (7:3). Non specific binding was blocked with 2% BSA in PBS for 30 min at RT. Specimens were incubated with the primary antibody for 1 h at 37°C, washed

extensively, and incubated with the secondary antibody under the same conditions. The primary antibody against collagen type II (II-II-6B3, Developmental Studies Hybridoma Bank, University of Iowa, USA) was applied in PBS with a dilution of 1:50. Negative controls were incubated in PBS only.

For collagen type I IHC, cryosections were washed in PBS, fixed for 30 min in 5% formaldehyde, at RT and permeabilized with 1% Triton-X-100 in PBS for 15 min at RT. Unspecific binding was blocked with 2% BSA in PBS, for 30 min at RT and samples were incubated with the primary antibody for 12 h at 4°C, washed extensively with PBS and incubated with the secondary antibody for 1 h at 37°C. The monoclonal antibody against collagen type I (C2456) was applied in a 1:1000 dilution in PBS. Negative controls were incubated in PBS only.

Detection in all samples and negative controls, was performed with FITC-conjugated goat anti-mouse IgG (Invitrogen, Basel, Switzerland) diluted 1:500 in PBS. DNA was stained with Hoechst 33258 in UPW (1µg/ml) for 15 min at 37°C. Samples were washed extensively with PBS, and embedded.

Histological stains

For Alcian blue staining for proteoglycans, Alcian blue working solution was prepared by dissolving 0.025% (w/v) Alcian blue (Alcian blue 8GX) in 3% (v/v) acetic acid (Carlo Erba, Rodano, Italy) containing 0.15 M sodium chloride, and 0.06 M magnesium chloride (Hänseler AG, Herisau, Switzerland). Cryosections were washed with PBS, fixed in 5% formaldehyde for 30 min at RT and incubated in Alcian blue working solution overnight. Sections were washed in PBS, nuclei were stained with Haematoxylin solution (Haematoxylin solution according to Delafield) for 2 min, blued in tap water, washed in PBS and embedded.

For phalloidin stain of actin stress fibers, cryosections were washed with PBST (PBS with 0.1% (v/v) Triton-X-100) and fixed for 1 h at 37°C with 100 mM 4-(2-Hydroxyethyl)piperazine-1-ethanesulfonic acid, 100 mM HEPES, 50 mM Ethylene glycol-bis(2-aminoethylether)-*N,N,N',N'*-tetraacetic acid (EGTA), 10 mM MgSO₄, 2% (v/v) Formaldehyde, and 0.2% (v/v) Triton X-100. Samples were washed with PBST three times for ten minutes, and actin was stained with Alexa-488 labeled phalloidin

(Invitrogen, Basel, Switzerland) 1:200 in PBS supplemented with 3% (w/v) BSA and 0.1% (v/v) Triton-X-100 at 37° for 1 h. DNA was stained with Hoechst 33258 in UPW (1µg/ml) for 15 min at 37°C; samples were washed extensively with PBS, and embedded.

Quantitative assays

Specimens for quantitative assays were lyophilized and the dry weight was determined. Each sample was then digested for 16 h with 0.6 ml papain solution (2.375 U/ml; Worthington, Lakewood, USA) in buffer (0.1 M disodium hydrogen phosphate, 0.01 M EDTA disodium salt, 14.4 mM L-cysteine), at 60°C. One part of the digest was directly used to determine the GAG content; one part was frozen at -20°C, to subsequently determine the DNA content.

To quantify chondrocyte ECM production during the culture period, *GAG content* of the final constructs was determined in triplicates, spectrophotometrically at 525 nm, following binding to the dimethylmethylene blue dye (AxonLab, Baden Dättwil, Switzerland) dissolved at 16 mg/l in 0.01 M HCl with 40.5 mM Glycine and 40.5 mM NaCl. Chondroitin sulfate was used as a standard. To determine the amount of DNA, and thus cells, in the constructs after the culture period, *DNA content* was measured fluorometrically from a 96-well black flat-bottom microtiter plate, by using the PicoGreen assay (Molecular Probes, Basel, Switzerland), according to manufacturer`s instructions (excitation wavelength, 480 nm; emission wavelength, 528 nm).

Diffusibility of soft and stiff hydrogels: To obtain an indication for the nutrient diffusion into hydrogels with different elasticities, BSA incorporation into unseeded hydrogels was determined. Scaffolds with either 0.75% or 3.5 % agarose were incubated in 4 mg/ml BSA in PBS for up to 48 h at 37°C. Samples were taken after 1, 3, 6, 12, 24 and 48 h, and washed with PBS. Samples were subsequently melted at 60°C and protein content was analyzed with a Bradford Assay (Bradford Reagent) according to manufacturer`s instructions.

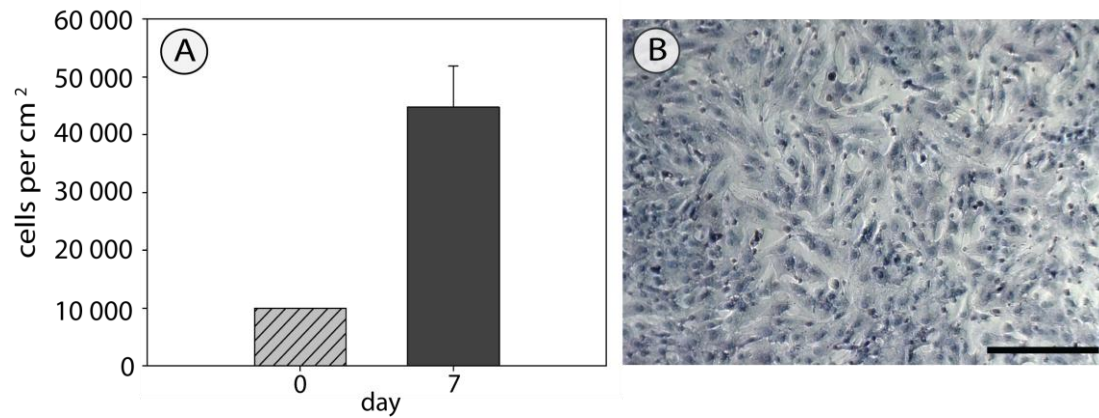


Figure 5.12: Chondrocyte expansion. **A:** Cell number significantly increases over the culture period of 7 days (note: numbers on day zero are cell numbers seeded). **B:** Brightfield image of cells after expansion (nuclei stained with Haematoxylin). Cells reach confluency during the expansion period. Scale bar: 200µm.

Statistical analyses

All statistical analyses were performed with the SPSS 17.0 software (SPSS inc., Chicago, USA). Statistical significance was determined by an ANOVA followed by Fisher's LSD with a significance level of $p < 0.05$. BSA uptake was analyzed with incubation time and elasticity as fixed factors. All results are displayed as mean \pm SD, $n = 5$ unless stated otherwise.

5.3.3 Results

Chondrocytes were expanded in monolayer for seven days. Phenotypical changes during the expansion period were monitored and cells were incorporated into hydrogels with different adhesion site densities and different mechanical properties (Figure 5.11).

Expansion of chondrocytes

During seven days of culture, cell numbers increased from the seeded 10'000 to $44'768 \pm 7'071$ cells/cm² (Figure 5.12 A). Cellular doubling time was calculated to be 78.7 ± 7.5 h, cellular proliferation rate 0.307 ± 0.03 cells per day and cells reached confluency during the expansion period (Figure 5.12 B).

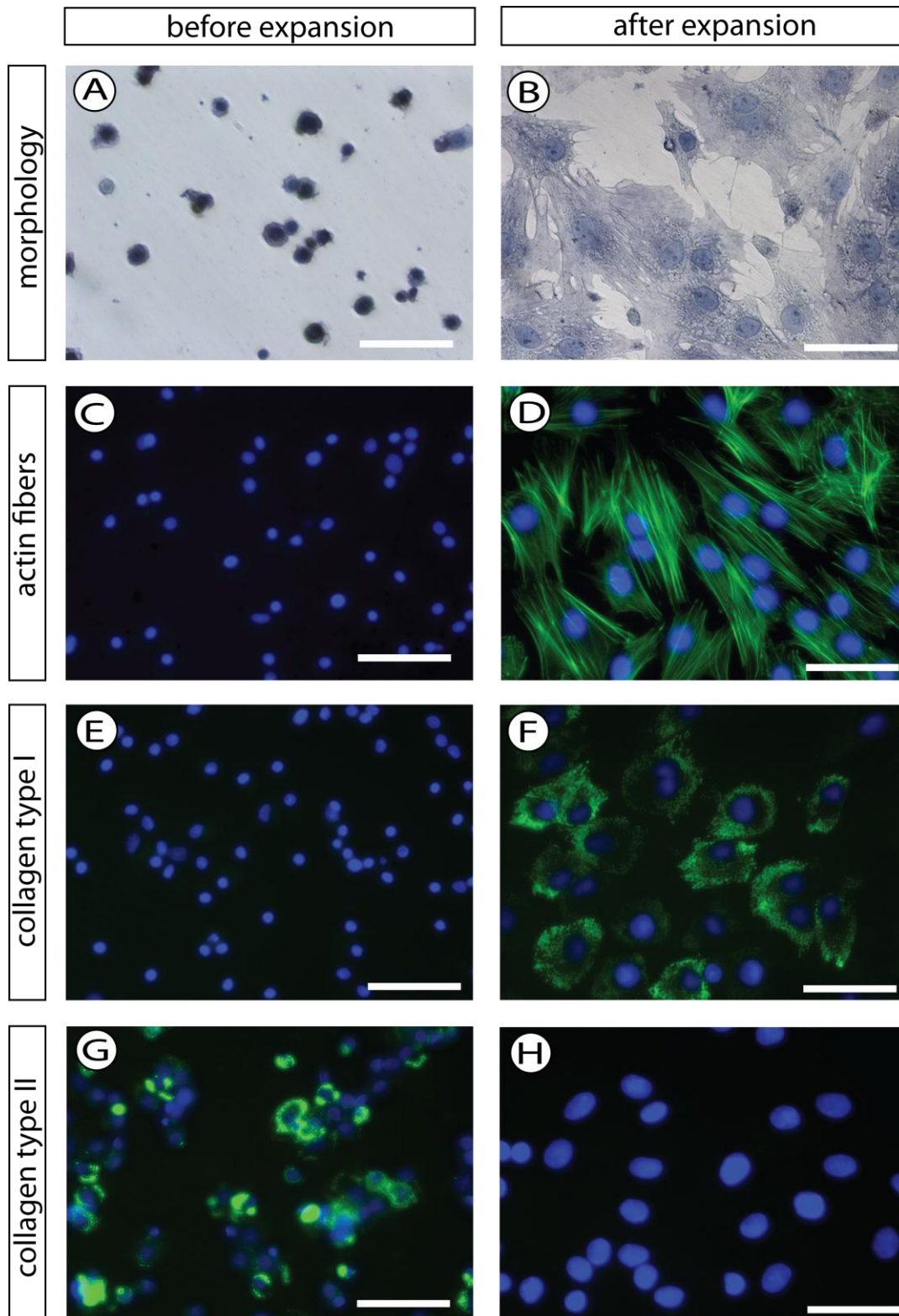


Figure 5.13: Chondrocyte dedifferentiation. Characterization of cells before (**A to D**) and after (**E to H**) expansion on cell culture plastic. Upon expansion, cells spread out, developed organized actin fibers and started to synthesize collagen type I instead of type II. **A, B:** Cellular morphology before and after expansion: Brightfield image, nuclei were stained with Haematoxylin. **C, D:** Phalloidin stain (green) for actin fibers. **E, F:** IHC for collagen type II (green). **G, H:** IHC for collagen type I (green). DNA was stained with Hoechst (blue), scale bar: 50 μm .

Upon expansion, chondrocytes clearly changed their phenotype. They changed from a chondrogenic, round morphology to a spread out, fibroblastoid, morphology (Figure 5.13 A, B; also note the increase in size of the nucleus on all pictures). This was accompanied by the development of highly organized actin-stress fibers (Figure 5.13 C, D). The expression of ECM molecules changed accordingly: While cells were negative for collagen type I and positive for collagen type II before expansion (Figure 5.13 E, G), this pattern was reversed after expansion, with a negative stain for collagen type II and positive stain for collagen type I (Figure 5.13 F, H). Cells, thus, displayed all common markers for a loss of the chondrogenic phenotype.

Redifferentiation in a 3D-environment

After expansion, cells were detached and incorporated into hydrogels with different RGD densities and different mechanical properties. Specimens were cultured for two weeks to facilitate redifferentiation.

The effect of adhesion site density on redifferentiation

To investigate the influence of adhesion site density on the chondrogenic phenotype, cells were stained for collagen type II, as a marker for the differentiated phenotype, and collagen type I, as a marker for the dedifferentiated phenotype. Cells incorporated into plain agarose produced high amounts of collagen type II during the two weeks of culture in 3D while collagen type II production seemed slightly diminished in 200 μ M RGD, and visibly diminished in hydrogels with 400 μ M RGD agarose hydrogels (Figure 5.14 A-C).

Sections of specimens with plain agarose were also clearly negative for collagen type I, while a slight positive stain for collagen type I was seen in some of the samples modified with 200 μ M RGD and many of the cells in specimens with 400 μ M RGD stained even clearly positive for collagen type I (Figure 5.14 D-F).

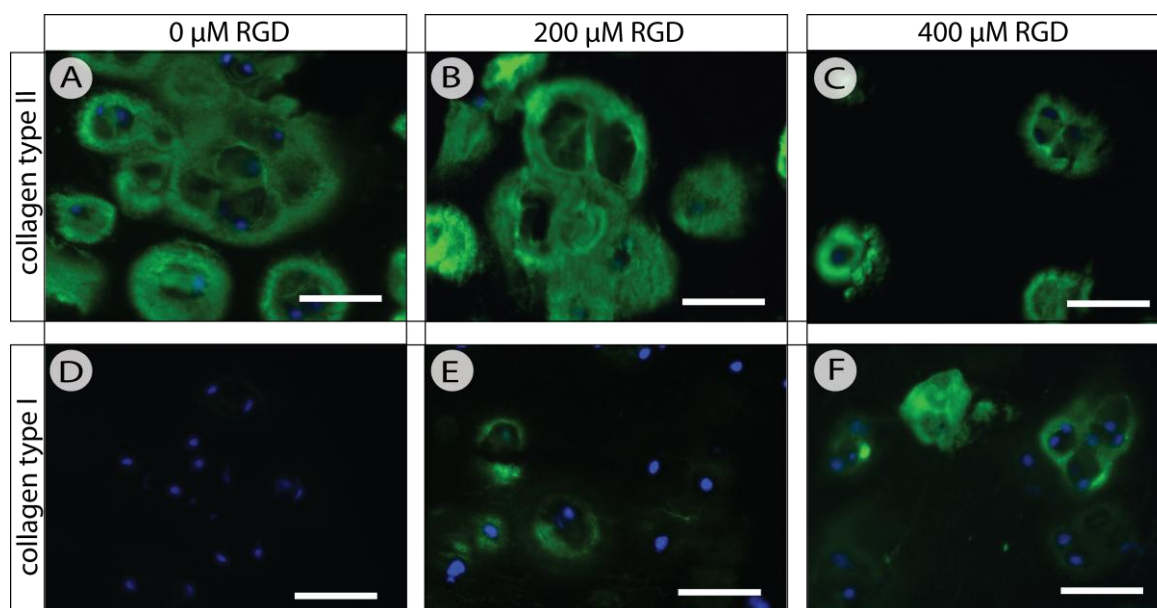


Figure 5.14: A-C: IHC for collagen type II (a marker for the differentiated phenotype) and D-F: collagen type I (a marker for the dedifferentiated phenotype). DNA was stained with Hoechst (blue). Redifferentiation was affected by the amount of RGD in the gel. Hydrogels with 0 μM RGD showed the highest amount of collagen type II and were clearly negative for collagen type I. Gels with 200 μM RGD showed slightly less collagen type II and, partly a positive stain for collagen type I. Gels with 400 μM RGD showed visibly less collagen type II and more collagen type I production. Scale bar: 50 μm

Quantitative analysis of the specimens showed that DNA content after two weeks of culture was not significantly influenced by the amount of RGD in the gel (Figure 5.15 A), while the amount of GAG per sample decreased with an increase in RGD concentration (Figure 5.15 IB). The amount of GAG produced per DNA (and thus per cell) decreased visibly, and was significantly different between plain agarose, agarose modified with 200 μM RGD ($p = 0.008$), and agarose modified with 400 μM RGD ($p < 0.001$) (Figure 5.15 IB, C).

Findings from the quantitative assays were confirmed in Alcian blue stained sections, where cells in plain agarose displayed the highest amount of GAG-production, and cells in 400 μM RGD-agarose the lowest amount of GAG-production (Figure 5.15 IIA-C).

The effect of stiffness on redifferentiation

The study in the first section of this chapter showed that the equilibrium modulus of modified agarose can be increased from 3.7 ± 1.9 kPa (soft) to 53.2 ± 14.64 kPa (stiff), by increasing the concentration of agarose from 0.75% to 3.5%.

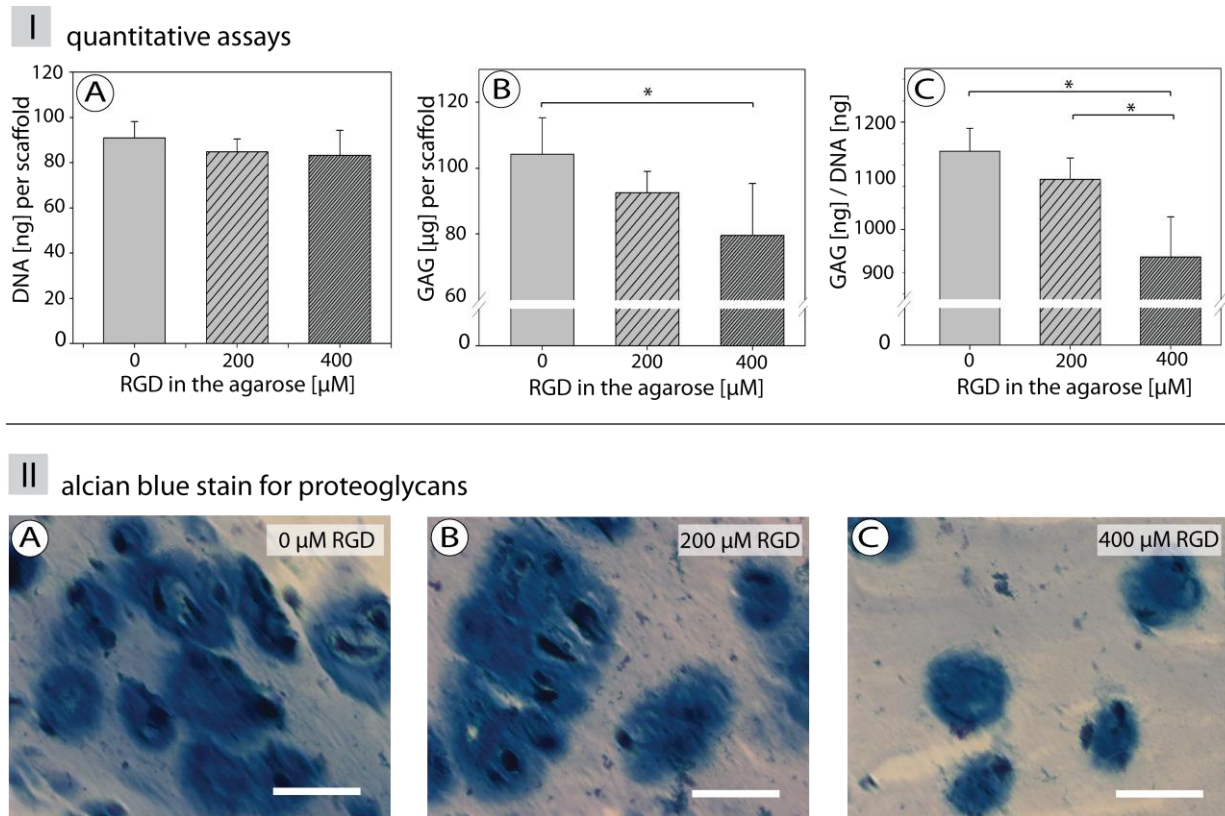


Figure 5.15: I: Quantitative data from agarose modified with different molarities of agarose. **A:** DNA content per scaffold is not different in different scaffolds. **B:** GAG content per scaffold is significantly different between the highest RGD concentration and plain agarose **C:** GAG content per DNA is significantly different between plain agarose and agarose modified with both, 200 μM and 400 μM . Values displayed as mean + SD, $n = 5$, $*p < 0.05$. **II:** Alcian blue staining for GAG produced by cells in **A:** plain agarose; **B:** agarose modified with 200 μM **C:** RGD modified with 400 μM RGD. In accordance with quantitative data, GAG production seemed diminished through RGD-modification. Nuclei were stained with Haematoxylin. Scale bar 50 μm .

I hypothesized that an increase in stiffness would have a similar negative effect on the redifferentiation process as an increase in adhesion site density. To investigate this hypothesis redifferentiation in stiff substrates of plain or 200 μM RGD-agarose was compared to redifferentiation in soft substrates of plain or 200 μM RGD-agarose.

An increase in stiffness did not inhibit the redifferentiation process, independently of the availability of adhesion sites: cells in stiff substrates stained negatively for collagen type I and positively for collagen type II with visibly smaller but seemingly denser ECM clusters (Figure 5.16).

However, stiff gels showed a significantly lower amount of DNA than soft gels ($p < 0.001$) (Figure 5.17 IA), a finding that was independent of the availability of adhesion

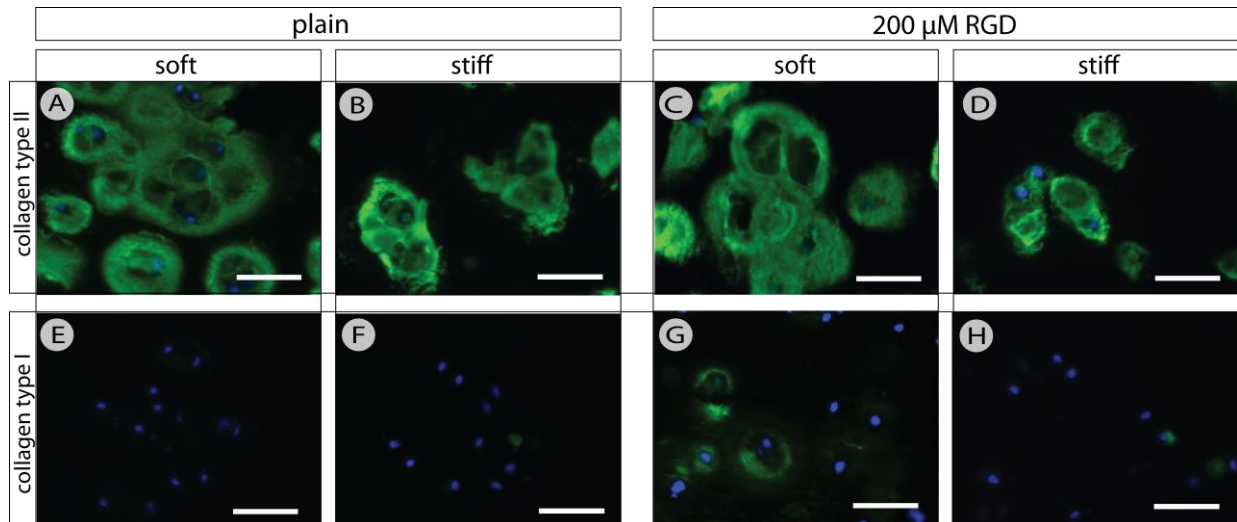
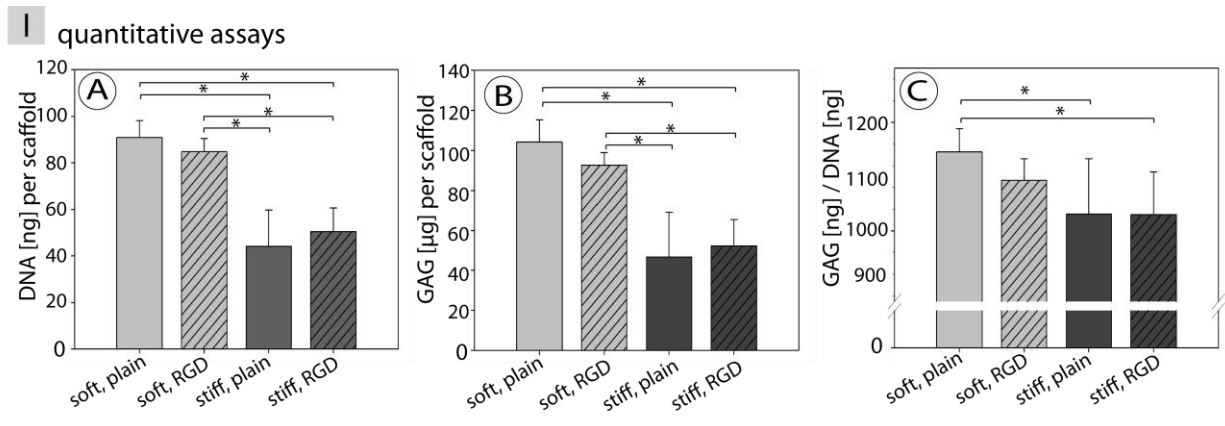


Figure 5.16: A-D: IHC for collagen type II and E-H: collagen type I. DNA was stained with Hoechst. The increase in stiffness did not induce an elevation of collagen type I production. ECM cluster of collagen type II seemed smaller in size but denser in stiff, when compared to soft substrates, independent of the type of modification. Scale bar = 50 μm .



II alcian blue stain for proteoglycans

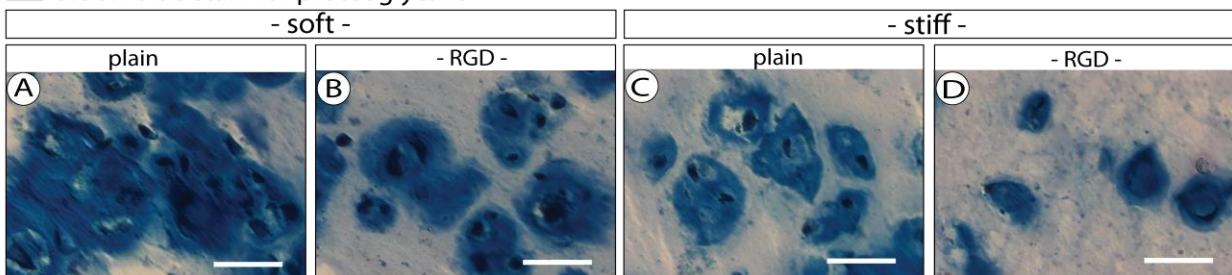


Figure 5.17: I: Quantitative data from agarose with different stiffnesses, with and without RGD modification. **A:** DNA content per scaffold was significantly different in stiff and soft gels. **B:** GAG content per scaffold was significantly different between stiff and soft gels. **C:** GAG content per DNA was only slightly different in different scaffolds. Values displayed as mean + SD, $n = 5$, $*p < 0.05$. **II:** Alcian blue staining for GAG produced by cells in **A:** plain, soft agarose; **B:** modified, soft agarose; **C:** plain, stiff agarose; **D:** modified, stiff agarose. The staining confirmed the findings from quantitative assays that softer gels contained more GAG than stiffer gels. Scale bar: 50 μm .

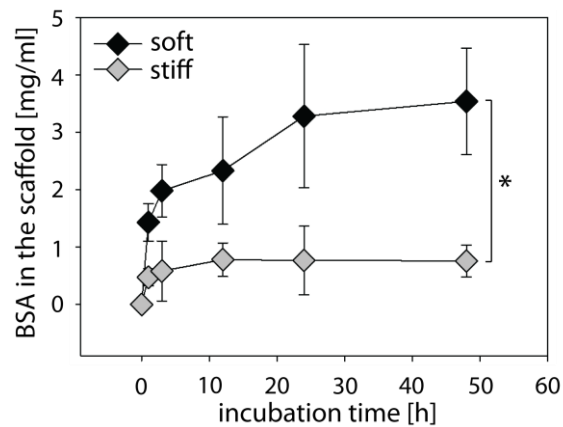


Figure 5.18: BSA uptake into hydrogels with different stiffnesses. BSA uptake was significantly higher ($p = 0.002$) in soft gels when compared to stiff gels. Values displayed as mean \pm SD, $n = 5$, $*p < 0.05$.

sites: Stiff, RGD-modified hydrogels contained only 60% of the DNA content of the respective soft gels; stiff, plain hydrogels contained only 48% of the DNA content of the respective soft gels.

Stiffer gels correspondingly showed a significantly lower amount of GAG per scaffold ($p < 0.001$) with only 56% GAG content in RGD-modified and 45% in plain, stiff agarose, when compared to the respective soft hydrogels (Figure 5.17 IB). The average GAG production per cell was higher in softer substrates (Figure 5.17 IC) and was hereby highest in plain, soft hydrogels, with 1145.5 ng GAG/ng DNA, and lowest in stiff, RGD-modified hydrogels with 1030.2 ng GAG/ng DNA. The impact of an increase in stiffness on these values was not as high as the one observed from an increase in adhesion site density (Figure 5.15 IC). Stiff gels showed a significantly lower amount of DNA than soft gels ($p < 0.001$) (Figure 4.17 IA), a finding that was independent of the availability of adhesion sites: Stiff, RGD-modified hydrogels contained only 60% of the DNA content of the respective soft gels and stiff, plain hydrogels contained only 48% of the DNA content of the respective soft gels.

To investigate a possible impact of nutrient diffusion on cellular proliferation, I representatively investigated BSA uptake into hydrogels with different mechanical

properties. Over the whole incubation period of 48 h, BSA uptake was significantly higher ($p = 0.002$) in softer hydrogels, with a maximum of 3.5 ± 0.9 mg/ml when compared to stiffer gels with a maximal uptake of 0.76 ± 0.27 mg/ml (Figure 5.18).

5.3.4 Discussion

Cells isolated from non-load bearing regions of cartilage need to be expanded to obtain sufficient cell numbers for the formation of functional cartilage substitutes *in vitro*. In this study, chondrocytes were expanded on cell culture plastic and their phenotypical changes were monitored. Different previous studies aimed at optimizing the expansion and redifferentiation process with the help of various soluble factors [205, 217, 218]. Since I was not interested in the effect of soluble factors, and in order to avoid adding further complexity to the study, cells were expanded in basal medium only. Cellular doubling time was, hereby, in agreement with doubling times of cells cultured in basal medium in other publications [205] and the cellular changes, correlated with a loss of the chondrogenic phenotype, could be clearly observed.

Cells were then transferred into a 3D hydrogel culture system to induce redifferentiation. I hypothesized, that the properties of this 3D environment, namely adhesion site density and stiffness, would influence the redifferentiation process, with a negative impact of high adhesion site densities and stiff substrates.

After a successful redifferentiation process, cells should produce substantial amounts of GAG and collagen type II instead of type I to form functional tissue substitutes. In agreement with my hypothesis, an increase in adhesion site density had a negative impact on all of these features. Cells in hydrogels with high adhesion site densities produced significantly less GAG, and could not completely reverse the collagen production. This was in contrast to cells cultured in gels that did not provide adhesion sites. These findings are in also agreement with findings from other studies in 2D environments, where an increase in adhesivity was shown to increase dedifferentiation of articular chondrocytes [219] and inhibit the redifferentiation capacity of nasal chondrocytes [220].

Connelly et al. [193] also used a model system, very similar to the one used here. The study showed that RGD has an inhibitory effect on the chondrogenic differentiation of

MSCs. I observed the same effect during the redifferentiation of dedifferentiated chondrocytes. This might indicate similarities between the mechanisms involved in the chondrogenic differentiation of MSCs and the redifferentiation of dedifferentiated chondrocytes. However, further studies about integrin expression profiles and cytoskeletal assembly in the early events of the redifferentiation phase should be performed to gain further insight into the similarity of the involved mechanisms.

The hypothesis that stiff substrates have a negative effect the redifferentiation process was not confirmed in my study: neither GAG production per cell (DNA) nor the reversal of collagen type I back to collagen type II production was affected by the stiffness of the hydrogels. My results, additionally, indicate that the influence of stiffness on cellular behavior in 2D cannot be easily translated into the 3D environment. While proliferation was increased on stiff substrates in our 2D system [184], contrary results were found in 3D with significantly higher DNA content in soft, when compared to stiff gels. This reversal has already been shown with other cell types [80] and stresses the differences between 2D and 3D environments and the resulting need to further transfer this field of research into the third dimension, to gain an understanding of the processes that might be involved *in vivo*.

I showed in the 2D study that a matrix which has an elasticity that is approximately in the range of freshly developed PCM [184], has a positive effect on the differentiated phenotype. [170]. This elasticity had no positive effect on the chondrogenic phenotype in my 3D study. It did, however, lead to the highest cell numbers, which resembles the behavior of fully differentiated chondrocytes in the previous section. While a favorable effect of tissue level elasticity on cellular differentiation, as found in studies with stem cells [7], cannot be persuasively confirmed in our 3D system, a positive effect on overall GAG content could, therefore, be observed. However, this effect was also seen in cells cultured in hydrogels that did not provide adhesion sites. This was, again, in agreement with the findings from the study with fully differentiated chondrocytes and may be cautiously interpreted as a result of two factors. First at a later stage of the redifferentiation period, cells might sense the resistance of the matrix through attachment to their own ECM rather than through attachment to RGD. Secondly, differences in the mesh size of hydrogels of different stiffnesses might alter the diffusivity of nutrients into

the gel.

A previous study indicated that chondrocytes can respond to external mechanical stimulation through binding to their own ECM: chondrocytes were responsive to mechanical stimulation when encapsulated in inert hydrogels, an effect that was reversed upon addition of soluble RGD [221]. I, therefore, postulate that they can also respond to the intrinsic mechanical stimulus of the seemingly denser, and therefore most likely stiffer, ECM surrounding them in stiff hydrogels.

Since differences in nutrient and serum uptake in hydrogels of different stiffness could be one possible explanation for the big difference in both, plain and modified hydrogels, I, representatively, I could hereby show that BSA uptake into stiff hydrogels was significantly lower, than its uptake into soft hydrogels.

While these results seem of high interest for TE applications, the findings also imply a need for further studies to investigate the involved processes. Cells constantly change their environment, as through the deposition of ECM proteins, or new intercellular contacts through proliferation. The initial response of cells to different substrate properties might, therefore, be very different from the long-term response and should be addressed in future studies.

5.3.5 Conclusions

This study provides interesting findings about the influence of isolated material properties on the redifferentiation process of expanded chondrocytes and might be used in the design of novel materials for the formation of cartilage substitutes.

The results indicate that cellular binding to RGD impairs redifferentiation. Accordingly, materials that do not require cellular attachment, as hydrogels where cells can be immobilized by incorporation, might be favorable for these applications. Softer hydrogels seem to facilitate higher amounts of DNA and corresponding GAG deposition, but the resulting advantages will have to be weighed against possible disadvantages through their initial mechanical instability.

Additionally, further studies are necessary to investigate the mechanisms involved in the

response to substrate adhesivity and stiffness, and segregate initial events in this response from later events in the redifferentiation process.

6 Synthesis

6.1 Innovations

To facilitate the intentional design of biomaterials for cartilage TE, knowledge about the influence of isolated material properties on cellular behavior needs to be acquired. I hypothesized that the elasticity of a material, as one of these properties, influences chondrocyte differentiation and proliferation and should, therefore, be considered as a design variable in cartilage TE. To provide a comprehensive investigation of this hypothesis, chondrocyte response to matrix elasticity in the different possible culture scenarios in cartilage TE should be investigated. The formulated specific aims were, hereby, the adaptation of a 2D culture system to study chondrocyte response to elasticity when cultured in monolayer, the identification or, if necessary, development of a suitable model system for 3D culture and the investigation of an influence of matrix elasticity on differentiated or dedifferentiated chondrocytes cultured in 3D. In the following, the achievements of this thesis, with respect to an adaptation or implementation of suitable model systems, as well as new insights into chondrocyte response to matrix elasticity, are highlighted. Additionally, limitations of the studies, performed in the scope of the thesis, and possible future work are discussed.

6.1.1 Model systems to study chondrocyte response to matrix elasticity

Chapter 3 of this thesis shows that the 2D PA system can be adapted for the culture of chondrocytes and can, thus, be used to study stiffness sensing in chondrocytes. Besides the advantage of using a system that has been very well characterized in other studies of the field, this also allows a comparison of the response of chondrocytes to matrix elasticity to the response of other cell types.

In a next step, a suitable 3D model should be identified or implemented. I showed in Chapter 4 that porous systems are not suitable to study stiffness sensing in 3D due to their heterogeneous mechanical properties and the limited contact between cells and

substrate. However, they can be used to investigate if cells respond to the pore size of the scaffold. Since changing the pore size in the micrometer range did not significantly change cell proliferation or the chondrogenic phenotype I concluded that a change of pore size in the nanometer range (as in a hydrogel-based system) would also not be likely to impact these factors.

Based on the experiences in the porous system a tunable hydrogel system was developed in Chapter 5. This provides a well-defined environment to study stiffness sensing. It allows the alteration of matrix elasticity independent of changes in microstructure or adhesion site density and provides the possibility for a modification with other adhesion proteins for future studies. The study with dedifferentiated chondrocytes further stresses the superiority of this system compared with some protein-based systems in which a change in stiffness cannot be separated from a change in adhesion site density. The increase in adhesion site number inhibited redifferentiation of expanded chondrocytes while an increase in stiffness reduced proliferation of the cells. These two effects would not be clearly assignable to the respective material properties in these protein-based systems.

6.1.2 Chondrocyte response to matrix elasticity

The aim of this thesis was to provide a comprehensive study of chondrocyte response to matrix elasticity. I hypothesized, that the elasticity of the matrix influences proliferation and differentiation state of chondrocytes and should, as a consequence, be considered as a design variable in cartilage TE. To investigate this hypothesis, chondrocyte response to matrix elasticity in different possible scenarios of chondrocyte culture for cartilage TE applications was studied: (i) a 2D culture system after chondrocyte isolation, for instance prior to reinjection of cells into a site of defect; (ii) culture and expansion of chondrocytes in a 3D setting after isolation and (iii) redifferentiation of chondrocytes that were expanded on cell culture plastic, prior to implant formation.

I applied the validated 2D PA system to show that chondrocytes sense the elasticity of the substrate they are cultured on and react to it. The stiffness directly influences morphology, proliferation and ECM secretion in 2D culture and soft substrates support the chondrogenic phenotype, in contrast to stiff substrates. This knowledge could be used

for the design of 2D culture systems that optimally support the chondrogenic phenotype and, hereby, delay the transition into a fibroblastoid phenotype.

My studies about stiffness sensing in a defined 3D environment show that knowledge obtained in 2D-settings cannot be easily transferred into 3D: Matrix elasticity does not influence the chondrogenic phenotype of cells cultured in 3D. However, it seems to influence cellular proliferation in the gel and the size of cell clusters that could be formed against the resistance of the hydrogel. This effect did not depend on the incorporation of adhesion sites into the material. A possible explanation for this is that the fully differentiated cells reshape their immediate environment through the secretion of ECM proteins early on in the culture period. Although results in the 3D system are very different from findings in the 2D setting, they confirm the positive impact of soft substrates on chondrocyte behavior. However, the observed differences also stress the importance of bringing research in the field of stiffness sensing into the third dimension. Transferred to cartilage TE applications, my results suggest that freshly isolated chondrocytes can be expanded in a 3D setting. Neither the availability of adhesion sites nor the stiffness induces a loss of the chondrogenic phenotype and proliferation is increased in soft materials.

In a last step, the 3D model system was applied to investigate the influence of both adhesion site density and stiffness on the redifferentiation of expanded chondrocytes. The results indicate that matrix elasticity has no effect on the redifferentiation process and that the highest cell number can be obtained in soft gels. Cells regained their differentiated phenotype independent of the elasticity of the material but again showed the highest proliferation in the softer hydrogels. Adhesion sites, in contrast, seem to inhibit the redifferentiation process in a dose dependent manner. These findings may be used for the design of suitable scaffold materials for the formation of cartilage constructs from autologous chondrocytes after expansion. Soft substrates would, hereby, facilitate higher cell numbers. Culture systems that do not require cell attachment, as hydrogels where cells can be directly incorporated, would optimize the redifferentiation process.

6.2 Limitations and future work

The immediate environment of a cell, cultured in a biomaterial, is determined by a complex interplay of a wide range of physical and chemical material properties. Research conducted in the field of TE only starts to understand the influence of the single components in this environment.

Although this lack of knowledge clearly necessitates research to fill this gap, it also complicates certain aspects of it: Findings obtained in one material cannot easily be applied to predict cellular behavior in a different material, and a clear separation of an effect of stiffness sensing from an influence of other material properties remains difficult.

Even a model system designed to allow a clear separation of material properties is, hereby, subjected to some limiting factors: While the microstructure of the hydrogels does not seem to change with a change in stiffness, a certain structural change of the material is the prerequisite for a change in stiffness. Since even a change in nanotopology was shown to influence cellular behavior [89] a possible impact of structural changes always needs to be considered. Another issue that can hardly be controlled in 3D model systems seems to be the exchange of nutrients and waste. Even a minor change in pore size might impact this process and needs to be taken into account.

A 3D hydrogel system is, additionally, likely to restrict or even determine the shape of the incorporated cell: Most cells tend to adapt a spread out morphology on stiff substrates in 2D cultures [130, 198]. Stiff, 3D cultures in contrast can induce the opposite response when the higher material density impairs spreading [187]. The morphology, the cell is allowed to adapt, in turn, has a high influence on different aspects of cellular behavior, including differentiation and proliferation [99, 163]. This might account for some of the differences observed in 2D compared to 3D culture systems.

However, this rather young field of research also holds great opportunities for future work. Type and density of the protein occupied for cellular adhesion is likely to impact the response to matrix elasticity and both factors should be varied for a comprehensive understanding of stiffness sensing. An extension of my experimental setups to a larger set of different mechanical properties would additionally be valuable to confirm the observed

trends and identify possible plateaus in the response. This work could then be adapted to studies with MSCs to cover all currently relevant cell types for cartilage TE.

Furthermore, although I was able to gain fundamental knowledge about how chondrocytes respond to matrix elasticity, the cellular and molecular mechanisms involved in this response were not investigated in the scope of this thesis. A general issue in the determination of suitable mechanical properties is the high deviation in the mechanical testing procedures that are applied in the field. Further evaluation is needed to identify which mechanical test would resemble the way a cell senses the stiffness of a matrix the best. These investigations might be, furthermore, complemented by studies of stiffness sensing mechanisms for instance through an inhibition of nonmuscle myosins (that are likely to be part of the mechanism) or through an analysis of integrin expression profiles.

6.3 Conclusions

This thesis provides a comprehensive work about chondrocyte response to matrix elasticity in different scenarios. The obtained knowledge may help to specifically tailor the properties of materials used for chondrocyte culture in order to optimize cell-material interactions. However, since this field of research is still young, scientists only start to understand the complex interplay of cells and the insoluble cues in their environment. Extensive future work, therefore, remains necessary to deepen the understanding of the involved processes.

References

1. Chung C, Burdick JA. Engineering cartilage tissue. *Adv Drug Deliv Rev* 2008 Jan 14;60(2):243-262.
2. Boontheekul T, Hill EE, Kong HJ, Mooney DJ. Regulating myoblast phenotype through controlled gel stiffness and degradation. *Tissue Eng* 2007 Jul;13(7):1431-1442.
3. Bryant SJ, Anseth KS. Hydrogel properties influence ECM production by chondrocytes photoencapsulated in poly(ethylene glycol) hydrogels. *J Biomed Mater Res* 2002 Jan;59(1):63-72.
4. Buxton PG, Bitar M, Gellynck K, Parkar M, Brown RA, Young AM, et al. Dense collagen matrix accelerates osteogenic differentiation and rescues the apoptotic response to MMP inhibition. *Bone* 2008 Aug;43(2):377-385.
5. Balgude AP, Yu X, Szymanski A, Bellamkonda RV. Agarose gel stiffness determines rate of DRG neurite extension in 3D cultures. *Biomaterials* 2001 May;22(10):1077-1084.
6. Engler AJ, Griffin MA, Sen S, Bonnemann CG, Sweeney HL, Discher DE. Myotubes differentiate optimally on substrates with tissue-like stiffness: pathological implications for soft or stiff microenvironments. *J Cell Biol* 2004 Sep 13;166(6):877-887.
7. Engler AJ, Sen S, Sweeney HL, Discher DE. Matrix elasticity directs stem cell lineage specification. *Cell* 2006 Aug 25;126(4):677-689.
8. Darling EM, Athanasiou KA. Rapid phenotypic changes in passaged articular chondrocyte subpopulations. *J Orthop Res* 2005 Mar;23(2):425-432.
9. Peterson L, Minas T, Brittberg M, Nilsson A, Sjogren-Jansson E, Lindahl A. Two- to 9-year outcome after autologous chondrocyte transplantation of the knee. *Clin Orthop Relat Res* 2000 May(374):212-234.
10. Wang Y, Kim UJ, Blasioli DJ, Kim HJ, Kaplan DL. In vitro cartilage tissue engineering with 3D porous aqueous-derived silk scaffolds and mesenchymal stem cells. *Biomaterials* 2005 Dec;26(34):7082-7094.
11. Gellynck K, Verdonk PC, Van Nimmen E, Almqvist KF, Gheysens T, Schoukens G, et al. Silkworm and spider silk scaffolds for chondrocyte support. *J Mater Sci Mater Med* 2008 Nov;19(11):3399-3409.
12. Griffon DJ, Sedighi MR, Schaeffer DV, Eurell JA, Johnson AL. Chitosan scaffolds: interconnective pore size and cartilage engineering. *Acta Biomater* 2006 May;2(3):313-320.
13. Lien SM, Ko LY, Huang TJ. Effect of pore size on ECM secretion and cell growth in gelatin scaffold for articular cartilage tissue engineering. *Acta Biomater* 2009 Feb;5(2):670-679.
14. Lu XL, Mow VC. Biomechanics of articular cartilage and determination of material properties. *Med Sci Sports Exerc* 2008 Feb;40(2):193-199.
15. Alexopoulos LG, Setton LA, Guilak F. The biomechanical role of the chondrocyte pericellular matrix in articular cartilage. *Acta Biomater* 2005 May;1(3):317-325.
16. Knudson CB, Knudson W. Cartilage proteoglycans. *Semin Cell Dev Biol* 2001 Apr;12(2):69-78.
17. Cremer MA, Rosloniec EF, Kang AH. The cartilage collagens: a review of their structure, organization, and role in the pathogenesis of experimental arthritis in animals and in human

- rheumatic disease. *J Mol Med* 1998 Mar;76(3-4):275-288.
18. Nestic D, Whiteside R, Brittberg M, Wendt D, Martin I, Mainil-Varlet P. Cartilage tissue engineering for degenerative joint disease. *Adv Drug Deliv Rev* 2006 May 20;58(2):300-322.
 19. Elisseeff J. Injectable cartilage tissue engineering. *Expert Opin Biol Ther* 2004 Dec;4(12):1849-1859.
 20. Ruano-Ravina A, Jato Diaz M. Autologous chondrocyte implantation: a systematic review. *Osteoarthritis Cartilage* 2006 Jan;14(1):47-51.
 21. Newman AP. Articular cartilage repair. *Am J Sports Med* 1998 Mar-Apr;26(2):309-324.
 22. Rand JA. Role of arthroscopy in osteoarthritis of the knee. *Arthroscopy* 1991;7(4):358-363.
 23. Kim HK, Moran ME, Salter RB. The potential for regeneration of articular cartilage in defects created by chondral shaving and subchondral abrasion. An experimental investigation in rabbits. *J Bone Joint Surg Am* 1991 Oct;73(9):1301-1315.
 24. Johnson LL. Arthroscopic abrasion arthroplasty historical and pathologic perspective: present status. *Arthroscopy* 1986;2(1):54-69.
 25. Insall J. The Pridie debridement operation for osteoarthritis of the knee. *Clin Orthop Relat Res* 1974 Jun(101):61-67.
 26. Ficat RP, Ficat C, Gedeon P, Toussaint JB. Spongialization: a new treatment for diseased patellae. *Clin Orthop Relat Res* 1979 Oct(144):74-83.
 27. Kreuz PC, Steinwachs MR, Erggelet C, Krause SJ, Konrad G, Uhl M, et al. Results after microfracture of full-thickness chondral defects in different compartments in the knee. *Osteoarthritis Cartilage* 2006 Nov;14(11):1119-1125.
 28. Hangody L, Kish G, Karpati Z, Szerb I, Udvarhelyi I. Arthroscopic autogenous osteochondral mosaicplasty for the treatment of femoral condylar articular defects. A preliminary report. *Knee Surg Sports Traumatol Arthrosc* 1997;5(4):262-267.
 29. Marlovits S, Zeller P, Singer P, Resinger C, Vecsei V. Cartilage repair: generations of autologous chondrocyte transplantation. *Eur J Radiol* 2006 Jan;57(1):24-31.
 30. Brittberg M. Autologous chondrocyte transplantation. *Clin Orthop Relat Res* 1999 Oct(367 Suppl):S147-155.
 31. French MM, Rose S, Canseco J, Athanasiou KA. Chondrogenic differentiation of adult dermal fibroblasts. *Ann Biomed Eng* 2004 Jan;32(1):50-56.
 32. Deng Y, Hu JC, Athanasiou KA. Isolation and chondroinduction of a dermis-isolated, aggrecan-sensitive subpopulation with high chondrogenic potential. *Arthritis Rheum* 2007 Jan;56(1):168-176.
 33. Hegert C, Kramer J, Hargus G, Muller J, Guan K, Wobus AM, et al. Differentiation plasticity of chondrocytes derived from mouse embryonic stem cells. *J Cell Sci* 2002 Dec 1;115(Pt 23):4617-4628.
 34. Kramer J, Bohrsen F, Schlenke P, Rohwedel J. Stem cell-derived chondrocytes for regenerative medicine. *Transplant Proc* 2006 Apr;38(3):762-765.
 35. Kramer J, Hargus G, Rohwedel J. Derivation and characterization of chondrocytes from embryonic stem cells in vitro. *Methods Mol Biol* 2006;330:171-190.
 36. Kramer J, Hegert C, Hargus G, Rohwedel J. Chondrocytes derived from mouse embryonic stem cells. *Cytotechnology* 2003 Mar;41(2-3):177-187.
 37. Goessler UR, Bugert P, Bieback K, Sadick H, Verse T, Baisch A, et al. In vitro analysis of matrix proteins and growth factors in dedifferentiating human chondrocytes for tissue-engineered cartilage. *Acta Otolaryngol* 2005 Jun;125(6):647-653.
 38. Buschmann MD, Gluzband YA, Grodzinsky AJ, Kimura JH, Hunziker EB. Chondrocytes in agarose culture synthesize a mechanically functional extracellular matrix. *J Orthop Res* 1992 Nov;10(6):745-758.
 39. Erickson GR, Gimble JM, Franklin DM, Rice HE, Awad H, Guilak F. Chondrogenic

- potential of adipose tissue-derived stromal cells in vitro and in vivo. *Biochem Biophys Res Commun* 2002 Jan 18;290(2):763-769.
40. Pittenger MF, Mackay AM, Beck SC, Jaiswal RK, Douglas R, Mosca JD, et al. Multilineage potential of adult human mesenchymal stem cells. *Science* 1999 Apr 2;284(5411):143-147.
 41. Johnstone B, Hering TM, Caplan AI, Goldberg VM, Yoo JU. In vitro chondrogenesis of bone marrow-derived mesenchymal progenitor cells. *Exp Cell Res* 1998 Jan 10;238(1):265-272.
 42. Coleman RM, Case ND, Guldberg RE. Hydrogel effects on bone marrow stromal cell response to chondrogenic growth factors. *Biomaterials* 2007 Apr;28(12):2077-2086.
 43. Williams CG, Kim TK, Taboas A, Malik A, Manson P, Elisseeff J. In vitro chondrogenesis of bone marrow-derived mesenchymal stem cells in a photopolymerizing hydrogel. *Tissue Eng* 2003 Aug;9(4):679-688.
 44. Hofmann S, Knecht S, Langer R, Kaplan DL, Vunjak-Novakovic G, Merkle HP, et al. Cartilage-like tissue engineering using silk scaffolds and mesenchymal stem cells. *Tissue Eng* 2006 Oct;12(10):2729-2738.
 45. Mauck RL, Yuan X, Tuan RS. Chondrogenic differentiation and functional maturation of bovine mesenchymal stem cells in long-term agarose culture. *Osteoarthritis Cartilage* 2006 Feb;14(2):179-189.
 46. De Franceschi L, Grigolo B, Roseti L, Facchini A, Fini M, Giavaresi G, et al. Transplantation of chondrocytes seeded on collagen-based scaffold in cartilage defects in rabbits. *J Biomed Mater Res A* 2005 Dec 1;75(3):612-622.
 47. Fujisato T, Sajiki T, Liu Q, Ikada Y. Effect of basic fibroblast growth factor on cartilage regeneration in chondrocyte-seeded collagen sponge scaffold. *Biomaterials* 1996 Jan;17(2):155-162.
 48. Wang Y, Blasioli DJ, Kim HJ, Kim HS, Kaplan DL. Cartilage tissue engineering with silk scaffolds and human articular chondrocytes. *Biomaterials* 2006 Sep;27(25):4434-4442.
 49. Awad HA, Quinn Wickham M, Leddy HA, Gimble JM, Guilak F. Chondrogenic differentiation of adipose-derived adult stem cells in agarose, alginate, and gelatin scaffolds. *Biomaterials* 2004;25(16):3211-3222.
 50. Benya PD, Shaffer JD. Dedifferentiated chondrocytes reexpress the differentiated collagen phenotype when cultured in agarose gels. *Cell* 1982 Aug;30(1):215-224.
 51. Buckley CT, Thorpe SD, Kelly DJ. Engineering of large cartilaginous tissues through the use of microchanneled hydrogels and rotational culture. *Tissue Eng Part A* 2009 Nov;15(11):3213-3220.
 52. Binette F, McQuaid DP, Haudenschild DR, Yaeger PC, McPherson JM, Tubo R. Expression of a stable articular cartilage phenotype without evidence of hypertrophy by adult human articular chondrocytes in vitro. *J Orthop Res* 1998 Mar;16(2):207-216.
 53. Rowley JA, Madlambayan G, Mooney DJ. Alginate hydrogels as synthetic extracellular matrix materials. *Biomaterials* 1999 Jan;20(1):45-53.
 54. Sechriest VF, Miao YJ, Niyibizi C, Westerhausen-Larson A, Matthew HW, Evans CH, et al. GAG-augmented polysaccharide hydrogel: a novel biocompatible and biodegradable material to support chondrogenesis. *J Biomed Mater Res* 2000 Mar 15;49(4):534-541.
 55. Marcacci M, Berruto M, Brocchetta D, Delcogliano A, Ghinelli D, Gobbi A, et al. Articular cartilage engineering with Hyalograft C: 3-year clinical results. *Clin Orthop Relat Res* 2005 Jun(435):96-105.
 56. Martens PJ, Bryant SJ, Anseth KS. Tailoring the Degradation of Hydrogels Formed from Multivinyl Poly(ethylene glycol) and Poly(vinyl alcohol) Macromers for Cartilage Tissue Engineering. *Biomacromolecules* 2003;4(2):283-292.
 57. Bryant SJ, Arthur JA, Anseth KS. Incorporation of tissue-specific molecules alters chondrocyte metabolism and gene expression in photocrosslinked hydrogels. *Acta Biomaterialia*

2005;1(2):243-252.

58. Bryant SJ, Nicodemus GD, Villanueva I. Designing 3D Photopolymer Hydrogels to Regulate Biomechanical Cues and Tissue Growth for Cartilage Tissue Engineering. *Pharm Res* 2008 May 29.
59. Stephanie J. Bryant KSA. Hydrogel properties influence ECM production by chondrocytes photoencapsulated in poly(ethylene glycol) hydrogels. *Journal of Biomedical Materials Research* 2002;59(1):63-72.
60. Sakai S, Hashimoto I, Kawakami K. Synthesis of an agarose-gelatin conjugate for use as a tissue engineering scaffold. *J Biosci Bioeng* 2007 Jan;103(1):22-26.
61. Zhao H, Ma L, Gong Y, Gao C, Shen J. A polylactide/fibrin gel composite scaffold for cartilage tissue engineering: fabrication and an in vitro evaluation. *J Mater Sci Mater Med* 2009 Jan;20(1):135-143.
62. Hsu SH, Chang SH, Yen HJ, Whu SW, Tsai CL, Chen DC. Evaluation of biodegradable polyesters modified by type II collagen and Arg-Gly-Asp as tissue engineering scaffolding materials for cartilage regeneration. *Artif Organs* 2006 Jan;30(1):42-55.
63. Lee HJ, Lee JS, Chansakul T, Yu C, Elisseeff JH, Yu SM. Collagen mimetic peptide-conjugated photopolymerizable PEG hydrogel. *Biomaterials* 2006 Oct;27(30):5268-5276.
64. Karageorgiou V, Kaplan D. Porosity of 3D biomaterial scaffolds and osteogenesis. *Biomaterials* 2005 Sep;26(27):5474-5491.
65. Vickers SM, Squitieri LS, Spector M. Effects of cross-linking type II collagen-GAG scaffolds on chondrogenesis in vitro: dynamic pore reduction promotes cartilage formation. *Tissue Eng* 2006 May;12(5):1345-1355.
66. Woodfield TB, Malda J, de Wijn J, Peters F, Riesle J, van Blitterswijk CA. Design of porous scaffolds for cartilage tissue engineering using a three-dimensional fiber-deposition technique. *Biomaterials* 2004 Aug;25(18):4149-4161.
67. Zeltinger J, Sherwood JK, Graham DA, Mueller R, Griffith LG. Effect of pore size and void fraction on cellular adhesion, proliferation, and matrix deposition. *Tissue Eng* 2001 Oct;7(5):557-572.
68. Khor HL, Kuan Y, Kukula H, Tamada K, Knoll W, Moeller M, et al. Response of cells on surface-induced nanopatterns: fibroblasts and mesenchymal progenitor cells. *Biomacromolecules* 2007 May;8(5):1530-1540.
69. Yim EK, Reano RM, Pang SW, Yee AF, Chen CS, Leong KW. Nanopattern-induced changes in morphology and motility of smooth muscle cells. *Biomaterials* 2005 Sep;26(26):5405-5413.
70. Peyton SR, Ghajar CM, Khatiwala CB, Putnam AJ. The emergence of ECM mechanics and cytoskeletal tension as important regulators of cell function. *Cell Biochem Biophys* 2007;47(2):300-320.
71. Pelham RJ, Jr., Wang YL. Cell locomotion and focal adhesions are regulated by the mechanical properties of the substrate. *Biol Bull* 1998 Jun;194(3):348-349; discussion 349-350.
72. Kong HJ, Polte TR, Alsberg E, Mooney DJ. FRET measurements of cell-traction forces and nano-scale clustering of adhesion ligands varied by substrate stiffness. *Proc Natl Acad Sci U S A* 2005 Mar 22;102(12):4300-4305.
73. Paszek MJ, Zahir N, Johnson KR, Lakins JN, Rozenberg GI, Gefen A, et al. Tensional homeostasis and the malignant phenotype. *Cancer Cell* 2005 Sep;8(3):241-254.
74. Georges PC, Janmey PA. Cell type-specific response to growth on soft materials. *J Appl Physiol* 2005 Apr;98(4):1547-1553.
75. Yeung T, Georges PC, Flanagan LA, Marg B, Ortiz M, Funaki M, et al. Effects of substrate stiffness on cell morphology, cytoskeletal structure, and adhesion. *Cell Motil Cytoskeleton* 2005 Jan;60(1):24-34.
76. Discher DE, Janmey P, Wang YL. Tissue cells feel and respond to the stiffness of their

- substrate. *Science* 2005 Nov 18;310(5751):1139-1143.
77. Georges PC, Miller WJ, Meaney DF, Sawyer ES, Janmey PA. Matrices with compliance comparable to that of brain tissue select neuronal over glial growth in mixed cortical cultures. *Biophys J* 2006 Apr 15;90(8):3012-3018.
78. Balaban NQ, Schwarz US, Riveline D, Goichberg P, Tzur G, Sabanay I, et al. Force and focal adhesion assembly: a close relationship studied using elastic micropatterned substrates. *Nat Cell Biol* 2001 May;3(5):466-472.
79. Friedland JC, Lee MH, Boettiger D. Mechanically activated integrin switch controls alpha5beta1 function. *Science* 2009 Jan 30;323(5914):642-644.
80. Peyton SR, Kim PD, Ghajar CM, Seliktar D, Putnam AJ. The effects of matrix stiffness and RhoA on the phenotypic plasticity of smooth muscle cells in a 3-D biosynthetic hydrogel system. *Biomaterials* 2008 Jun;29(17):2597-2607.
81. Geiger B, Bershadsky A, Pankov R, Yamada KM. Transmembrane crosstalk between the extracellular matrix--cytoskeleton crosstalk. *Nat Rev Mol Cell Biol* 2001 Nov;2(11):793-805.
82. Giannone G, Sheetz MP. Substrate rigidity and force define form through tyrosine phosphatase and kinase pathways. *Trends Cell Biol* 2006 Apr;16(4):213-223.
83. Tilghman RW, Parsons JT. Focal adhesion kinase as a regulator of cell tension in the progression of cancer. *Semin Cancer Biol* 2008 Feb;18(1):45-52.
84. Ingber DE. Tensegrity I. Cell structure and hierarchical systems biology. *J Cell Sci* 2003 Apr 1;116(Pt 7):1157-1173.
85. Ingber DE. Tensegrity II. How structural networks influence cellular information processing networks. *J Cell Sci* 2003 Apr 15;116(Pt 8):1397-1408.
86. Ingber DE. Tensegrity: the architectural basis of cellular mechanotransduction. *Annu Rev Physiol* 1997;59:575-599.
87. Wang N, Tolic-Norrelykke IM, Chen J, Mijailovich SM, Butler JP, Fredberg JJ, et al. Cell prestress. I. Stiffness and prestress are closely associated in adherent contractile cells. *Am J Physiol Cell Physiol* 2002 Mar;282(3):C606-616.
88. Cukierman E, Pankov R, Stevens DR, Yamada KM. Taking cell-matrix adhesions to the third dimension. *Science* 2001 Nov 23;294(5547):1708-1712.
89. Arnold M, Cavalcanti-Adam EA, Glass R, Blummel J, Eck W, Kantlehner M, et al. Activation of integrin function by nanopatterned adhesive interfaces. *Chemphyschem* 2004 Mar 19;5(3):383-388.
90. Engler A, Bacakova L, Newman C, Hategan A, Griffin M, Discher D. Substrate compliance versus ligand density in cell on gel responses. *Biophys J* 2004 Jan;86(1 Pt 1):617-628.
91. Zaman MH, Trapani LM, Sieminski AL, Mackellar D, Gong H, Kamm RD, et al. Migration of tumor cells in 3D matrices is governed by matrix stiffness along with cell-matrix adhesion and proteolysis. *Proc Natl Acad Sci U S A* 2006 Jul 18;103(29):10889-10894.
92. Connelly JT, Garcia AJ, Levenston ME. Interactions between integrin ligand density and cytoskeletal integrity regulate BMSC chondrogenesis. *J Cell Physiol* 2008 Oct;217(1):145-154.
93. Peyton SR, Raub CB, Keschrums VP, Putnam AJ. The use of poly(ethylene glycol) hydrogels to investigate the impact of ECM chemistry and mechanics on smooth muscle cells. *Biomaterials* 2006;27(28):4881-4893.
94. Appelman TP, Mizrahi J, Elisseeff JH, Seliktar D. The differential effect of scaffold composition and architecture on chondrocyte response to mechanical stimulation. *Biomaterials* 2009 Feb;30(4):518-525.
95. Rosso F, Giordano A, Barbarisi M, Barbarisi A. From cell-ECM interactions to tissue engineering. *J Cell Physiol* 2004 May;199(2):174-180.
96. Mahmood TA, de Jong R, Riesle J, Langer R, van Blitterswijk CA. Adhesion-mediated signal transduction in human articular chondrocytes: the influence of biomaterial chemistry and tenascin-C. *Exp Cell Res* 2004 Dec 10;301(2):179-188.

97. Chen CS, Mrksich M, Huang S, Whitesides GM, Ingber DE. Geometric control of cell life and death. *Science* 1997 May 30;276(5317):1425-1428.
98. McBeath R, Pirone DM, Nelson CM, Bhadriraju K, Chen CS. Cell shape, cytoskeletal tension, and RhoA regulate stem cell lineage commitment. *Dev Cell* 2004 Apr;6(4):483-495.
99. Kim UJ, Park J, Li C, Jin HJ, Valluzzi R, Kaplan DL. Structure and properties of silk hydrogels. *Biomacromolecules* 2004 May-Jun;5(3):786-792.
100. Lee CR, Grodzinsky AJ, Spector M. The effects of cross-linking of collagen-glycosaminoglycan scaffolds on compressive stiffness, chondrocyte-mediated contraction, proliferation and biosynthesis. *Biomaterials* 2001 Dec;22(23):3145-3154.
101. Dadsetan M, Hefferan TE, Szatkowski JP, Mishra PK, Macura SI, Lu L, et al. Effect of hydrogel porosity on marrow stromal cell phenotypic expression. *Biomaterials* 2008 May;29(14):2193-2202.
102. Amsden B. Solute Diffusion within Hydrogels. Mechanisms and Models. *Macromolecules* 1998;31(23):8382-8395.
103. Peppas NA, Huang Y, Torres-Lugo M, Ward JH, Zhang J. Physicochemical foundations and structural design of hydrogels in medicine and biology. *Annu Rev Biomed Eng* 2000;2:9-29.
104. Peppas NA, Lustig SR. The role of cross-links, entanglements, and relaxations of the macromolecular carrier in the diffusional release of biologically active materials. Conceptual and scaling relationships. *Ann N Y Acad Sci* 1985;446:26-41.
105. Villanueva I, Hauschulz DS, Mejjic D, Bryant SJ. Static and dynamic compressive strains influence nitric oxide production and chondrocyte bioactivity when encapsulated in PEG hydrogels of different crosslinking densities. *Osteoarthritis Cartilage* 2008 Aug;16(8):909-918.
106. Harley BA, Kim HD, Zaman MH, Yannas IV, Lauffenburger DA, Gibson LJ. Microarchitecture of three-dimensional scaffolds influences cell migration behavior via junction interactions. *Biophys J* 2008 Oct;95(8):4013-4024.
107. Ma T, Li Y, Yang ST, Kniss DA. Effects of pore size in 3-D fibrous matrix on human trophoblast tissue development. *Biotechnol Bioeng* 2000 Dec 20;70(6):606-618.
108. Mygind T, Stiehler M, Baatrup A, Li H, Zou X, Flyvbjerg A, et al. Mesenchymal stem cell ingrowth and differentiation on coralline hydroxyapatite scaffolds. *Biomaterials* 2007 Feb;28(6):1036-1047.
109. Kim J, Yaszemski MJ, Lu L. Three-dimensional porous biodegradable polymeric scaffolds fabricated with biodegradable hydrogel porogens. *Tissue Eng Part C Methods* 2009 Dec;15(4):583-594.
110. Ikem VO, Menner A, Bismarck A. High-Porosity Macroporous Polymers Synthesized from Titania-Particle-Stabilized Medium and High Internal Phase Emulsions. *Langmuir* Feb 12.
111. McKegney M, Taggart I, Grant MH. The influence of crosslinking agents and diamines on the pore size, morphology and the biological stability of collagen sponges and their effect on cell penetration through the sponge matrix. *J Mater Sci Mater Med* 2001 Sep;12(9):833-844.
112. MacKintosh FC, Kas J, Janmey PA. Elasticity of semiflexible biopolymer networks. *Phys Rev Lett* 1995 Dec 11;75(24):4425-4428.
113. Semler EJ, Moghe PV. Engineering hepatocyte functional fate through growth factor dynamics: the role of cell morphologic priming. *Biotechnol Bioeng* 2001 Dec 5;75(5):510-520.
114. Wang YK, Wang YH, Wang CZ, Sung JM, Chiu WT, Lin SH, et al. Rigidity of collagen fibrils controls collagen gel-induced down-regulation of focal adhesion complex proteins mediated by alpha2beta1 integrin. *J Biol Chem* 2003 Jun 13;278(24):21886-21892.
115. McDaniel DP, Shaw GA, Elliott JT, Bhadriraju K, Meuse C, Chung KH, et al. The stiffness of collagen fibrils influences vascular smooth muscle cell phenotype. *Biophys J* 2007 Mar 1;92(5):1759-1769.
116. Erickson IE, Huang AH, Sengupta S, Kestle S, Burdick JA, Mauck RL. Macromer density influences mesenchymal stem cell chondrogenesis and maturation in photocrosslinked hyaluronic

- acid hydrogels. *Osteoarthritis Cartilage* 2009 Dec;17(12):1639-1648.
117. Buckley CT, Thorpe SD, O'Brien FJ, Robinson AJ, Kelly DJ. The effect of concentration, thermal history and cell seeding density on the initial mechanical properties of agarose hydrogels. *J Mech Behav Biomed Mater* 2009 Oct;2(5):512-521.
118. Cui FZ, Tian WM, Hou SP, Xu QY, Lee IS. Hyaluronic acid hydrogel immobilized with RGD peptides for brain tissue engineering. *J Mater Sci Mater Med* 2006 Dec;17(12):1393-1401.
119. Connelly JT, Garcia AJ, Levenston ME. Inhibition of in vitro chondrogenesis in RGD-modified three-dimensional alginate gels. *Biomaterials* 2007;28(6):1071-1083.
120. Drury JL, Mooney DJ. Hydrogels for tissue engineering: scaffold design variables and applications. *Biomaterials* 2003;24(24):4337-4351.
121. Zhang WJ, Laue C, Hyder A, Schrezenmeir J. Purity of alginate affects the viability and fibrotic overgrowth of encapsulated porcine islet xenografts. *Transplant Proc* 2001 Nov-Dec;33(7-8):3517-3519.
122. Kong HJ, Wong E, Mooney DJ. Independent Control of Rigidity and Toughness of Polymeric Hydrogels. *Macromolecules* 2003;36(12):4582-4588.
123. Ahearne M, Yang Y, El Haj AJ, Then KY, Liu K-K. Characterizing the viscoelastic properties of thin hydrogel-based constructs for tissue engineering applications. *Journal of The Royal Society Interface* 2005;2(5):455-463.
124. Genes NG, Rowley JA, Mooney DJ, Bonassar LJ. Effect of substrate mechanics on chondrocyte adhesion to modified alginate surfaces. *Archives of Biochemistry and Biophysics* 2004;422(2):161-167.
125. LeRoux MA, Guilak F, Setton LA. Compressive and shear properties of alginate gel: effects of sodium ions and alginate concentration. *J Biomed Mater Res* 1999 Oct;47(1):46-53.
126. Hsiong SX, Carampin P, Kong HJ, Lee KY, Mooney DJ. Differentiation stage alters matrix control of stem cells. *J Biomed Mater Res A* 2008 Apr;85(1):145-156.
127. Harris AK, Stopak D, Wild P. Fibroblast traction as a mechanism for collagen morphogenesis. *Nature* 1981 Mar 19;290(5803):249-251.
128. Hinz B, Celetta G, Tomasek JJ, Gabbiani G, Chaponnier C. Alpha-smooth muscle actin expression upregulates fibroblast contractile activity. *Mol Biol Cell* 2001 Sep;12(9):2730-2741.
129. Pelham RJ, Jr., Wang Y. Cell locomotion and focal adhesions are regulated by substrate flexibility. *Proc Natl Acad Sci U S A* 1997 Dec 9;94(25):13661-13665.
130. Ehrbar M, Rizzi SC, Schoenmakers RG, Miguel BS, Hubbell JA, Weber FE, et al. Biomolecular hydrogels formed and degraded via site-specific enzymatic reactions. *Biomacromolecules* 2007 Oct;8(10):3000-3007.
131. Park Y, Lutolf MP, Hubbell JA, Hunziker EB, Wong M. Bovine primary chondrocyte culture in synthetic matrix metalloproteinase-sensitive poly(ethylene glycol)-based hydrogels as a scaffold for cartilage repair. *Tissue Eng* 2004 Mar-Apr;10(3-4):515-522.
132. Nguyen KT, West JL. Photopolymerizable hydrogels for tissue engineering applications. *Biomaterials* 2002;23(22):4307-4314.
133. Chirag B. Khatiwala SRPMMAJP. The regulation of osteogenesis by ECM rigidity in MC3T3-E1 cells requires MAPK activation. *Journal of Cellular Physiology* 2007;211(3):661-672.
134. Rizzi SC, Hubbell JA. Recombinant Protein-co-PEG Networks as Cell-Adhesive and Proteolytically Degradable Hydrogel Matrixes. Part I: Development and Physicochemical Characteristics. *Biomacromolecules* 2005;6(3):1226-1238.
135. Shapira-Schweitzer K, Seliktar D. Matrix stiffness affects spontaneous contraction of cardiomyocytes cultured within a PEGylated fibrinogen biomaterial. *Acta Biomaterialia* 2007;3(1):33-41.
136. Salinas CN, Cole BB, Kasko AM, Anseth KS. Chondrogenic differentiation potential of human mesenchymal stem cells photoencapsulated within poly(ethylene glycol)-arginine-glycine-aspartic acid-serine thiol-methacrylate mixed-mode networks. *Tissue Eng* 2007 May;13(5):1025-

- 1034.
137. Benoit DS, Anseth KS. The effect on osteoblast function of colocalized RGD and PHSRN epitopes on PEG surfaces. *Biomaterials* 2005 Sep;26(25):5209-5220.
138. Sikavitsas VI, Temenoff JS, Mikos AG. Biomaterials and bone mechanotransduction. *Biomaterials* 2001 Oct;22(19):2581-2593.
139. Khatiwala CB, Peyton SR, Putnam AJ. Intrinsic mechanical properties of the extracellular matrix affect the behavior of pre-osteoblastic MC3T3-E1 cells. *Am J Physiol Cell Physiol* 2006 Jun;290(6):C1640-1650.
140. Khatiwala CB, Peyton SR, Metzke M, Putnam AJ. The regulation of osteogenesis by ECM rigidity in MC3T3-E1 cells requires MAPK activation. *J Cell Physiol* 2007 Jun;211(3):661-672.
141. Irie K, Ejiri S, Sakakura Y, Shibui T, Yajima T. Matrix mineralization as a trigger for osteocyte maturation. *J Histochem Cytochem* 2008 Jun;56(6):561-567.
142. Rattner A, Sabido O, Le J, Vico L, Massoubre C, Frey J, et al. Mineralization and alkaline phosphatase activity in collagen lattices populated by human osteoblasts. *Calcif Tissue Int* 2000 Jan;66(1):35-42.
143. Yang F, Williams CG, Wang DA, Lee H, Manson PN, Elisseeff J. The effect of incorporating RGD adhesive peptide in polyethylene glycol diacrylate hydrogel on osteogenesis of bone marrow stromal cells. *Biomaterials* 2005 Oct;26(30):5991-5998.
144. Thyberg J, Hedin U, Sjolund M, Palmberg L, Bottger BA. Regulation of differentiated properties and proliferation of arterial smooth muscle cells. *Arteriosclerosis* 1990 Nov-Dec;10(6):966-990.
145. Kim BS, Nikolovski J, Bonadio J, Smiley E, Mooney DJ. Engineered smooth muscle tissues: regulating cell phenotype with the scaffold. *Exp Cell Res* 1999 Sep 15;251(2):318-328.
146. Adelow C, Segura T, Hubbell JA, Frey P. The effect of enzymatically degradable poly(ethylene glycol) hydrogels on smooth muscle cell phenotype. *Biomaterials* 2008 Jan;29(3):314-326.
147. Subramanian A, Lin HY. Crosslinked chitosan: its physical properties and the effects of matrix stiffness on chondrocyte cell morphology and proliferation. *J Biomed Mater Res A* 2005 Dec 1;75(3):742-753.
148. Lo CM, Wang HB, Dembo M, Wang YL. Cell movement is guided by the rigidity of the substrate. *Biophys J* 2000 Jul;79(1):144-152.
149. Domke J, Radmacher M. Measuring the Elastic Properties of Thin Polymer Films with the Atomic Force Microscope. *Langmuir* 1998;14(12):3320-3325.
150. Westra KL, Thomson DJ. Effect of tip shape on surface roughness measurements from atomic force microscopy images of thin films. *Journal of Vacuum Science & Technology B: Microelectronics and Nanometer Structures* 1995;13(2):344-349.
151. Hertz H. Über die Berührung fester elastischer Körper. *J Reine Angew Mathematik* 1882;92:156-171.
152. C. L. Bauer RJF. Determination of poisson's ratio for polyimide films. *Polymer Engineering & Science* 1989;29(16):1107-1110.
153. Glowacki J, Trepman E, Folkman J. Cell shape and phenotypic expression in chondrocytes. *Proc Soc Exp Biol Med* 1983 Jan;172(1):93-98.
154. Schnabel M, Marlovits S, Eckhoff G, Fichtel I, Gotzen L, Vecsei V, et al. Dedifferentiation-associated changes in morphology and gene expression in primary human articular chondrocytes in cell culture. *Osteoarthritis Cartilage* 2002 Jan;10(1):62-70.
155. Archer CW, Rooney P, Wolpert L. Cell shape and cartilage differentiation of early chick limb bud cells in culture. *Cell Differ* 1982 Jun;11(4):245-251.
156. Mallein-Gerin F, Garrone R, van der Rest M. Proteoglycan and collagen synthesis are correlated with actin organization in dedifferentiating chondrocytes. *Eur J Cell Biol* 1991

Dec;56(2):364-373.

157. Jeffrey JJ, Martin GR. The role of ascorbic acid in the biosynthesis of collagen. II. Site and nature of ascorbic acid participation. *Biochim Biophys Acta* 1966 Jun 29;121(2):281-291.
158. Clark AG, Rohrbaugh AL, Otterness I, Kraus VB. The effects of ascorbic acid on cartilage metabolism in guinea pig articular cartilage explants. *Matrix Biol* 2002 Mar;21(2):175-184.
159. Gunson R, Gillespie G, W FC. Optimisation of PCR reactions using primer chessboarding. *J Clin Virol* 2003 Apr;26(3):369-373.
160. Iwig M, Czeslick E, Muller A, Gruner M, Spindler M, Glaesser D. Growth regulation by cell shape alteration and organization of the cytoskeleton. *Eur J Cell Biol* 1995 Jun;67(2):145-157.
161. Assoian RK. Anchorage-dependent cell cycle progression. *J Cell Biol* 1997 Jan 13;136(1):1-4.
162. Assoian RK, Zhu X. Cell anchorage and the cytoskeleton as partners in growth factor dependent cell cycle progression. *Curr Opin Cell Biol* 1997 Feb;9(1):93-98.
163. Margadant C, van Opstal A, Boonstra J. Focal adhesion signaling and actin stress fibers are dispensable for progression through the ongoing cell cycle. *J Cell Sci* 2007 Jan 1;120(Pt 1):66-76.
164. Wang HB, Dembo M, Wang YL. Substrate flexibility regulates growth and apoptosis of normal but not transformed cells. *Am J Physiol Cell Physiol* 2000 Nov;279(5):C1345-1350.
165. Deroanne CF, Lapiere CM, Nussgens BV. In vitro tubulogenesis of endothelial cells by relaxation of the coupling extracellular matrix-cytoskeleton. *Cardiovasc Res* 2001 Feb 16;49(3):647-658.
166. Engler AJ, Sweeney HL, Discher DE, Schwarzbauer JE. Extracellular matrix elasticity directs stem cell differentiation. *J Musculoskelet Neuronal Interact* 2007 Oct-Dec;7(4):335.
167. Freeman PM, Natarajan RN, Kimura JH, Andriacchi TP. Chondrocyte cells respond mechanically to compressive loads. *J Orthop Res* 1994 May;12(3):311-320.
168. Koay EJ, Shieh AC, Athanasiou KA. Creep indentation of single cells. *J Biomech Eng* 2003 Jun;125(3):334-341.
169. Jones WR, Ting-Beall HP, Lee GM, Kelley SS, Hochmuth RM, Guilak F. Alterations in the Young's modulus and volumetric properties of chondrocytes isolated from normal and osteoarthritic human cartilage. *J Biomech* 1999 Feb;32(2):119-127.
170. Ng L, Hung HH, Sprunt A, Chubinskaya S, Ortiz C, Grodzinsky A. Nanomechanical properties of individual chondrocytes and their developing growth factor-stimulated pericellular matrix. *J Biomech* 2007;40(5):1011-1023.
171. Guilak F, Alexopoulos LG, Haider MA, Ting-Beall HP, Setton LA. Zonal uniformity in mechanical properties of the chondrocyte pericellular matrix: micropipette aspiration of canine chondrons isolated by cartilage homogenization. *Ann Biomed Eng* 2005 Oct;33(10):1312-1318.
172. Guilak F, Jones WR, Ting-Beall HP, Lee GM. The deformation behavior and mechanical properties of chondrocytes in articular cartilage. *Osteoarthritis Cartilage* 1999 Jan;7(1):59-70.
173. Nemir S, West JL. Synthetic Materials in the Study of Cell Response to Substrate Rigidity. *Ann Biomed Eng* 2009 Oct 9.
174. Kim UJ, Park J, Kim HJ, Wada M, Kaplan DL. Three-dimensional aqueous-derived biomaterial scaffolds from silk fibroin. *Biomaterials* 2005 May;26(15):2775-2785.
175. Panilaitis B, Altman GH, Chen J, Jin HJ, Karageorgiou V, Kaplan DL. Macrophage responses to silk. *Biomaterials* 2003 Aug;24(18):3079-3085.
176. Meinel L, Hofmann S, Karageorgiou V, Zichner L, Langer R, Kaplan D, et al. Engineering cartilage-like tissue using human mesenchymal stem cells and silk protein scaffolds. *Biotechnol Bioeng* 2004 Nov 5;88(3):379-391.
177. Horan RL, Antle K, Collette AL, Wang Y, Huang J, Moreau JE, et al. In vitro degradation of silk fibroin. *Biomaterials* 2005 Jun;26(17):3385-3393.

178. Zaoming W, Codina R, Fernandez-Caldas E, Lockey RF. Partial characterization of the silk allergens in mulberry silk extract. *J Investig Allergol Clin Immunol* 1996 Jul-Aug;6(4):237-241.
179. Hofmann S, Hagenmuller H, Koch AM, Muller R, Vunjak-Novakovic G, Kaplan DL, et al. Control of in vitro tissue-engineered bone-like structures using human mesenchymal stem cells and porous silk scaffolds. *Biomaterials* 2007 Feb;28(6):1152-1162.
180. Hildebrand T, Laib A, Muller R, Dequeker J, Rueggsegger P. Direct three-dimensional morphometric analysis of human cancellous bone: microstructural data from spine, femur, iliac crest, and calcaneus. *J Bone Miner Res* 1999 Jul;14(7):1167-1174.
181. Bolfarine H, Valenca DM. Testing homogeneity in Weibull-regression models. *Biom J* 2005 Oct;47(5):707-720.
182. Stok KS, Lisignoli G, Cristino S, Facchini A, Muller R. Mechano-functional assessment of human mesenchymal stem cells grown in three-dimensional hyaluronan-based scaffolds for cartilage tissue engineering. *J Biomed Mater Res A* 2009 May 29.
183. Spilker RL, Suh JK, Mow VC. A finite element analysis of the indentation stress-relaxation response of linear biphasic articular cartilage. *J Biomech Eng* 1992 May;114(2):191-201.
184. Schuh E, Kramer J, Rohwedel J, Notbohm H, Muller R, Gutschmann T, et al. Effect of matrix elasticity on the maintenance of the chondrogenic phenotype. *Tissue Eng Part A* 2009 Nov 10.
185. Semler EJ, Lancin PA, Dasgupta A, Moghe PV. Engineering hepatocellular morphogenesis and function via ligand-presenting hydrogels with graded mechanical compliance. *Biotechnol Bioeng* 2005 Feb 5;89(3):296-307.
186. Nuttelman CR, Benoit DS, Tripodi MC, Anseth KS. The effect of ethylene glycol methacrylate phosphate in PEG hydrogels on mineralization and viability of encapsulated hMSCs. *Biomaterials* 2006 Mar;27(8):1377-1386.
187. Dikovskiy D, Bianco-Peled H, Seliktar D. Defining the role of matrix compliance and proteolysis in three-dimensional cell spreading and remodeling. *Biophys J* 2008 Apr 1;94(7):2914-2925.
188. Mauck RL, Wang CCB, Oswald ES, Ateshian GA, Hung CT. The role of cell seeding density and nutrient supply for articular cartilage tissue engineering with deformational loading. *Osteoarthritis and Cartilage* 2003;11(12):879-890.
189. Mauck RL, Soltz MA, Wang CC, Wong DD, Chao PH, Valhmu WB, et al. Functional tissue engineering of articular cartilage through dynamic loading of chondrocyte-seeded agarose gels. *J Biomech Eng* 2000 Jun;122(3):252-260.
190. Lee KY, Mooney DJ. Hydrogels for tissue engineering. *Chem Rev* 2001 Jul;101(7):1869-1879.
191. Normand V, Lootens DL, Amici E, Plucknett KP, Aymard P. New insight into agarose gel mechanical properties. *Biomacromolecules* 2000 Winter;1(4):730-738.
192. Gu WY, Yao H, Huang CY, Cheung HS. New insight into deformation-dependent hydraulic permeability of gels and cartilage, and dynamic behavior of agarose gels in confined compression. *J Biomech* 2003 Apr;36(4):593-598.
193. Connelly JT, Garcia AJ, Levenston ME. Interactions between integrin ligand density and cytoskeletal integrity regulate BMSC chondrogenesis. *J Cell Physiol* 2008 May 1.
194. Rowlands AS, George PA, Cooper-White JJ. Directing osteogenic and myogenic differentiation of MSCs: interplay of stiffness and adhesive ligand presentation. *Am J Physiol Cell Physiol* 2008 Oct;295(4):C1037-1044.
195. Pek YS, Wan AC, Ying JY. The effect of matrix stiffness on mesenchymal stem cell differentiation in a 3D thixotropic gel. *Biomaterials* Jan;31(3):385-391.
196. Xiong JY, Narayanan J, Liu XY, Chong TK, Chen SB, Chung TS. Topology evolution

- and gelation mechanism of agarose gel. *J Phys Chem B* 2005 Mar 31;109(12):5638-5643.
197. Lund AW, Stegemann JP, Plopper GE. Inhibition of ERK promotes collagen gel compaction and fibrillogenesis to amplify the osteogenesis of human mesenchymal stem cells in three-dimensional collagen I culture. *Stem Cells Dev* 2009 Mar;18(2):331-341.
198. Kramer J, Hegert C, Rohwedel J. In vitro differentiation of mouse ES cells: bone and cartilage. *Methods Enzymol* 2003;365:251-268.
199. Johnson EM, Berk DA, Jain RK, Deen WM. Hindered diffusion in agarose gels: test of effective medium model. *Biophys J* 1996 Feb;70(2):1017-1023.
200. Leddy HA, Awad HA, Guilak F. Molecular diffusion in tissue-engineered cartilage constructs: effects of scaffold material, time, and culture conditions. *J Biomed Mater Res B Appl Biomater* 2004 Aug 15;70(2):397-406.
201. Lundberg P, Kuchel PW. Diffusion of solutes in agarose and alginate gels: ^1H and ^{23}Na PFGSE and ^{23}Na TQF NMR studies. *Magn Reson Med* 1997 Jan;37(1):44-52.
202. Bryant SJ, Anseth KS. The effects of scaffold thickness on tissue engineered cartilage in photocrosslinked poly(ethylene oxide) hydrogels. *Biomaterials* 2001 Mar;22(6):619-626.
203. Freed LE, Marquis JC, Langer R, Vunjak-Novakovic G. Kinetics of chondrocyte growth in cell-polymer implants. *Biotechnol Bioeng* 1994 Mar 25;43(7):597-604.
204. Schuh E, Kramer J, Rohwedel J, Notbohm H, Muller R, Gutschmann T, et al. Effect of Matrix Elasticity on the Maintenance of the Chondrogenic Phenotype. *Tissue Eng Part A* Feb 11.
205. Jakob M, Demartean O, Schafer D, Hintermann B, Dick W, Heberer M, et al. Specific growth factors during the expansion and redifferentiation of adult human articular chondrocytes enhance chondrogenesis and cartilaginous tissue formation in vitro. *J Cell Biochem* 2001 Mar 26;81(2):368-377.
206. Cook JL, Williams N, Kreeger JM, Peacock JT, Tomlinson JL. Biocompatibility of three-dimensional chondrocyte grafts in large tibial defects of rabbits. *Am J Vet Res* 2003 Jan;64(1):12-20.
207. Rahfoth B, Weisser J, Sternkopf F, Aigner T, von der Mark K, Brauer R. Transplantation of allograft chondrocytes embedded in agarose gel into cartilage defects of rabbits. *Osteoarthritis Cartilage* 1998 Jan;6(1):50-65.
208. Pfeiffer E, Vickers SM, Frank E, Grodzinsky AJ, Spector M. The effects of glycosaminoglycan content on the compressive modulus of cartilage engineered in type II collagen scaffolds. *Osteoarthritis Cartilage* 2008 Oct;16(10):1237-1244.
209. Miot S, Woodfield T, Daniels AU, Suetterlin R, Peterschmitt I, Heberer M, et al. Effects of scaffold composition and architecture on human nasal chondrocyte redifferentiation and cartilaginous matrix deposition. *Biomaterials* 2005 May;26(15):2479-2489.
210. Newman P, Watt FM. Influence of cytochalasin D-induced changes in cell shape on proteoglycan synthesis by cultured articular chondrocytes. *Exp Cell Res* 1988 Oct;178(2):199-210.
211. D'Souza SE, Ginsberg MH, Plow EF. Arginyl-glycyl-aspartic acid (RGD): a cell adhesion motif. *Trends Biochem Sci* 1991 Jul;16(7):246-250.
212. Villanueva I, Weigel CA, Bryant SJ. Cell-matrix interactions and dynamic mechanical loading influence chondrocyte gene expression and bioactivity in PEG-RGD hydrogels. *Acta Biomater* 2009 Oct;5(8):2832-2846.
213. Alsberg E, Anderson KW, Albeiruti A, Rowley JA, Mooney DJ. Engineering growing tissues. *Proc Natl Acad Sci U S A* 2002 Sep 17;99(19):12025-12030.
214. Borkenhagen M, Clemence JF, Sigrist H, Aebischer P. Three-dimensional extracellular matrix engineering in the nervous system. *J Biomed Mater Res* 1998 Jun 5;40(3):392-400.
215. del Rio A, Perez-Jimenez R, Liu R, Roca-Cusachs P, Fernandez JM, Sheetz MP. Stretching single talin rod molecules activates vinculin binding. *Science* 2009 Jan 30;323(5914):638-641.

-
216. Schwartz MA. Cell biology. The force is with us. *Science* 2009 Jan 30;323(5914):588-589.
217. Brandl A, Angele P, Roll C, Prantl L, Kujat R, Kinner B. Influence of the growth factors PDGF-BB, TGF-beta1 and bFGF on the replicative aging of human articular chondrocytes during in vitro expansion. *J Orthop Res* 2009 Oct 1;28(3):354-360.
218. Koo J, Kim KI, Min BH, Lee GM. Controlling medium osmolality improves the expansion of human articular chondrocytes in serum-free media. *Tissue Eng Part C Methods* 2009 Dec 9.
219. Mahmood TA, Miot S, Frank O, Martin I, Riesle J, Langer R, et al. Modulation of chondrocyte phenotype for tissue engineering by designing the biologic-polymer carrier interface. *Biomacromolecules* 2006 Nov;7(11):3012-3018.
220. Woodfield TB, Miot S, Martin I, van Blitterswijk CA, Riesle J. The regulation of expanded human nasal chondrocyte re-differentiation capacity by substrate composition and gas plasma surface modification. *Biomaterials* 2006 Mar;27(7):1043-1053.
221. Chowdhury TT, Salter DM, Bader DL, Lee DA. Integrin-mediated mechanotransduction processes in TGFbeta-stimulated monolayer-expanded chondrocytes. *Biochem Biophys Res Commun* 2004 Jun 11;318(4):873-881.

Scientific manuscripts

MANUSCRIPT 1:

Schuh E, Kramer J, Rohwedel J, Notbohm H, Müller R, Gutschmann T, Rotter N. Effect of matrix elasticity on the maintenance of the chondrogenic phenotype. *Tissue Eng Part A*. 2009. *Tissue Eng Part A*. 2010 Apr; 16(4):1281-90.

MANUSCRIPT 2:

Schuh E, Hofmann S, Stok K, Notbohm H, Müller R, Rotter N. The influence of matrix elasticity on chondrocyte behavior in 3D. Under Revision at *Tissue Engineering*.

MANUSCRIPT 3:

Schuh E, Hofmann S, Notbohm H, Müller R, Rotter N. Chondrocyte redifferentiation in 3D: the effect of adhesion site density and substrate stiffness. Submitted to *TERM*.